EXPLOITING DIVERSITY BY OPPORTUNISTIC SCHEDULING IN ENERGY HARVESTING WIRELESS NETWORKS

A Dissertation

by

HANG LI

Submitted to the Office of Graduate and Professional Studies of
Texas A&M University
in partial fulfillment of the requirements for the degree of

DOCTOR OF PHILOSOPHY

Chair of Committee,	Shuguang Cui
Committee Members,	Zixiang Xiong
	I-Hong Hou
	William B. Johnson
Head of Department,	Miroslav M. Begovic

August 2016

Major Subject: Electrical Engineering

ABSTRACT

It is in recent years that harvesting energy from ambient energy sources (e.g., solar, wind, or vibration) has been commercialized, which is a promising technique to fulfil sustainable operations for many kinds of electrical systems. To advocate reducing the emission of greenhouse gases, people in communication society are seeking to accommodate and take advantage of this new technology for wireless systems, such as sensor networks, Internet of Things, and heterogeneous networks.

In this dissertation, we focus on energy harvesting (EH) based wireless networks, where multiple users are powered by energy harvesters and share limited spectrum resources. In this system, the design of efficient access schemes plays a crucial role in optimizing the system performance. Moreover, different from the conventional wireless systems, there are two random processes that must be jointly counted in the transmission design: the channel fading and the dynamics of the EH powered battery.

Specifically, we narrow down the design onto two typical network setups. First, in a single channel access scenario, an *ad hoc* network with multiple transmitter-receiver pairs is considered, where all EH-based transmitters share one channel by random access. Two EH rate models are applied: Constant and i.i.d. (i.e., independent and identically distributed) EH rate models. To quantify the roles of both the energy and channel state information, a distributed opportunistic scheduling framework is proposed such that the average throughput of the network is maximized.

Second, in a multi-channel access scenario, we study an uplink transmission under a heterogeneous network hierarchy, where each EH-based mobile user (MU) is capable of both deterministically accessing to a large network via one private channel, and dynamically accessing a small network with a certain probability via one common channel

shared by multiple MUs. Considering a time-correlated EH model, we study an opportunistic transmission scheme to maximize the average throughput for each MU by jointly exploiting the statistics of the system states.

Finally, back to the single channel access setup, we investigate the *multiuser energy diversity* by analyzing the fundamental scaling law of the throughput over the number of EH-based users under both centralized and distributed access schemes. We reveal the throughput gain coming from both the increase of total available energy harvested over time/space and the combined dynamics of batteries.

DEDICATION

To my parents,

Shuxiang Li and Suzhen Wang.

ACKNOWLEDGEMENTS

I would like to thank all the people who have offered me their help during my Ph.D program at Texas A&M University, the Aggieland located in East-Central Texas.

I would like to genuinely thank my family members who are behind me all the time. Thank my parents for their endless love and support, and thank my wife for her believing in me regardless of the long distance through all these years. They gave me cheers no matter how big the achievement I got, and also gave me comforts whenever I was depressed.

I would like to especially thank my advisor, Prof. Shuguang Cui, for offering me the opportunity to undertake the cutting-edge research in wireless communications. Moreover, from him, I learned what a qualified researcher should be: He must be able to think boldly and work cautiously; he must stand in the audiences' shoes when he speaks; and he must know haste makes waste. Besides, my advisor also thinks and cares about my personal life, such as my future career and family reunion.

I would like to exceptionally thank Prof. Chuan Huang, who guided me like a mentor on the path of executing research. It is no doubt that I cannot achieve what I have done without his efforts. He shared plenty of life experiences with me as well, which were more practical knowledge beyond those in textbooks.

I would like to sincerely thank all my friends, Yao Liu, Dr. Muxi Yan, Dr. Di Li, Liang Ge, Amir Salimi, Dr. Edwin Collado, Dr. Weijia Han, and the ladies in our office, Dan Lv and Yanyan Zhang. They make my life colorful and full of joyness. They are and will be my friends forever.

Finally, I would like to thank all my committee members, Prof. Zixiang Xiong, Prof. I-Hong Hou, Prof. William B. Johnson, and Prof. Jim Ji, for their time and support on my prelim exam, defense and the dissertation. Their valuable comments help me a lot in

improving the quality of my work.

TABLE OF CONTENTS

Page

LIST OF FIGURES

FIGURE Page

LIST OF TABLES

TABLE Page

1. INTRODUCTION*

It is in recent years that energy harvesting (EH) has raised substantial research interests since it is expected to have abundant applications in future wireless communication networks to power transceivers by utilizing the environmental energy such as solar, thermal, wind, and kinetic energy. Compared against systems with the conventional power supplies that convert fossil fuels into electric energy, EH-based systems are not only more environment friendly, but also more cost-effective by cutting down the service provider utility bills [17]. For example, in cellular networks, solar panels and wind farms have been deployed to power base stations, which could considerably lower the expenses on energy bills as well as reduce the level of carbon dioxide emissions. For other systems, e.g, wireless sensor networks, Internet of Things [27], and heterogeneous networks [18], it is expected that EH could also be a good substitute of the conventional power supplies [42,54], prolonging the operation time to almost infinity, at least theoretically.

Despite the promising potential, there are two major challenges that hold back the operation of EH wireless systems.

1) EH Uncertainty. The power generated by EH is non-deterministic in general due to the dynamic and intermittent characteristics of renewable energy sources, which may not provide a stable power supply for the wireless system. This implies that communications may suffer from unreliability due to the random shortage of energy. Some existing works have studied the impact of such uncertainty brought by EH. For example, the authors in [18] studied a heterogeneous network with multiple base stations (BSs) powered by EH solely. The non-outage probabilities of BSs were derived to analyze the availability region

*Part of this chapter is reprinted, with permission, from [Hang Li, Chuan Huang, Fuad Alsaadi, and Shuguang Cui, "Performance analysis for energy harvesting communication systems: from throughput to energy diversity", in *Global Telecommunications Conference*, IEEE, Dec. 7-10, 2015]

of the network. For a large-scale *ad hoc* network, the author in [32] defined a notion called transmission probability to capture the portion of time when the sensor node has enough energy and transmits at a constant power level.

2) EH Constraints. These new transmission constraints mean that the available energy at the system up to any time is bounded by its accumulatively harvested energy by then. This is in contrast to conventional communication systems with fixed energy sources, in which the available energy at any time is either unbounded or only limited by the remaining energy in the storage device (e.g., battery). Many existing works have investigated the throughput optimal or suboptimal transmission strategies under EH constraints. For instance, the optimal throughput has been investigated in point-to-point channel [30, 44], Gaussian relay channel [31], and multiuser scenario [37]. In [57], a comprehensive review was provided on the recent development of EH communications, where throughput-optimal power allocations and scheduling policies were thoroughly discussed under various setups. Therefore, for EH-based wireless networks, the EH constraint should be carefully taken into account in the design of access schemes.

In this dissertation, we focus on the design of opportunistic scheduling for EH-based networks. First, we design a distributed opportunistic scheduling for a general ad hoc network, where all EH-based users share a common wireless channel for communications. Second, we consider a heterogeneous network that provides multiple wireless accesses for mobile users. To efficiently exploit the channel resources, we propose an opportunistic transmission schemes to maximize the throughput of each user. Finally, we investigate the fundamental the scaling law of the throughput over the number of users, which describes how the scheduling schemes exploit the multiuser energy diversity.

The main body of the dissertation includes three parts.

- In the first part, an ad hoc network with multiple transmitter-receiver pairs is con-

sidered, in which all transmitters are capable of harvesting renewable energy from the environment and compete for one shared channel by random access.

In particular, we focus on two different scenarios: the constant EH rate model where the EH rate remains constant within the time of interest and the i.i.d. EH rate model where the EH rates are independent and identically distributed across different contention slots. To quantify the roles of both the energy state information (ESI) and the channel state information (CSI), a distributed opportunistic scheduling (DOS) framework with two-stage probing and save-then-transmit energy utilization is proposed.

Then, the optimal throughput and the optimal scheduling strategy are obtained via one-dimension search, i.e., an iterative algorithm consisting of the following two steps in each iteration: First, assuming that the stored energy level at each transmitter is stationary with a given distribution, the expected throughput maximization problem is formulated as an optimal stopping problem, whose solution is proved to exist and then derived for both models; second, for a fixed stopping rule, the energy level at each transmitter is shown to be stationary and an efficient iterative algorithm is proposed to compute its steady state distribution. Finally, we validate our analysis by numerical results and quantify the throughput gain compared with the best-effort delivery scheme.

- In the second part, an multi-channel scenario is studied. Particulary, the heterogeneous system, where small networks (e.g., small cell or WiFi) boost the system throughput under the umbrella of a large network (e.g., cellular systems), is a promising architecture for the next generation wireless communication networks, where green and sustainable communication is a key aspect. Renewable energy based communication via energy harvesting (EH) devices is one of such green tech-

nology candidates.

In this part, we study an uplink transmission scenario under such a heterogeneous network hierarchy, where each mobile user (MU) is powered by a sustainable energy supply, capable of both deterministic access to the large network via one private channel, and dynamic access to a small network with certain probability via one common channel shared by multiple MUs. Considering a general EH model, i.e., energy arrivals are time-correlated, we study an opportunistic transmission scheme and aim to maximize the average throughput for each MU, which jointly exploits the statistics and current states of the private channel, battery level, and EH rate, together with the availability of the common channel. Applying a simple yet efficient "save-then-transmit" scheme, the throughput maximization problem is cast as a "rate-of-return" optimal stopping problem. The optimal stopping rule is proved to has a time-dependent threshold-based structure for the case with general Markovian system dynamics, and degrades to a pure threshold policy for the case with independent and identically system dynamics. As performance benchmarks, the optimal power allocation scheme with conventional power supplies is also examined.

- Based on the above results, it is found that in EH networks, the multiuser diversity comes from not only the channel effect, but also from the dynamics of the stored energy. In the third part, we study multiuser diversity with respect to the energy availability. To facilitate the analysis, we eliminate the effect of fading channel by considering additive white Gaussian noise (AWGN) channel models only.

  We investigate the scaling of the available energy across all the users and the scaling of average throughput. Specifically, we reveal the throughput gain coming from the increase of total available energy harvested over time/space and from the combined dynamics of batteries. Considering both centralized and distributed access schemes,

the scaling of the average throughput over the number of transmitters is studied, along with the scaling of corresponding available energy in the batteries.

2. SINGLE-CHANNEL ACCESS: AD HOC WIRELESS NETWORKS*

2.1 Introduction

In this chapter, we focus on a typical ad hoc wireless network where multiple transmitter-receiver pairs share one common channel for communication purpose. To better distinguish the contribution of our study, it is helpful to briefly go over the existing literatures about the EH-based communication systems.

For the point-to-point wireless systems, the authors in [30] [44] considered the throughput maximization problem over a finite horizon for both the cases that the harvested energy information is non-causally and causally known to the transmitter, where the optimal solutions were obtained by the proposed one-dimension search algorithm and dynamic programming (DP) techniques, respectively. In [31], the authors extended the results to the classic three-node Gaussian relay channel with EH source and relay nodes, where the optimal power allocation algorithms were proposed. With a more practical circuit model by considering the half-duplex constraint of the battery, the authors in [40] proposed a save-then-transmit protocol, which divides each transmission frame into two parts: the first one for harvesting energy and the other for data transmission. For wireless networks with EH constraints, the authors in [33] investigated the performance of some standard medium access control protocols, e.g., TDMA, framed-Aloha, and dynamic-framed-Aloha.

In related works on *ad hoc* networking, opportunistic scheduling has been known as an effective method to utilize the wireless resource [4, 38, 58]. In particular, a distributed opportunistic scheduling (DOS) scheme was introduced in [65, 66], where only local

*©[2016] IEEE. Reprinted, with permission, from [Hang Li, Chuan Huang, Ping Zhang, Shuguang Cui, and Junshan Zhang, "Distributed opportunistic scheduling for energy harvesting based wireless networks: a two-stage probing approach." *Networking, IEEE/ACM Transactions on*, 24(3):1618–1631, June 2016]

channel state information (CSI) is available to each transmitter. By applying optimal stopping theory [20], it has been shown in [65, 66] that the optimal solution for the expected throughput maximization problem has a threshold-based structure. When channel estimation is imperfect, the authors in [55] proposed a two-level channel probing framework that allows the accessing transmitter to perform one more round of channel estimation before data transmission to improve the quality of estimated CSI and possibly increase the system throughput. The optimal scheduling policy of the two-level probing framework was proven to be threshold-based as well by referring to the optimal stopping with two-level incomplete information [53].

Different from the conventional energy supplies (e.g., non-rechargeable batteries, power grid) in the conventional networks [4, 38, 55, 58, 65, 66], we consider the network powered by energy harvesters that could generate electric energy from different renewable energy sources. Among various types of renewable energy sources, we consider two typical energy harvesting rate models in this chapter[1]:

1. *Constant energy harvesting rate model*: The EH rate (specifically, the amount of harvested energy per unit time) can be approximated as a constant within the entire time duration of interest. For example, the power variation coherence time of wind and solar EH systems is on the order of multiple seconds [7, 16], while the duration of one communication block is about several milliseconds. Thus, over thousands of communication blocks, the EH rate keeps almost the same.

2. *Independent and identically distributed (i.i.d.) energy harvesting rate model*: Compared to the constant rate model, the EH rate for this case changes much faster, i.e., comparable to the duration of one communication block. For example, the energy from light, thermal, kinetic, or ambient-radiation sources, usually changes every

[1] A more general case is that the transmitter only has causal information about EH rates, which could be modeled as a Markov process. This model has been used in the point-to-point wireless system [30, 44].

several milliseconds. Accordingly, EH rates can be modeled as an i.i.d. [33, 44] random process.

With the above two EH models, we investigate the DOS problem for a heterogeneous EH-based network, where the channel gains across different links and the EH rates across different transmitters are non-identical. The system works in a two-stage pattern as follows. In the first stage, all transmitters adopt random access and do channel probing (CP), during which the successful link can obtain the CSI via channel contentions, similar to those in [55,65,66]. In the second stage, the successful transmitter at the first stage has the option to spend certain time to harvest more energy, i.e., executes energy probing (EP); and then, with the updated energy state information (ESI), it decides either to transmit in the rest of the transmission block, or to stop probing and give up the channel. With EP, *since the total duration of the transmission block is fixed, although spending more time on harvesting energy could increase the energy level, it decreases the portion of the time for data transmission, which leads to a tradeoff to optimize*.

We propose a DOS framework for an *ad hoc* network powered by energy harvesters, which efficiently utilizes both the CSI and the ESI at each transmitter. In this framework, we adopt a "save-then-transmit" scheme, i.e., the transmitter keeps harvesting energy before it initiates the transmission that uses up all the available energy in the battery. Note that such a greedy power utilization scheme is suboptimal in general, while it is sensible when the number of transmitters is large.

The main contributions are summarized as follows:

1. First, by assuming that the battery state at each transmitter is stationary with a certain distribution, the throughput maximization problem for the considered network is cast as a rate-of-return problem. We prove the existence of the optimal stopping rules for both EP and CP, and further obtain:

- For the constant EH model, the optimal stopping rule of EP is determined by maximizing the throughput over the transmission block before starting EP, and it is either zero or a finite value according to the given CSI and ESI. Then, based on the stopping rule of EP, the optimal stopping rule of CP is shown to be a pure threshold policy (the threshold does not change over time) and the transmission decision is made right after each round of CP.
- For the i.i.d. EH model, the optimal stopping rule for EP is shown to be dynamic and threshold based, which is obtained by solving a stopping problem over a finite-time horizon. The stopping rule of CP is also threshold based and obtained based on the decision of EP, i.e., either transmit or start a new CP. Unlike the constant case, the transmission decision under i.i.d. EH model is made during the process of EP.

2. Next, with a fixed stopping rule, we show the existence of the steady-state distribution of the battery state by constructing a "super" Markov chain with its states being jointly determined by all transmitters. Moreover, we propose an efficient iterative algorithm to compute the steady-state distribution, executed at each transmitter in parallel. Particularly, it is shown that with the constant EH model, if the network consists of n transmitters and each one is with m possible energy states, the computational complexity for one iteration of the proposed algorithm is on the order of $O\left(n^2m^2\right)$, which is more efficient (when n and m are large) than that of the super Markov chain case, whose complexity for one iteration is on the order of $O\left(2m^{2n}\right)$.

3. Finally, by exploiting the structure of the rate-of-return problem, we show that the maximum throughput and the optimal scheduling strategy of the DOS framework could be obtained for both the two EH rate models, via one-dimension search by repeating the above two steps.

The rest of this chapter is organized as follows. Section 3.2.1 introduces the system model. In Section 3.2.2, the throughput maximization problem is formulated and solved under the assumption that the stationary distribution of the battery at each transmitter is known. Then, with the obtained stopping rule, we prove in Section 2.4 the existence of the steady-state distribution for each transmitter, and propose an iterative algorithm to compute it. Section 2.5 discusses the computation for the optimal throughput. In Section 2.6, numerical results are provided to validate our analysis and evaluate the throughput gain of our proposed scheduling scheme against the best-effort delivery. Finally, Section 2.7 concludes the chapter.

2.2 System Model

We consider a heterogeneous single-hop *ad hoc* network, where all the I transmitter-receiver pairs have independent but not necessarily identical statistical information of CSI and ESI. All pairs contend for one shared channel by random access. For each link, the transmitter is powered by a renewable energy source and utilizes a small rechargeable battery to temporally store the harvested energy. Note that the transmitter could keep harvesting energy until it initiates a data transmission. In addition, we do not consider the effect of inefficiency in energy storage and retrieval, nor the energy consumed other than data transmission, which can be approximately neglected by properly adjusting the energy model [30, 31, 33, 44]. Denote the duration of one channel contention as $l > 0$, and the length of one transmission block as L, which is an integer multiple of l.

As illustrated in Fig. 2.1, the DOS procedure of the whole network takes place in two stages: First, each transmitter probes the channel via random access and harvests energy at the same time; and then the successful transmitter may start the EP (to potentially increase the average transmission rate over the transmission block[2]) before the data transmission

[2]If the successful transmitter experiences a bad channel condition and a low energy level, it may skip the transmission.

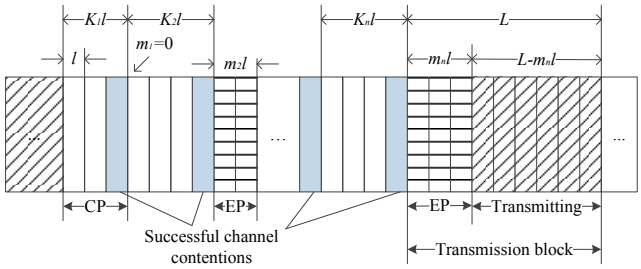

Figure 2.1: One realization for the DOS with two-stage probing.

process.

2.2.1 Channel Probing

In the first stage, a successful channel contention is defined as follows: All transmitters first independently contend for the channel until there is only one contending in a particular time slot. Furthermore, one round of CP is defined as the process to achieve one successful channel contention. Denote the probability that transmitter i contends for the channel as q_i, $1 \leq i \leq I$, with $0 \leq q_i \leq 1$. As such, the probability that the i-th transmitter successfully occupies the channel is given by $Q_i = q_i \prod_{j \neq i}(1-q_j)$. Then, the probability to achieve one successful channel contention at each time slot is given by $Q = \sum_{i=1}^{I} Q_i$, and it is easy to check that $Q \leq 1$ [1]. Accordingly, for the n-th round of CP, $n \geq 1$, we use K_n to denote the number of time slots needed to achieve a successful channel contention, which is a random variable and satisfies the geometric distribution with parameter Q [55, 65, 66]. In this way, the expected duration of one round of CP is given as l/Q. Denote the transmitted signal at transmitter i as x^i, and the received signal y^i is thus given by $y^i = h^i x^i + z^i$, where h^i is the complex channel gain and z^i is the circularly symmetric complex Gaussian (CSCG) noise with zero mean and variance σ^2 at the receiver. Across different links, $\{h^i\}_{1 \leq i \leq I}$ are independent with finite mean and variance, while not necessarily identically distributed. After one round of CP, the successful transmitter can perfectly estimate the

corresponding channel gain via certain feedback mechanisms, and thus h^i is assumed a known constant during the whole transmission block. After CP, the successful transmitter chooses one of the following actions based on its local CSI and ESI:

(a) releases the channel (if the CSI and ESI indicate that the transmission rate is lower than a threshold) and let all links re-contend; or

(b) directly transmits until the end of the transmission block; or

(c) holds the channel, starts EP.

Note that to complete one data transmission, it may take n rounds of CPs as depicted in Fig. 2.1. It is worth noting that each transmitter keeps harvesting energy until it starts a transmission, and after each round of CP, only the successful transmitter makes a choice among three actions as listed above.

2.2.2 Energy Probing

When the successful transmitter decides not to take action (a) or (b) defined above, it starts the second stage EP, i.e., action (c), to obtain more energy. During this stage, the transmitter chooses to continue harvesting energy slot by slot, and then ends EP by action (a) or (b), i.e., either releasing the channel or transmitting over the rest of the transmission block. As it is depicted in Fig. 2.1, one transmission is fulfilled with n rounds of CPs and m_n extra slots of EP.

For transmitter i, let $B^i_{n,m} \in \mathbf{\Delta}$ denote the energy level of the battery after the n-th round of CP and m additional time slots for EP, where $\mathbf{\Delta} = \{0, \delta, 2\delta, \cdots, B_{max}\delta\}$ is the set of all possible energy states, with δ being the minimum energy unit and $B_{max}\delta$ the capacity of the battery. We use E^i_t to denote the EH rate of transmitter i at time t. As noted in the previous section, we consider the following two types of scenarios:

1. *Constant EH rate model*: $\{E^i_t\}_{t\geq 1}$ are constants for each i, i.e., $E^i_t = E^i \in \mathbf{\Delta}$ for all $t \geq 1$, and $\{E^i\}$ can thus be learned and assumed non-causally known before

transmissions.

2. *I.i.d EH rate model*: The EH rates among different transmitters are independent. For transmitter i, $\{E_t^i\}_{t\geq 1}$ are i.i.d. across t, with finite mean and the probability mass function (PMF) $\Pr\{E_t^i = e\delta\} = F^i(e)$, where $e \in \{0, 1, 2, \cdots\}$.

Under the save-then-transmit scheme, the energy level will keep non-decreasing and drop to zero after the transmission, which forms a Markov chain (as described in Section 2.4 later). Thus, the energy level $B_{n,m}^i$ can be written as

$$B_{n,m}^i = \min\left\{B_{n,0}^i + l\sum_{k=0}^{m} E_k^i, B_{max}\delta\right\}, \tag{2.1}$$

where $n \geq 1$, $0 \leq m \leq L/l$, and $\min\{x, y\}$ denotes the smaller value between two real numbers x and y. Note that $B_{n,0}^i$ indicates the energy level after the successful contention round before taking any action. If $m = 0$, i.e., transmitter i does not do EP, we let $\sum_{k=0}^{m} E_k^i = E_0^i = 0$.

2.3 Transmission Scheduling

In this section, we target to derive the optimal scheduling policy that maximizes the average throughput for the considered network with the proposed two-stage access strategy, conditioned on the given battery state distribution. We point out that the results obtained in this section are based on the assumption that the energy level at transmitter i is stationary with a given distribution Π^i, for $1 \leq i \leq I$, which will be validated in Section 2.4.

2.3.1 Problem Formulation

After the n-th round of CP and m additional time slots, the CSI and the ESI at the successful transmitter are given as $\mathcal{F}_{n,m}^i = \left\{h_n^i, B_{n,m}^i\right\}$. Note that the channel gain h_n^i is now indexed by n, which is determined at the end of the n-th round of CP and assumed

fixed during the whole data transmission block. In particular, $\mathcal{F}_{n,0}^i = \left\{h_n^i, B_{n,0}^i\right\}$ denotes the initial information right after the n-th round of CP. For convenience, we omit the index i for either the CSI or the ESI in the sequel, and retrieve it when necessary.

By adopting the save-then-transmit scheme at the transmitters to fully take advantage of each channel use, the transmission rate over L/l time slots with state $\mathcal{F}_{n,m}$ is defined as

$$R_n(m) = \left(1 - \frac{ml}{L}\right) \log\left(1 + |h_n|^2 \frac{B_{n,m}}{(L - ml)\sigma^2}\right). \tag{2.2}$$

When $ml = L$, we set $R_n(m) = 0$ since there is no transmission in this case.

Remark 2.3.1 Some important properties of $R_n(m)$ are listed as follows.

- $\mathbb{E}\left[R_n(m)\right] < \infty$ *and* $\mathbb{E}\left[(R_n(m))^2\right] < \infty$*, which results from the fact that h_n has finite mean and variance and the energy level $B_{n,m}$ is also finite.*

- $\{R_n(m)\}_{n\geq 1}$ *are approximately independent random variables over n. To see this, recall that the channel gains and the battery states are independent across different transmitters at a given time slot; moreover, the probability is small for a transmitter to occupy the channel in two consecutive contentions when the number of user pairs is large. For example, in an* ad hoc *network with K pairs where each pair fairly competes for the channel use with probability $1/K$, such a probability is $\frac{1}{K^2}(1 - 1/K)^{2(K-1)}$ [1], which is as small as 0.0625 even when $K = 2$. Thus, $\{\mathcal{F}_{n,m}\}_{n\geq 1}$ are nearly independent over n, which implies that $\{R_n(m)\}_{n\geq 1}$ are independent over n.*

Let N be the stopping rule for CP, and M_n be the stopping rule for EP associated with the n-th CP for $1 \leq n \leq N$, which together tell the transmitter when to start the data transmission. Then, under these stopping rules, the transmission rate would be $R_N(M_N)$, and we let T_N be the total time duration for completing one data transmission. Here,

T_N contains the duration of $N-1$ rounds of CP, which is given by $l\sum_{n=1}^{N-1} K_n$, and $l\sum_{n=1}^{N-1} M_n$ time slots in which the transmitter probes the energy but gives up the channel after EP. Also, after the N-th round of CP with the time $K_N l$, the transmitter may use M_N slots for the EP and transmit within the duration $L - M_N l$ afterwards. Accordingly, we obtain

$$T_N = l\sum_{n=1}^{N-1} M_n + l\sum_{n=1}^{N} K_n + L. \tag{2.3}$$

If such a process is executed J times with $R_{N_j}(M_{N_j})L$ bits transmitted at each transmission, $1 \le j \le J$, we obtain the average throughput λ per transmission of the network:

$$\frac{L\sum_{j=1}^{J} R_{N_j}(M_{N_j})}{\sum_{j=1}^{J} T_{N_j}} \longrightarrow \lambda = \frac{L\mathbb{E}\left[R_N(M_N)\right]}{\mathbb{E}\left[T_N\right]} \text{ a.s.}$$

as $J \to \infty$ by the renewal theory [9]. Again, we point out that the energy level is stationary at the N_j-th round of CP for $j \ge 1$, as we assumed.

Our target is to maximize λ by adjusting the stopping rule N and $\{M_n\}_{1\le n\le N}$. It is easy to see that maximizing λ is in fact a "rate-of-return" stopping problem [20, 21] (for which the specific definition is given later). Instead of directly solving this problem, we examine the "net reward" of the considered network, which is given as

$$\begin{aligned} r_N(\lambda) &= R_N(M_N)L - \lambda T_N \\ &= (R_N(M_N) - \lambda)L - \lambda l\left[K_N + \sum_{n=1}^{N-1}(K_n + M_n)\right], \end{aligned} \tag{2.4}$$

for some $\lambda > 0$. The term $(R_N(M_N) - \lambda)L$ can be interpreted as the reward of transmission, $\lambda l K_n$ as the cost of CP, and $\lambda l M_n$ as the cost of failed EP for $1 \le n \le N-1$. We set $r_{-\infty}(\lambda) = -\infty$ since it is irrational that the system does not send any data forever. Then,

we define the maximum value of the expected net reward with $\lambda > 0$ as

$$S^*(\lambda) = \sup_{N \in \mathcal{N}, \{M_n\}_{1 \le n \le N}} \mathbb{E}\left[r_N(\lambda)\right], \tag{2.5}$$

where $\sup(\cdot)$ denotes the least upper bound for a set of real numbers, and

$$\begin{aligned} \mathcal{N} \triangleq \{N : N \ge 1,\ \mathbb{E}\left[T_N\right] < \infty, \\ \text{for } M_n \in [0, L/l] \text{ with } 1 \le n \le N\}. \end{aligned} \tag{2.6}$$

Remark 2.3.2 One important property of problem (2.5) is time invariance. We observe that before the system starts the N-th round of CP, the accumulated cost $\lambda l \sum_{n=1}^{N-1} (K_n + M_n)$ over the past $N-1$ rounds of CP has already been finalized, with no need to be further considered in the remaining decision process. Moreover, $\{R_n(M_n)\}_{1 \le n \le N}$ are independent over n as we mentioned before; it follows that the expected optimal reward before the N-th round of CP is the same as that of any previous round of CP. In other words, the system can obtain the expected optimal reward $S^*(\lambda)$ whenever a new round of CP is about to start. Therefore, we conclude that problem (2.5) is time invariant.

Recall from Section 3.2.1 that after each round of CP, the successful transmitter will choose one of three actions (i.e., transmitting, giving up the channel, or starting EP) according to the stopping rule of CP, which needs the expected reward of EP depending on the stopping rule of EP. Thus, we will first introduce the formulation and the optimal stopping rule for EP, and then for CP.

2.3.1.1 Formulation for EP

When the successful transmitter starts EP after the n-th round of CP, where $1 \le n \le N$, it will end up with one of the two actions: transmitting or giving up the channel without transmission. Specifically, we define the expected optimal reward at the k-th slot of EP,

$0 \leq k \leq L/l$, as

$$U_k(\mathcal{F}_{n,k}) = \max_{k \leq M_n \leq L/l} \mathbb{E}\left[\max\left\{(R_n(M_n) - \lambda)L, \right.\right. \\ \left.\left. -\lambda l M_n + S^*(\lambda)\right\} \mid \mathcal{F}_{n,k}\right], \tag{2.7}$$

where $-\lambda l M_n + S^*(\lambda)$ is the expected value of giving up the channel after M_n slots of EP. If $k = 0$, $U_0(\mathcal{F}_{n,0})$ denotes the maximum of the expected net reward right after the n-th round of CP. In other words, we want to find the optimal stopping rule M_n^* of EP which attains

$$U_0(\mathcal{F}_{n,0}) = \max_{0 \leq M_n \leq L/l} \mathbb{E}\left[\max\left\{(R_n(M_n) - \lambda)L, \right.\right. \\ \left.\left. -\lambda l M_n + S^*(\lambda)\right\} \mid \mathcal{F}_{n,0}\right]. \tag{2.8}$$

Note that M_n^* exists since problem (2.8) is an optimal stopping problem over a finite time horizon [20, 45].

2.3.1.2 Formulation for CP

By choosing $\{M_n^*\}_{1 \leq n \leq N}$, we define

$$\lambda^* = \sup_{N \in \mathcal{N}} \frac{L\mathbb{E}\left[R_N(M_N^*)\right]}{\mathbb{E}\left[T_N\right]},\ N^* = \arg\sup_{N \in \mathcal{N}} \frac{L\mathbb{E}\left[R_N(M_N^*)\right]}{\mathbb{E}\left[T_N\right]}. \tag{2.9}$$

Note that if the optimal stopping rule $N^* \notin \mathcal{N}$, we would claim that N^* does not exist. Thus, λ^* is the optimal average throughput of the original rate-of-return problem.

The connection between the transformed problem (2.5) and the original problem (2.9) is introduced in the following lemma. It is worth noticing that with the optimal stopping rule $\{M_n^*\}_{1 \leq n \leq N}$ for EP, problem (2.5) boils down to a one-level stopping problem with stopping rule N.

Lemma 2.3.1 (i) If there exists λ^* such that $S^*(\lambda^*) = 0$, this λ^* is the optimal throughput defined in (2.9). Moreover, if $S^*(\lambda^*) = 0$ is attained at $N^*(\lambda^*)$, the stopping rule N^* defined in (2.9) is the same as $N^*(\lambda^*)$, i.e., $N^* = N^*(\lambda^*)$.

(ii) Conversely, if (2.9) is true, there is $S^*(\lambda^*) = 0$, which is attained at N^* given by (2.9).

This lemma directly follows Theorem 1 in Chapter 6 of [20].

The next proposition secures the existence of the optimal stopping rule for CP.

Proposition 2.3.1 With the EP stopping rule $\{M_n^*\}_{0\leq n\leq N}$, the optimal stopping rule $N^*(\lambda)$ for problem (2.5) exists. Moreover, for $N \geq 1$, the following equation holds

$$S^*(\lambda) = U_0(\mathcal{F}_{N,0}) - \lambda l K_N. \tag{2.10}$$

The proof is given in Appendix A.

Remark 2.3.3 The equation (2.10) is obtained from the optimality equation of the CP. The calculation of the optimal throughput relies on this equation, which will be shown in Section 2.5.

Now, we are ready to derive the optimal stopping rules N^* and $\{M_n^*\}$ that jointly maximize the expected value of $r_N(\lambda)$ for the two different EH models. As we mentioned above, the stopping rule N for CP relies on the form of M_N (the stopping rule for EP). We will find the optimal stopping rule M_N^* before N^*. After obtaining the forms of the optimal stopping rules, the calculation for the optimal throughput will be discussed.

2.3.2 Optimal Stopping Rule for Constant EH Model

For notation simplicity, we omit the index N of CP when we derive the stopping rule M in this subsection. Then, we will derive the stopping rule N based on the results of EP.

When the EH rate is constant, the transmission rate $R(M)$ is deterministic for a given $\mathcal{F}_0$ over the transmission block. Then, we obtain a simplified version of $U_0(\mathcal{F}_0)$ (2.8) as

$$U_0(\mathcal{F}_0) = \max_{0\le M\le L/l} \max\left\{(R(M)-\lambda)L, -\lambda l M + S^*(\lambda)\right\}.$$

The value of $U_0(\mathcal{F}_0)$ can be obtained simply by comparing $-\lambda l M + S^*(\lambda)$ and $(R(M)-\lambda)L$, whose values can be computed individually. Clearly, the first one achieves its maximum $S^*(\lambda)$ at $M=0$. For the second term, only $R(M)$ is changing over M with a given $\mathcal{F}_0$. Therefore, we settle down to the following auxiliary problem:

$$V^* = \arg \max_{0\le V\le L/l} R(V). \tag{2.11}$$

Then, we could use the optimal V^* to find M^* without difficulty. Note that when $Vl = L$, it follows that $R(V) = 0$ according to our definition in Section 3.2.1, which implies that $V = L/l$ cannot be optimal, and thus we take $0 \le V \le L/l - 1$. We first consider a related continuous version of $R(V)$ by relaxing Vl/L as ρ, $0 \le \rho < 1$:

$$\begin{aligned}\max_{0\le\rho<1} R(\rho) = &\max_{0\le\rho<1}(1-\rho)\\ &\cdot \log\left(1+|h|^2\frac{\min\{B_0+\rho LE, B_{max}\delta\}}{(1-\rho)L\sigma^2}\right).\end{aligned} \tag{2.12}$$

After solving (2.12), we will show how to obtain the optimal solution of problem (2.11).

First, we establish some properties for the objective function of problem (2.12).

Proposition 2.3.2 For arbitrary $a, b \ge 0$, we have that

1. *the function $y(x) = (1-x)\log\left(1+\frac{a+bx}{1-x}\right)$ is concave over $[0,1)$, and $\lim_{x\to 1^-} y'(x) < 0$;*
2. *the function $g(x) = (1-x)\log\left(1+\frac{a}{1-x}\right)$ is concave and non-increasing over $[0,1)$.*

The proof is given in Appendix A.

Since $\rho \in [0, 1)$, when $\frac{B_{max}\delta - B_0}{LE} \geq 1$, $R(\rho)$ is simply concave over ρ on $[0, 1)$ according to part 1) of Proposition 2.3.2. When $\frac{B_{max}\delta - B_0}{LE} < 1$, according to Proposition 2.3.2, $R_N(\rho)$ is concave over $\left[0, \frac{B_{max}\delta - B_0}{LE}\right]$, and is non-increasing on $\left[\frac{B_{max}\delta - B_0}{LE}, 1\right)$. Thus, $R(\rho)$ cannot achieve its maximum on $\left(\frac{B_{max}\delta - B_0}{LE}, 1\right)$. Therefore, we treat this fact as a new constraint over ρ, and rewrite problem (2.12) as

$$\begin{aligned} &\max G(\rho) = \max (1-\rho) \log \left(1 + |h|^2 \frac{B_0 + \rho LE}{(1-\rho) L\sigma^2}\right) \\ &\text{s.t. } B_0 + \rho LE \leq B_{max}\delta,\ 0 \leq \rho < 1. \end{aligned} \tag{2.13}$$

Next, we establish the following proposition to solve problem (2.13), where the obtained solution is optimal for problem (2.12) as well.

Proposition 2.3.3 The optimal solution ρ^* for problem (2.13) is given by:

$$\rho^* = \begin{cases} \min\left\{\rho_0, \frac{B_{max}\delta - B_0}{LE}\right\}, & \textit{when } \frac{C+D}{1+C} \geq \log(1+C); \\ 0, & \textit{otherwise,} \end{cases}$$

where $C = \frac{|h|^2 B_0}{L\sigma^2}$, $D = \frac{|h|^2 E}{\sigma^2}$, and ρ_0 is the unique solution for the equation $\log\left(1 + \frac{C+D\rho}{1-\rho}\right) = \frac{C+D}{1-\rho+C+D\rho}$ when $\frac{C+D}{1+C} \geq \log(1+C)$.

The proof is given in Appendix A.

Based on the optimal solution ρ^*, the optimal V^* for $R(V)$ in (2.11) can be obtained easily: We only need to compare $R(\lfloor \rho^* L/l \rfloor)$ against $R(\lceil \rho^* L/l \rceil)$, and V^* should attain the larger value. Specifically, we have the following result.

Proposition 2.3.4 The optimal V^* of the problem (2.11) is given by

$$V^* = \begin{cases} \lfloor \rho^* L/l \rfloor, & \text{if } R(\lfloor \rho^* L/l \rfloor) \geq R(\lceil \rho^* L/l \rceil); \\ \lceil \rho^* L/l \rceil, & \text{if } R(\lceil \rho^* L/l \rceil) > R(\lfloor \rho^* L/l \rfloor); \\ 0, & \text{otherwise.} \end{cases} \tag{2.14}$$

where ρ^* is obtained by Proposition 2.3.3. Thus, the optimal stopping rule M^* is given by

$$M^* = \begin{cases} 0, & \text{if } (R(V^*) - \lambda)L < S^*(\lambda); \\ V^*, & \text{otherwise.} \end{cases} \tag{2.15}$$

The optimal reward $U_0(\mathcal{F}_0)$ with constant EH rate model is

$$U_0(\mathcal{F}_0) = \max\left\{(R(V^*) - \lambda)L, S^*(\lambda)\right\}. \tag{2.16}$$

Next, the following proposition formally quantifies the optimal stopping rule N^* and the equation to compute the optimal throughput λ^*.

Proposition 2.3.5 The optimal stopping rule to solve problem (2.5) is given by

$$N^* = \min\left\{n \geq 1 : R_n(V^*) \geq \lambda^*\right\}, \tag{2.17}$$

with V^* given in Proposition 2.3.4. Moreover, λ^* satisfies the following equation

$$\sum_{i=1}^{I} Q_i \mathbb{E}\left[\left(R^i\left(V^*\right) - \lambda^*\right)^+\right] = \frac{\lambda^* l}{L}, \tag{2.18}$$

where the function $(x)^+$ means $\max\{x, 0\}$ for some real number x, and Q_i is the probability of a successful channel contention at transmitter i, defined in Section 3.2.1. The index n for $R^i\left(V^*\right)$ in (2.18) is removed since $\{R_n\left(V^*\right)\}_{n\geq 1}$ are ergodic for $1 \leq i \leq I$.

Proof: Following (2.16) in Proposition 2.3.4, the stopping rule N^* has the form

$$N^* = \min\left\{n \geq 1 : (R_n(V^*) - \lambda^*)L \geq S^*(\lambda^*)\right\}. \tag{2.19}$$

Thus, we can obtain N^* by plugging $S^*(\lambda^*) = 0$ into (2.19), which results in (2.17). Finally, equation (2.18) can be obtained by plugging $S^*(\lambda^*) = 0$ into (2.10) and taking the expectation on both sides. ■

Remark 2.3.4 Note that the stopping rule (2.19) implies that each transmitter has the same threshold that is globally determined even when all transmitters have different statistics of the CSI and ESI. The intuition is similar to that in [65]: In order to guarantee the overall system performance, the transmitter with a bad channel condition and a low energy level should "sacrifice" its own reward, while the one with good conditions should transmit more data.

Directly following Propositions 2.3.4 and 2.3.5, the next proposition gives the DOS under the constant EH model.

Proposition 2.3.6 After the n-th round of CP, it is optimal for the successful transmitter to take one of the following two options:

1. *release the channel immediately if $R_n(V^*) < \lambda^*$ (which is equivalent to $M^* = 0$), and let all transmitters perform the next round of CP;*
2. *otherwise, transmit after V^* slots for EH, where V^* is given by Proposition 2.3.4.*

2.3.3 Optimal Stopping Rule for i.i.d. EH Model

Similarly as in the previous subsection, we first consider problem (2.8) to find the optimal stopping rule M^*, then the optimal stopping rule N^* afterwards.

Under the i.i.d. EH model, $U_0(\mathcal{F}_0)$ has the form in (2.8). As we mentioned in Section 2.3.1, it is a finite-horizon stopping problem [20, 45], and the solution of problem (2.8) could be directly generalized in the next proposition.

Proposition 2.3.7 For $0 \leq k \leq L/l$ *and some* $\lambda > 0$*, the* optimality equation *for problem (2.8) is given by*

$$U_k(\mathcal{F}_k) = \max\{(R(k) - \lambda)L, -\lambda kl + S^*(\lambda), \mathbb{E}[U_{k+1}(\mathcal{F}_{k+1}) \mid \mathcal{F}_k]\}, \tag{2.20}$$

and the optimal stopping rule has the following form:

$$M^* = \min\{0 \leq k \leq L/l : U_k(\mathcal{F}_k) = \max\{(R(k) - \lambda)L, -\lambda kl + S^*(\lambda)\}\}. \tag{2.21}$$

The stopping rule M^* given in (2.21) suggests that the EP would stop at M^* by either transmitting or giving up the channel, which also indicates the final decision for the current round of CP. Thus, the optimal stopping rule N^* could be obtained by reorganizing (2.21).

Proposition 2.3.8 The optimal stopping rule of CP under the i.i.d. EH model has the form as:

$$N^* = \min\{n \geq 1 : U_{M^*}(\mathcal{F}_{n,M^*}) = (R_n(M^*) - \lambda^*)L\}, \tag{2.22}$$

where M^* *is the optimal stopping rule of EP given in Proposition 2.3.7. The optimal throughput* λ^* *satisfies the following equation*

$$\sum_{i=1}^{I} Q_i \mathbb{E}\left[\mathbb{E}\left[\max\{R^i(M^*) - \lambda^*, -\lambda^* M^* l/L\} \mid \mathcal{F}_0\right]^+\right] = \frac{\lambda^* l}{L}. \tag{2.23}$$

The proof is analogous to the constant EH rate case, which is omitted here.

The next proposition, which directly follows Propositions 2.3.7 and 2.3.8, concludes the overall DOS under i.i.d. EH model.

Proposition 2.3.9 After the n-th round of CP, it is optimal for the successful transmitter to take one of the following two options:

1. *if* $\max\{(R_n(0)-\lambda^*)L, \mathbb{E}[U_1(\mathcal{F}_{n,1}) \mid \mathcal{F}_{n,0}]\} < 0$*, release the channel immediately and let all transmitters start the next round of CP.*

2. *otherwise, start EP following the optimal stopping rule M_n^* given in Proposition 2.3.7.*

Remark 2.3.5 Propositions 2.3.6 and 2.3.9 summarize the DOS under the constant and i.i.d. EH models, respectively. We observe that under the constant EH model, the EP could be "forecasted" by finding the optimal V^*; then the decision of transmission would be made before starting EP. On the contrary, when the EH rates are i.i.d., such decision can only be made step by step during the EP.

2.4 Battery Dynamics

In this section, we validate the assumption made in Section 3.2.2 that the energy level at each transmitter is stationary with some distribution. Firstly, we show that under the constant EH model, the energy level stored at each transmitter forms a Markov chain over time, while the state transition probabilities for different transmitters are coupled together. However, we propose an iterative algorithm to compute the corresponding steady-state distribution, which is shown converging to the global optimal point. Then, we extend our analysis to the case with i.i.d. EH rate model.

2.4.1 Battery with Constant EH Model

Note that after CP, if the successful transmitter releases the channel immediately, then the next round of CP starts, and the battery continues to be charged. If the transmitter starts

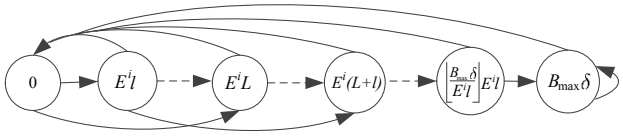

Figure 2.2: State transition of the energy level under the constant EH rate model.

the transmission, its energy level will become zero at the end of the transmission block according to Section 3.2.1. During this time, all other transmitters will keep harvesting energy within this period. Thus, the energy level transition over the transmission block can be determined. To simplify our analysis, the transmission block is treated as one time slot with length L for the purpose of counting battery state transitions. In addition, we assume that the battery works in half-duplex mode, i.e., it cannot be charged when the transmitter transmits data.

For transmitter i with EH rate E^i, $1 \leq i \leq I$, the set of its energy states is given by $B_t^i \in \mathbf{\Delta}_i = \left\{0, E^i l, 2E^i l \cdots, \left\lfloor \frac{B_{max}\delta}{E^i l} \right\rfloor E^i l, B_{max}\delta \right\}$, where $t \geq 1$ is the slot index. The state transition is depicted in Fig. 2.2. In addition, we denote the distribution of the energy level for transmitter i at time t as $\Pi_t^i = \left[\pi_{t,0}^i \cdots \pi_{t,B_{max}}^i\right]$.

Next, we consider the state transition probability. Suppose that transmitter i is at energy level $u_i \in \mathbf{\Delta}_i$, there are three events that may happen at time slot t:

(i) It occupies the channel and transmits. According to Section 3.2.1, transmitter i consumes all the energy for the transmission, and transfers to the energy level 0 after the transmission. Thus, the transition probability is given by

$$p_{u_i,0}^i = Q_i p_{tr}^i(u_i), \tag{2.24}$$

where Q_i is the probability that the i-th transmitter occupies the channel, and $p_{tr}^i(u_i)$ is the probability that it successfully transmits with the energy level u_i. Furthermore, according

to (2.17), $p_{tr}^{i}(u_i)$ can be computed as

$$\begin{aligned} p_{tr}^{i}(u_i) &= \mathbb{P}\left\{R^i(V^*) \geq \lambda^*\right\} \\ &= \mathbb{P}\left\{\log\left(1+|h^i|^2\frac{u_i+V^*lE^i}{(L/l-V^*)l\sigma_i^2}\right) \geq \frac{\lambda^*}{1-\frac{V^*l}{L}}\right\}, \end{aligned} \tag{2.25}$$

where V^* is defined by (2.14) in Proposition 2.3.4. Note that in (2.25), $|h^i|^2$ is the only random variable and its distribution is known.

(ii) Other transmitters occupy the channel and transmit. If anyone among the other $I-1$ transmitters sends data, transmitter i will harvest E^iL units of energy during this period, and then attain level $v_i = \min\{u+E^iL, B_{max}\delta\}$. Suppose that the j-th transmitter transmits. Similar to the first case, the probability of transmission performed by the j-th transmitter is given by $Q_j\sum_{b=0}^{B_{max}}\pi_{t,b}^{j}p_{tr}^{j}(bE^jl)$, where $bE^jl \in \mathbf{\Delta}_j$ and thus $b \in \left\{0,1,2,\cdots,\left\lfloor\frac{B_{max}\delta}{E^jl}\right\rfloor, B_{max}\right\}$. Since there are in total $I-1$ transmitters, the transition probability for the transmitter i from level u_i to v_i is given by

$$p_{u_i,v_i}^{i} = \sum_{j\neq i}Q_j\sum_{b=0}^{B_{max}}\pi_{t,b}^{j}p_{tr}^{j}(bE^jl). \tag{2.26}$$

(iii) No transmission happens. In this case, transmitter i just harvests E^il units of the energy and goes into state $w_i = \min\{u_i+E^il, B_{max}\delta\}$. The probability of this case happening can be directly obtained as

$$p_{u_i,w_i}^{i} = 1 - p_{u_i,0}^{i} - p_{u_i,v_i}^{i}. \tag{2.27}$$

Note that when $\widetilde{u}_i = v_i = w_i$, the transition probability is just given by

$$\begin{aligned} p^i_{u_i,\widetilde{u}_i} &= p^i_{u_i,v_i} + p^i_{u_i,w_i} \\ &= p^i_{u,v_i} + 1 - p^i_{u_i,0} - p^i_{u_i,v_i} \\ &= 1 - p^i_{u_i,0}. \end{aligned} \tag{2.28}$$

In this way, we can compute all $\{p^i_{u_i,\widetilde{u}_i}\}$ for $1 \leq i \leq I$, where $u_i \in \mathbf{\Delta}_i$ and $\widetilde{u}_i \in \{0, v_i, w_i, B_{max}\delta\}$. The transition probability matrix is nothing but $\mathbf{P}^i_t = \{p^i_{u_i,\widetilde{u}_i}\}$ with dimension $\left(\lceil \frac{B_{max}\delta}{E^i l} \rceil + 1\right) \times \left(\lceil \frac{B_{max}\delta}{E^i l} \rceil + 1\right)$. Obviously, $\mathbf{P}^i_t$ is a stochastic matrix, i.e, a square matrix in which all elements are nonnegative and the row sum is 1. However, $\mathbf{P}^i_t$ depends on t since $p^i_{u_i,v_i}$ depends on the state distribution Π^j_t for all $j \neq i$. Therefore, $\{B^i_t\}_{t\geq 0}$ is a non-homogeneous Markov chain, whose state evolution is given by

$$\Pi^i_{t+1} = \Pi^i_t \mathbf{P}^i_t, \ t \geq 0. \tag{2.29}$$

We propose Algorithm 2.1, which is summarized in Table I, to compute the steady-state distribution for all transmitters. Here, the infinity norm is applied, which is defined as $\| \mathbf{a} \|_\infty = \max_{1\leq i\leq n} |a_i|$ for $\mathbf{a} = [a_1 \ \cdots a_n]$.

Proposition 2.4.1 For any given initial state distribution Π^i_0, $\Pi^i_t = \left[\pi^i_{t,0} \cdots \pi^i_{t,B_{max}}\right]$ *that is generated by Algorithm 2.1, converges to a unique steady-state distribution* Π^i *for all* $1 \leq i \leq I$.

The proof is given in Appendix A.

Remark 2.4.1 The steady-state distribution for all transmitters can be obtained by the iterative computation $\mathbf{\Pi}_{t+1} = \mathbf{\Pi}_t \mathbf{P}$ *over the "super" Markov system as well, which is constructed in Appendix D. However, this is not as efficient as Algorithm 2.1. From the*

Table 2.1: Algorithm 2.1: Compute the steady-state distribution for all transmitters.

- Initialize Π_0^i for $1 \leq i \leq I$, ε, and compute $p_{u_i,0}^i$ by (2.24) for all $u_i \in \mathbf{\Delta}_i$ and $1 \leq i \leq I$;
- Set $t = 0$, compute $\mathbf{P}_0^i$ by (2.26)–(2.28) for all $1 \leq i \leq I$, and compute Π_1^i by (2.29) for all $1 \leq i \leq I$. Then:
  - While $\max_{1 \leq i \leq I} \parallel \Pi_{t+1}^i - \Pi_t^i \parallel_\infty > \varepsilon$, repeat:
    1. $t = t + 1$;
    2. Update $\mathbf{P}_t^i$ by (2.26)–(2.28) for all $1 \leq i \leq I$;
    3. Compute Π_{t+1}^i by (2.29) for all $1 \leq i \leq I$;
  - end.
- Algorithm ends.

computational complexity point of view, suppose that each transmitter has m energy levels, and there are n transmitters in total. The number of the states in the "super" Markov chain is m^n. If there is only one processer, the floating-point calculation for one iteration of the state distribution for the "super" Markov chain is approximately on the order of $O\left(2m^{2n}\right)$. On the contrary, by using Algorithm 2.1, (2.26) requires n^2m^2 calculations, and updating $\{\mathbf{P}_t^i\}$ requires about nm calculations according to (2.27). In addition, $\{\Pi_t^i \mathbf{P}_t^i\}$ requires $2nm^2$ calculations. Overall, one iteration for all transmitters is approximately on the order of $O\left(n^2m^2\right)$, which is more efficient than the case for the "super" Markov chain especially when m and n are large. Moreover, our algorithm can also be operated in a parallel way, i.e., computing $\Pi_{t+1}^i = \Pi_t^i \mathbf{P}_t^i$ for $1 \leq i \leq n$ at the same time over different cores.

2.4.2 Battery with i.i.d. EH Model

The argument that the battery state evolves as a Markov process for the random case is analogous to that of the constant case in the previous subsection. The main difference

is that the probability $p_{tr}^i(u_i)$ defined by (2.25) is changed, which needs to be further developed under the i.i.d. EH rate model.

We now consider the calculation of $p_{tr}^i(u_i)$. When transmitter i grabs the channel with energy level u_i, according to the stopping rule M^* (2.21) and N^* (2.22), the transmitter checks the condition $\max\{(R(0)-\lambda)L, -\lambda l + \mathbb{E}[U_1(\mathcal{F}_1) \mid \mathcal{F}_0]\} \geq 0$. If it is true, the transmitter starts EP until the M^*-th slot and transmits when $(R(M^*)-\lambda^*)L \geq -\lambda^* M^* l$ according to (2.22). Specifically, given $U_0(u_i, |h^i|^2) \geq 0$, the transmitter continues EP at slot k for $0 \leq k \leq M^*-1$, which is equivalent to $\max\{(R(k)-\lambda^*)L, -\lambda^* kl\} < \mathbb{E}[U_{k+1}(\mathcal{F}_{k+1}) \mid \mathcal{F}_k]$, where $\mathcal{F}_k = \{u_i + l\sum_{j=0}^k E_j^i, |h^i|^2\}$. Then, at slot $M^* = m \leq L/l$, the transmitter stops EP and transmits when $(R(m)-\lambda^*)L \geq \max\{-\lambda^* ml, \mathbb{E}[U_{m+1}(\mathcal{F}_{m+1}) \mid \mathcal{F}_m]\}$. Thus, we obtain

$$p_{tr}^i(u_i) = \int_0^\infty \mathbb{P}\left\{\text{Transmits at } M^* \mid U_0(u_i, d|h^i|^2) \geq 0\right\} \cdot \mathbb{P}\left\{U_0(u_i, d|h^i|^2) \geq 0\right\} f(|h^i|^2) d|h^i|^2, \tag{2.30}$$

where $f(|h^i|^2)$ is the probability density function (PDF) of the channel power gain. The probability $\mathbb{P}\{U_0(u_i, d|h^i|^2) \geq 0\}$ can be computed based on Proposition 2.3.7. For notation simplicity, we omit the condition $U_0(u_i, d|h^i|^2) \geq 0$, and the first term in the integral of (2.30) can be expanded as

$$\mathbb{P}\{\text{Transmits at } M^*\} = \sum_{m=0}^{L/l} \left(\prod_{k=0}^{m-1} \mathbb{P}\{\alpha_k < 0\}\right) \mathbb{P}\{\beta_m \leq 0\} \tag{2.31}$$

where $\alpha_k = \max\{(R(k)-\lambda^*)L, -\lambda kl\} - \mathbb{E}[U_{k+1}(\mathcal{F}_{k+1}) \mid \mathcal{F}_k]$, and $\beta_m = \max\{-\lambda ml, \mathbb{E}[U_{m+1}(\mathcal{F}_{m+1}) \mid \mathcal{F}_m]\} - (R(m)-\lambda^*)L$. Note that in $\mathbb{P}\{\alpha_k < 0\}$, $R(k)$ and $\mathbb{E}[U_{k+1}(\mathcal{F}_{k+1}) \mid \mathcal{F}_k]$ are random since they are the functions of $\sum_{j=0}^k E_j^i$, where $\left\{E_j^i\right\}_{1 \leq j \leq k}$ are i.i.d. with a known distribution and $E_0^i = 0$. Thus, $\mathbb{P}\{\alpha_k < 0\}$ can be computed. Using the simi-

lar argument, it is easy to see that $\mathbb{P}\{\beta_m \leq 0\}$ can be computed as well. Therefore, the probability given in (2.31) is computable. Overall, we could obtain $p_{tr}^i(u_i)$ after plugging (2.31) into (2.30).

After obtaining $p_{tr}^i(u_i)$, the transition probability $\{p_{u_i,\widetilde{u}_i}^i\}$, where $u_i \in \mathbf{\Delta}$, and $\widetilde{u}_i \in \{0, u_i, u_i+\delta, \cdots, B_{max}\delta\}$, can be calculated similarly as the case of constant EH rate. In addition, Algorithm 2.1 and Proposition 2.4.1 could be modified, such that they could suit the i.i.d. EH model, which is omitted.

2.5 Computation of the Optimal Throughput

The optimal throughput λ^* hinges upon the optimal stopping rules in (2.17) and (2.22). Thus, to fully obtain the optimal scheduling policy of the proposed DOS, we next turn our attention to computing the value of λ^*.

By Propositions 2.3.5 and 2.3.8, λ^* can be obtained by solving (2.18) or (2.23) under the constant or i.i.d. EH model, respectively. Next, we briefly introduce the idea why there exists λ^* such that the equation (2.18) or (2.23) holds, and how to search λ^*. For brevity, we focus the constant EH rate case.

Note that $R(V^*)$ is a function of random variables h^i and B_0^i; we could calculate the expectation on the left-hand side of (2.18) for each given $\lambda \geq 0$. Such expectation requires the distribution of B_0^i, i.e., the steady-state distribution Π^i, which could be approximately computed as shown in Section 2.4. In addition, for a given λ, an upper bound of this expectation can be obtained by fixing $\Pi^i = [0, \ \cdots 0, \ 1]$. As λ increases from zero to infinity, this upper bound decreases to zero at some $\widetilde{\lambda} < \infty$. Since the right-hand side of (2.18) is strictly increasing over λ within the range $[0, +\infty)$, there at least exists one λ^* satisfying (2.18). Therefore, an exhaustive one-dimension search can be applied to obtain the optimal throughput over the range $\left[0, \widetilde{\lambda}\right]$. Note that during each iteration of the exhaustive search, Algorithm 2.1 (given in Section 2.4) is used to obtain the steady-state

distribution for a given $\lambda \in \left[0, \widetilde{\lambda}\right]$, and then we check if the equation (2.18) or (2.23) holds. Finally, λ^* should be the largest one in $\left[0, \widetilde{\lambda}\right]$ that makes the equation (2.18) or (2.23) hold.

In summary, the above search can characterize the optimal stopping rules given in Propositions 2.3.5 and 2.3.8, which completes the proposed DOS framework.

2.6 Numerical Results

In this section, we first validate Propositions 2.3.5 and 2.3.8 to show that the optimal throughput λ^* exists and can be found via one-dimension search. Second, we investigate the throughput gain of our proposed DOS with two-level probing over the best-effort delivery method, where the data is transmitted whenever the channel contention is successful. Note that such a method can be realized in the proposed DOS framework by fixing $M = 0$ and setting $N = 1$ in (2.17) and (2.22). Let λ_0 denote the throughput obtained by the best-effort scheme, which can be calculated as

$$\lambda_0 = \frac{\sum_{i=1}^{I} \frac{Q_i}{Q} \mathbb{E}\left[L \log\left(1 + |h_n^i|^2 \frac{B_{n,0}^i}{L\sigma^2}\right)\right]}{\frac{l}{Q} + L}. \tag{2.32}$$

In general, a typical button cell battery has the capacity of 150 mAh with the end-point voltage of 0.9 V, which is equal to 150 mAh $\times$ 3600 s/h $\times$ 0.9 V = 486 J. A thin-film rechargeable battery can offer 50 μAh with 3.3 V, which is equal to 0.594 J. Since a typical transmission time interval is on the time scale of milliseconds, we let the energy unit be $\delta = 10^{-3}$ J in the simulation. Accordingly, we set the capacity of the battery $B_{max}\delta = 10^5\delta$, which falls between the capacity volume of a thin-film battery and that of a button cell battery. Also, the current commercial solar panel can provide power from 1 W to about 400 W, which is equivalent to $1\delta{\cdot}\text{ms}^{-1} \sim 400\delta{\cdot}\text{ms}^{-1}$. According to this fact, in our simulation, we let the EH rate vary within the range $[0, 40\delta]$. In addition, the

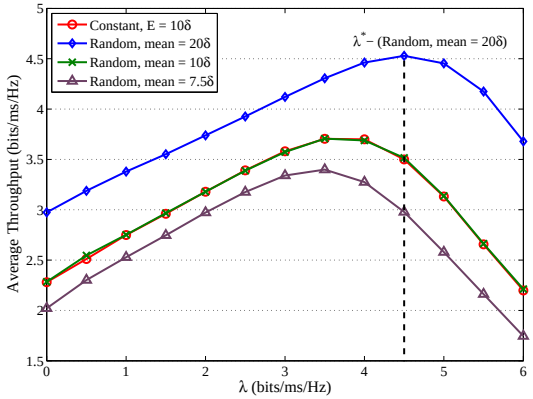

Figure 2.3: λ vs. the average throughput.

channel gains are i.i.d for different links and the channel power gains follow an exponential distribution with mean 5. The variance of the noise is set to be 10 mW. The length of one time slot is unified as $l = 1$ ms and the length of a transmission block is $L = 100l$.

2.6.1 Validation of Propositions 2.3.5 and 2.3.8

In Fig. 2.3, we illustrate the variation of the average throughput as the "threshold" λ changes. Without loss of generality, we first consider a homogeneous network with 10 user pairs, i.e., all pairs are identical. For the constant EH model, the EH rate is set to be $E = 10\delta$ for all transmitters. For the i.i.d. EH case, we choose the Bernoulli model [35, 50]: The EH rate is either zero or of a finite value with probability 0.5. In our simulation, we consider three cases for the mean values in i.i.d. EH model: 7.5δ, 10δ, and 20δ.

First, we observe in Fig. 2.3 that as λ increases from zero, the average throughput is increasing then decreasing. Then, the optimal point is achieved at λ^*, where the average throughput is at its apex that is also approximately of the same value as λ^*. Taking the case of i.i.d. EH model with mean 20δ as an example in Fig. 2.3, the value of the optimal throughput $\lambda = \lambda^*$ is approximately 4.5, and the actual optimal average throughput is

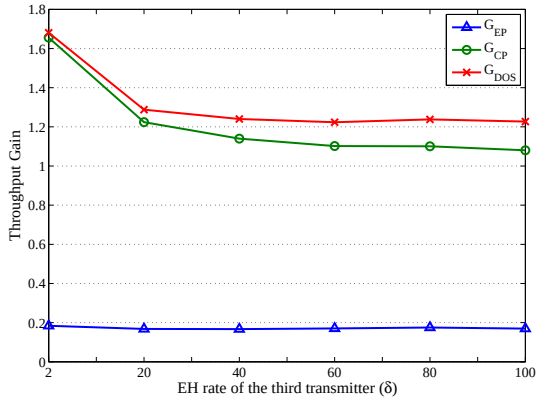

Figure 2.4: The throughput gain vs. EH rate of the third transmitter.

about 4.5 as well. Therefore, this observation validates our Propositions 2.3.5, 2.3.8 and discussions in Section 2.5. Second, we observe that the average throughput is almost the same when the mean of the EH rate in the i.i.d. EH model is equal to the EH rate in the constant EH model. Thus, the type of EH rate models does not directly determine the average throughput performance.

2.6.2 Throughput Gain

We use λ_{EP} to denote the throughput where only EP is adopted, i.e., setting $N = 0$ and $M = M^*$, and λ_{CP} to denote the throughput where only CP is adopted, i.e., setting $N = N^*$ and $M = 0$. Thus, the throughput gains are defined as:

$$\begin{cases} G_{EP} = \frac{\lambda_{EP}-\lambda_0}{\lambda_0}, & \text{gain from EP;} \\ G_{CP} = \frac{\lambda_{CP}-\lambda_0}{\lambda_0}, & \text{gain from CP;} \\ G_{DOS} = \frac{\lambda^*-\lambda_0}{\lambda_0}, & \text{gain from CP + EP.} \end{cases} \tag{2.33}$$

In Fig. 2.4, we evaluate the above throughput gains for the network with $I = 3$ user pairs. Recall from Section 3.2.1 that our analysis is applicable for $I \geq 2$. Since the con-

stant and i.i.d. EH rate models could attain the same throughput performance over λ, we only consider the constant EH model in this case. Particularly, we study a heterogeneous case where the first two transmitters have the same EH rates 2δ, while the EH rate of the third transmitter varies from 2δ to 100δ.

We observe in Fig. 2.4 that as the EH rate of the third transmitter increases, G_{EP} almost keeps constant and can achieve a gain about 19%. It implies that after the channel contention, the successful transmitter with any EH rate could do EP to enhance its average transmission rate over the transmission block. Thus, the ESI of the successful transmitter does not have obvious impact on the throughput. However, we notice that G_{CP} achieves its maximum when all transmitters are identical (with the same EH rate 2δ) and then decreases slowly as the EH rate of the third transmitter increases. The intuition is that when the difference among EH rates becomes larger, the stopping rule of CP will more likely let the transmitter with relatively low energy level to give up the channel, which results in a longer time on CP and then the throughput gain is lower than the case when all transmitters are identical. Regarding G_{DOS}, our proposed DOS with two-stage probing can achieve the highest throughput gain among three schemes. It is worth noticing that as the EH rate of the third transmitter increases, the efficiency of DOS becomes more apparent, although slowly, than the scheme with pure CP, which implies that the second stage probing brings more benefits. Our intuition is that a larger difference among the EH rates leads to a bigger difference of energy levels. Since EP allows the successful transmitter with relatively lower energy level to possibly harvest more energy after CP, EP will plays a more important role as the difference among the EH rates increases.

In Fig. 2.5, we illustrate how the size of the network influences the throughput gains. In this scenario, we start from a three-pair network with EH rates 2δ, 2δ, and 80δ, respectively. Then, we keep adding pairs with EH rate 2δ at the transmitter side. We observe that the throughput gain G_{CP} is increasing a little as the size of the network is increasing.

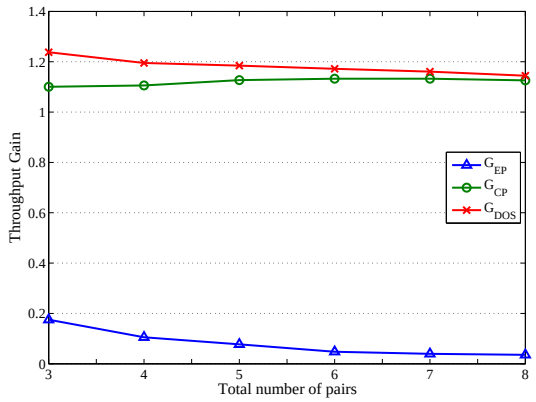

Figure 2.5: The throughput gain vs. the size of the network.

It is reasonable since CP could utilize the multi-user diversity of both channel gains and energy levels. We see that G_{CP} increases slowly, since we only add a low-EH-rate transmitter at each time. We also observe that G_{EP} is decreasing. The reason is that the more transmitters in the network, the less probability to transmit for each transmitter, and then more transmitters would maintain a high energy level. Thus, EP is rarely triggered after a channel contention. For the same reason, G_{DOS} would approach G_{CP} as the size of the network increases.

2.7 Conclusion

In this chapter, we proposed a DOS framework for a heterogeneous single-hop *ad hoc* network, in which each transmitter is powered by a renewable energy source and accesses the channel randomly. Our DOS framework includes two successive processes: All transmitters first probe the channel via random access, and then the successful transmitter decides whether to give up the channel or to optimally probe the energy before data transmission. The optimal scheduling policy of the DOS framework is obtained as follows: First, assuming the battery state is stationary at each transmitter, the expected throughput maximization problem was formulated as a rate-of-return optimal stopping problem,

which was solved for both the constant and i.i.d. EH rate models; second, by fixing the stopping rule, the stored energy level at each transmitter was shown to own a steady-state distribution as time goes to infinity, where we also proposed an efficient iterative algorithm for its computation; finally, the optimal throughput and the scheduling policy is obtained via one-dimension search with the above two steps (i.e., finding the form of the optimal stopping rule and calculating the steady-state distribution) repeated in each iteration. Numerical results were also provided to validate our analysis; the proposed DOS with two-level probing was shown to outperform the best-effort delivery method.

3. MULTI-CHANNEL ACCESS: HETEROGENEOUS NETWORKS

3.1 Introduction

3.1.1 Motivations

Heterogeneous networks (HetNets), where small networks (e.g., femtocell or WiFi) composed of low-power access points (APs) are placed under the coverage of a large network (e.g., cellular network), evolve into a new type of network deployment that could enhance the overall system capacity with reasonable cost and power consumption [2, 24]. Standardization bodies, such as ETSI and 3GPP, have paid much attention to this shifting of network paradigm and have made femtocells part of the current and future cellular standards, like UMTS and LTE/LTE-A. Now, commercial femtocell deployments could be found globally, operated by various cellular carrier companies [3].

In a cellular network, a mobile user (MU) is usually assigned a dedicated channel to access the base station (BS), while this link may experience bad channel conditions due to the possible severe path loss and fading between the MU and the BS. In such cases, however, the desired quality-of-service (QoS) could still be satisfied by allowing the MU to access a nearby AP in an underlying small network via a common channel, whose channel condition is relatively good. Essentially, the MU in the above HetNet constructs a multi-channel access scheme: The messages from MU could be directly delivered to the cellular BS, or if available, to a nearby low-power AP as well [39]. In general, there are two modes of access control for small networks (e.g., for femtocells): restricted access, i.e., only pre-registered users could access the corresponding AP [3, 39]; and open access, i.e., any local users in the small network could gain the access. It is worth noting that the small network could either share the same band with the large network, or operate over a band orthogonal to the large network: e.g., WiFi uses the unlicensed band [8] and

femtocells could be allocated with different bands from the large network via orthogonal frequency division multiple access (OFDMA) or time division multiple access [3, 62]. In practice, the MU may fail to establish a dedicated link to the small network due to the limited spectrum resources or the relatively large distance to the AP, which introduces another type of channel randomness beyond channel fading in the conventional cellular system.

Another significant advantage enabled by the aforementioned HetNet is that the MU could potentially enjoy a longer lifetime since its power consumption is reduced by communicating with the local AP instead of the distanced BS. However, since the lifetime of an MU is still limited by the stored energy in the batteries [30], the MU should seek an "active" way to recharge itself, especially in a green fashion. Such renewable energy powered nodes will play critical roles in the next generation wireless system, which is designed to be environment friendly and to support diversified applications such as machine-to-machine communications and Internet of things (IoT). A promising "self-charging" technology is energy harvesting (EH), which can efficiently convert certain renewable energy sources (e.g., solar, radiation, and vibration) to electric energy [54]. In this way, the MU could prolong the battery life almost infinitely, and fulfil the increasing demands of green systems [60]. Compared with the conventional constant power supply, such a renewable energy supply raises a new design constraint as pointed out in previous chapters: The consumed energy up to any time should be bounded by the harvested energy until this point, which is named as the EH constraint [30].

In this chapter, we study a simple uplink HetNet scenario depicted in Fig. 3.1, where each EH-based MU has an individual link, namely a *private channel*, to the large network BS for deterministic access. Moreover, a local AP of a small network offers a *common channel*, which is randomly shared by all nearby MUs. Here we consider a scenario that each MU could access the common channel with a certain probability at each time slot.

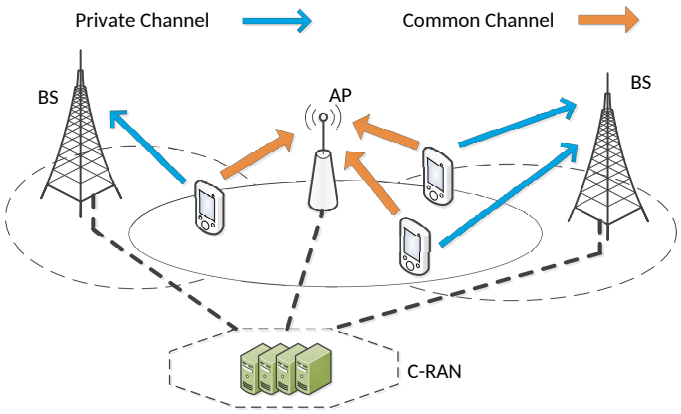

Figure 3.1: The uplink HetNet with multi-channel access, where each MU is powered by energy harvesters, and accesses to the BS and AP via private and common channels, respectively.

Thus, based on this multi-channel access setup, the MU could fulfil a transmission by using the harvested energy via either its private channel solely or via both the private and common channels simultaneously. Joint information processing is done in a cloud-based radio access network (C-RAN) platform [15, 29].

On the MU side, there are two types of state information that could be causally known before the transmission: the channel state information (CSI) of the links to the large network and the small network (if the AP was successfully occupied by the MU); and the energy state information (ESI), i.e., the EH rate (the harvested energy per unit time) and the battery state at the MU. Therefore, the MU could decide when to start a transmission with both CSI and ESI at hand. Obviously, a longer waiting time before transmissions to probe those information may accumulate a higher transmission power, and create a higher likelihood to secure the common channel, while it may reduce the average effective throughput since the effective transmission time is decreased. Thus, this leaves us an interesting tradeoff to optimize: channel-energy probing time vs. transmission time. In addition, we consider a "save-then-transmit" scheme such that each transmission would

consume all the harvested energy at the MU. This suboptimal power utilization scheme is able to deploy the largest instantaneous transmit power such that the short-term transmission rate is maximized, and is more tractable for analysis as well.

3.1.2 Contributions

First, we propose an opportunistic transmission scheme for the multi-channel HetNet uplink powered by sustainable energy supplies, and aim to enhance the average throughput for each user by jointly exploiting the stochastic CSI and ESI. More precisely, the throughput maximization is cast as a "rate-of-return" optimal stopping problem. With Markovian private channel and EH models, the optimal stopping rule is proved to exist and have a state-dependent threshold-based structure with both the finite and infinite battery capacities. The optimal throughput is proved to be strictly increasing over the access probability of the common channel.

Second, we study the case when the private channel gains and the EH rates are respectively independent and identically distributed (i.i.d.) across different communication blocks. The corresponding optimal stopping rule is proved to be a pure-threshold policy, i.e., the threshold does not change over time, which could be found via a one-dimension search. With such a fixed threshold, the mean probing time is proved to be decreasing polynomially over the access probability to the common channel. We also show via simulations that the randomness of EH rates, termed "EH diversity", influences the throughput performance and could be exploited by our proposed pure-threshold policy: Specifically, we find that the more dynamically the EH rate varies, the higher the average throughput that the MU could achieve.

Finally, we study the case with conventional constant power supplies, showing that the optimal power allocation has a "water-filling" structure, where the water level is jointly determined by the statistics of both the private and common channels, and the common

channel access probability.

3.1.3 Related Works and Organization

Most of existing works related to the uplink of heterogeneous cellular networks (HCNs) assume certain deterministic access control of the underlying small networks [3, 12, 49, 62]. From the views of both the femtocell owner and the overall network operator, authors in [62] evaluated the femtocell performance with open and restricted accesses. It was shown that with nonorthogonal (in terms of frequency or time) multiple access, i.e., CDMA, for mobile users, the open access benefits both the femtocell owner and the network operator; and for the orthogonal case, time-division multiple access (TDMA) or orthogonal frequency-division multiple access (OFDMA), the femtocell access control (open or restricted) is closely related to the user density. In [12], by adopting open access, the outage behaviors of both femtocell and macrocell users were analyzed by using the stochastic geometry to model the locations of both the femtocell APs and the cellular users. The authors also presented several interference avoidance methods to enhance the per-user capacity. In [49], each macrocell user was assumed one direct link to the marcocell BS, and one relay link to the femtocell AP. Playing a non-cooperative game against the others, each user could seek its preferred open-access femtocell and split the rates between the BS and the AP to maximize its own utility. In contrast to these existing works, here we consider users with random, not deterministic, access to the local AP, which is more realistic in WiFi based HetNets.

On the other hand, the study of wireless transmitters powered by renewable energy has also drawn a lot of attention in recent years. Particularly, with noncausal (i.e., offline) knowledge on energy arrival processes, the throughput maximization problem was investigated for both non-fading and fading channels in [30, 44], in addition to the classic three-node Gaussian relay channel [31]. With causal (i.e., online) knowledge, the optimal

throughput in fading channels over finite-time horizons was obtained via dynamic programming techniques in [30, 44]. A save-then-transmit protocol was proposed in [40], where each communication block is divided into two parts: the first one for harvesting energy and the other for data transmission. Here, on the contrary, we consider the save-then-transmit strategy over infinite number of communication blocks.

In some cases, wireless users may first potentially ask for more channel resources and then transmit. In [26], the authors discussed how a transmitter probes a relay channel with some additional time cost when its direct channel is undesirable. In addition, similar channel selection problems for WiFi and cognitive radio were investigated in [34] and [52], respectively. For [26,34,52], the key idea is that the sender may spend time on probing the channel quality before starting a transmission. We here adopt a similar idea; however, we need to face a different and more challenging scenario: Besides the large network channel quality, we also need to probe the resource availability in the small network, and the local battery status that is dynamic due to the energy arrival and withdrawal.

The remainder of this chapter is organized as follows. The specific system model and the problem formulation are described in Section 3.2. The throughput optimization problem is solved for both Markovian and i.i.d. models in Section 3.3. The optimal power allocation with traditional power supplies is discussed in Section 3.4. Finally, Section 3.5 concludes the chapter.

3.2 System Model and Problem Formulation

3.2.1 System Model

As shown in Fig. 3.1, an uplink HetNet communication scenario is considered: One private channel to the large network BS is assigned to each EH-based MU, and one common channel to a given small network AP is randomly accessed by all nearby users. All private and common channels are orthogonal in frequency, slotted equally in time, and

synchronized. The duration of each time slot is unified. Moreover, in each slot, an MU can access at most one local AP through the common channel with probability p_s, called the *access probability*. Similar to a WiFi system, the MU cannot hold the common channel all the time, and it is required to release the channel after one successful access.

Under the above setup, an MU can fulfill a transmission: 1) via the private channel only; 2) or via both the private and common channels.

- In case 1), the received signal in the t-th time slot at the BS is given by

$$y_t = h_t\sqrt{P_t}x_t + z_t, \tag{3.1}$$

  where h_t is the channel gain of the MU-to-BS link, P_t is the transmit power, x_t is the transmitted signal with zero mean and unit variance, and z_t is the circularly symmetric complex Gaussian (CSCG) noise with zero mean and unit variance. Define $\{H_t = |h_t|^2\}$ on a state space $\mathcal{H}$ with finite mean and variance.

- In case 2), the received signal in the t-th time slot at the BS is the same as (3.1), and that at the AP is given by

$$y_t^c = h_t^c\sqrt{P_t^c}x_t^c + z_t^c, \tag{3.2}$$

  where h_t^c is the channel gain of the MU-to-AP link, P_t^c is the transmit power over the common channel, x_t^c and z_t^c are defined similar as (3.1). Define $\{H_t^c = |h_t^c|^2\}$ on a space $\mathcal{H}_c$ with finite mean and variance.

Here, we assume that H_t follows a more general Markovian model [63] while H_t^c follows an i.i.d. model, due to the fact that the MU-to-BS link usually experiences a much longer distance such that the channel may be under correlated shadowing, while the MU-to-AP link does not, given its much shorter distance. The CSI includes both H_t and H_t^c. For

simplicity, the time on channel probing for CSI is negligible compared to the length of one time slot.

We use $\{B_t\}_{t\geq 1}$ to denote the energy level at the battery for the considered MU at the beginning of time slot t, and the energy level is quantified into unit steps, i.e., $B_t \in \mathcal{B} = \{0, \delta, 2\delta, \ldots, B_{max}\delta\}$, where δ is the smallest energy unit, and B_{max} could be either a finite integer or infinity. For the case of $B_{max} = +\infty$, it is a good approximation when the battery capacity is large enough compared with the EH rate, e.g., an AA-sized NiMH battery has a capacity of 7.7 kJ, which requires a couple of hours to be fully charged by some commercial solar panels [51]. During time slot t, the MU can harvest E_t amount of energy. The sequence $\{E_t\}_{t\geq 1}$ is modeled as a homogeneous Markov process. Due to hardware limitations, the EH rate is represented over a finite state space $\mathcal{E} \subseteq \{E : E = k\delta, k \in \mathbb{N} \bigcup \{0\}\}$. The energy state information (ESI, i.e., EH rate and battery status) is causally known by the MU.

A power consumption model based on [36] is considered such that when the MU is transmitting, the circuit power is $C > 0$. Moreover, probing the private and common channels for CSI requires an instant power $S > 0$ (since we assume that the time on probing is negligible). At time slot t, the MU probes the channels if $B_t > S+C$; otherwise, it only harvests energy. It is assumed that if the MU probes channels, it can perfectly obtain CSI of the private and common channels (if accessed w.p. p_s).

Accounting the circuit power and probing power, we consider a "save-then-transmit" scheme over multiple time slots: The MU probes channels (if $B_t > S + C$) and harvests energy simultaneously, and then uses up the total available energy in the battery for each transmission. Such a scheme has the nature of maximizing the short-term transmission rate, and is practical in certain applications[1]. As such, if we let $t = 1$ as the first time slot

[1]For example, such scheme works when an MU needs to report a message approximately periodically, since the mean of save-then-transmit periods can be quantified, which will be shown later.

after one data transmission, B_t can be written as

$$B_t = \min\left\{\sum_{i=1}^{t-1} E_i - S\sum_{i=1}^{t-1} 1_{\{B_i > S+C\}}, B_{max}\delta\right\}. \tag{3.3}$$

When $t = 1$, there is $B_1 = E_0$, where E_0 is the accumulated energy during transmission slot in last save-then-transmit period. The MU decides when to stop "saving" and to start a transmission according to CSI and ESI. Based on the above discussions, at the beginning of time slot t, an MU acts as follows:

- If $B_t > S + C$, probe channels, and decide between the two operations based on CSI and ESI:
    1. transmit immediately during the current time slot (via either the private channel or both the private and common channels); or
    2. skip transmission, and release the common channel if it has been secured by the MU.
- Otherwise, do not probe and skip transmission.

In Fig. 3.2, we show one realization of the probing and access process, in which two users are assigned with two private channels, respectively, and share one common channel. In particular, MU 1 transmits only through its private channel at time T and MU 2 transmits via both its private and the common channel at time K.

3.2.2 Problem Formulation

We use Shannon capacity formula to represent the instant transmission rate R_t of the MU at time slot t. Then, based on the above channel model and applying a joint decoder

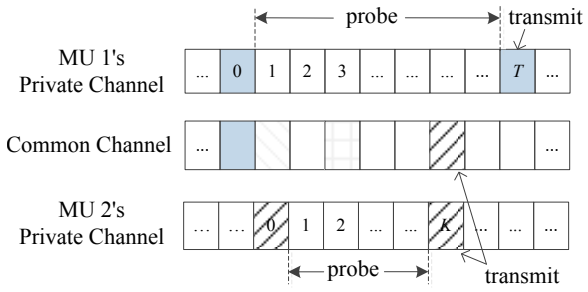

Figure 3.2: A realization of the proposed multi-channel access system.

at the receivers, the rate R_t with unit bandwidth is expressed as

$$R_t = \log\left(1 + H_t P_t\right) + \log\left(1 + \phi_t H_t^c P_t^c\right), \tag{3.4}$$

where the indicator ϕ_t following Bernoulli distribution such that $\phi_t = 0$ with probability (w.p.) $1 - p_s$ and $\phi_t = 1$ w.p. p_s. Due to the adopted save-then-transmit scheme, it is easy to see that $P_t + \phi_t P_t^c = (B_t - S - C)^+$. When $\phi_t = 0$, it follows $P_t = (B_t - S - C)^+$, since only the private channel is available; and when if $\phi_t = 1$, the power allocation follows the "water-filling" scheme given in the next lemma.

Lemma 3.2.1 When the MU can access both the private and common channels, i.e., $\phi_t = 1$*, it is optimal to allocate power as follows:*

- *If* $\left|\frac{1}{H_t^c} - \frac{1}{H_t}\right| < (B_t - S - C)^+$*, we have that* $P_t = \frac{1}{2}\left((B_t - S - C)^+ + \frac{1}{H_t^c} - \frac{1}{H_t}\right)$ *and* $P_t^c = \frac{1}{2}\left((B_t - S - C)^+ + \frac{1}{H_t} - \frac{1}{H_t^c}\right)$*;*
- *If* $\left|\frac{1}{H_t^c} - \frac{1}{H_t}\right| \geq (B_t - S - C)^+$ *and* $H_t > H_t^c$*, we have* $P_t = (B_t - S - C)^+$ *and* $P_t^c = 0$*;*
- *If* $\left|\frac{1}{H_t^c} - \frac{1}{H_t}\right| \geq ((B_t - S - C)^+$ *and* $H_t < H_t^c$*, we have* $P_t = 0$ *and* $P_t^c = (B_t - S - C)^+$.

Lemma 3.2.1 can be proved by using standard convex optimization techniques and thus the proof is omitted for brevity. For notation simplicity, we define state of the MU, including CSI and ESI, at time t as $\mathbf{F}_t = \{\phi_t, B_t, E_{t-1}, H_t, H_t^c\} \in \mathcal{F} = \{0,1\} \times \mathcal{B} \times \mathcal{E} \times \mathcal{H} \times \mathcal{H}_c$. In this way, $R_t = R(\mathbf{F}_t)$ is uniquely determined by $\mathbf{F}_t$. In addition, we make the following assumption:

Assumption: The steady-state distribution of $\{B_t\}$ exists.

It follows that the steady-station distribution of $\{\mathbf{F}_t\}$ also exists given that $\{E_t\}$ and $\{H_t\}$ are stationary, respectively. We will verify this assumption later by showing that our proposed transmission scheme will result in a stationary $\{B_t\}$.

Let T be some stopping rule indicating the time slot to stop probing and to start the transmission. Then, the transmission rate at the time slot T would be $R(\mathbf{F}_T)$. If we adopts this stopping rule T for infinitely many times, we obtain

$$\frac{\lim_{L\to\infty} \frac{1}{L} \sum_{l=1}^{L} R(\mathbf{F}_{T_l})}{\lim_{L\to\infty} \frac{1}{L} \sum_{l=1}^{L} T_l} = \frac{\mathbb{E}[R(\mathbf{F}_T)]}{\mathbb{E}[T]} = \lambda,$$

where the expectation is taken over the joint stationary distribution of $\mathbf{F}_t$ and T, and λ is the average throughput per save-then-transmit period. The maximum throughput λ^* and the optimal stopping rule T^* are defined as

$$\lambda^* \triangleq \sup_{T\geq 1} \frac{\mathbb{E}[R(\mathbf{F}_T)]}{\mathbb{E}[T]},\ T^* \triangleq \arg\sup_{T\geq 1} \frac{\mathbb{E}[R(\mathbf{F}_T)]}{\mathbb{E}[T]}. \tag{3.5}$$

In the next section, we will find T^* and λ^*.

3.3 Optimal Stopping Rule and Throughput

The problem defined in (3.5) is a "rate-of-return" problem and could be converted into a standard optimal stopping problem [20, 21]. For a certain $\lambda > 0$, we let $G_T(\lambda) =$

$R(\mathbf{F}_T) - \lambda T$, and consider a new problem:

$$\sup_{T \geq 1} \mathbb{E}[G_T(\lambda)]. \tag{3.6}$$

Under this interpretation, $R(\mathbf{F}_T)$ can be regarded as the offer at time T, λT is the cost, and $G_T(\lambda)$ is the net reward. We let $G_\infty = -\infty$ since it is irrational that a transmitter does not send any data forever. The following lemma, which is directly from Theorem 1 of chapter 6 in [20], connects problems (3.5) and (3.6):

Lemma 3.3.1 i) *If (3.5) holds, it follows that when* $\lambda = \lambda^* > 0$, $\sup_{T \geq 1} \mathbb{E}[G_T(\lambda^*)] = 0$ *and the supremum is attained at the same* T^* *in (3.5); and* ii) *conversely, if for some* $\lambda = \lambda^* > 0$, $\sup_{T \geq 1} \mathbb{E}[G_T(\lambda^*)] = 0$ *and it is attained by some* T^**, then (3.5) holds.*

Therefore, we will focus on finding the optimal stopping rule T^* for problem (3.6) and $\lambda = \lambda^* > 0$ such that $\sup_{T \geq 1} \mathbb{E}[G_T(\lambda^*)] = 0$. In the rest of this section, we first solve problem (3.6) with Markovian private channel states and EH rates. Then, we consider the corresponding i.i.d. case.

3.3.1 Solutions for Markovian Case

Given some $\lambda > 0$, we define the remaining expected maximum reward starting at time t as

$$V_t(\mathbf{F}_t) = \sup_{T \geq 1} \mathbb{E}\left[R(\mathbf{F}_T) - \lambda T \mid \mathbf{F}_t\right]. \tag{3.7}$$

The following proposition shows the existence and the form of the optimal stopping rule, whose proof is given in Appendix B.

Proposition 3.3.1 The optimal stopping rule for problem (3.6) exists with either $B_{max} <$

$+\infty$ *or* $B_{max} = +\infty$. *Moreover, it has the following form*

$$T^* = \min\left\{t \geq 1 : R(\mathbf{F}_t) - \lambda^* = V_1(\mathbf{F}_t)\right\}. \tag{3.8}$$

Moreover, the optimal throughput λ^* *satisfies*

$$\lambda^* = \mathbb{E}\left[\max\left\{R(\mathbf{F}_1), \mathbb{E}\left[V_1(\mathbf{F}_2) \mid \mathbf{F}_1\right]\right\}\right], \tag{3.9}$$

where $\mathbf{F}_1$ *is the initial state of the save-then-transmit period, which is a random vector defined over the space* $\mathcal{F}_1 \subseteq \mathcal{F}$ *with a certain stationary distribution.*

It is observed from (3.8) that the optimal stopping rule for problem (3.6) is state-dependent and has a threshold-base structure with a parameter λ^*. The structure is derived based on the optimality equation [20], or equivalently, the dynamic programming equation [6, 59]. The next proposition gives some properties of λ^*.

Proposition 3.3.2 λ^* *is uniquely determined by equation (3.9) and is strictly increasing over* p_s.

Proof: We first show the uniqueness of λ^*. We observe equation (3.9) that its left-hand side is monotonically increasing from zero to positive infinity over $\lambda^* \in [0, +\infty)$. In the right-hand side of (3.9), notice that

$$\mathbb{E}\left[V_1(\mathbf{F}_2) \mid \mathbf{F}_1\right] = \mathbb{E}\left[\sup_{T\geq 1} \mathbb{E}\left[R(\mathbf{F}_T) - \lambda^* T \mid \mathbf{F}_2\right] \middle| \mathbf{F}_1\right],$$

which is obtained according to (3.7). It follows that the right-hand side of (3.9) is monotonically deceasing from a finite number, i.e.,

$$\mathbb{E}\left[\max\left\{R(\mathbf{F}_1), \mathbb{E}\left[\sup_{T\geq 1} \mathbb{E}\left[R(\mathbf{F}_T) \mid \mathbf{F}_2\right] \middle| \mathbf{F}_1\right]\right\}\right],$$

to negative infinity over $\lambda^* \in [0, +\infty)$. Thus, there exists a unique λ^* that makes equation (3.9) hold.

For the monotonicity of λ^* over p_s, please see Appendix B. ■

Remark 3.3.1 Although λ^* is unique, the computation of λ^* is in general extremely difficult since the stationary distribution of the battery is unknown and the battery capacity could be infinite. Proposition 3.3.2 also shows the strict monotonicity of the optimal throughput λ^* over the access probability p_s, which implies that the common channel is helpful for sure in general.

Next, we will show the stationary distribution of $\{B_t\}$ exists. Note that when B_{max} is finite, the transition probability of the energy level is also determined under the stopping rule T^* and the stationary distribution of E_t. Moreover, all attainable states of the battery form a positive recurrent class. Thus, $\{B_t\}$ has a steady-state distribution.

When B_{max} is infinite, our proposed transmission scheme can still keep $\{B_t\}$ stationary. From the perspective of queueing theory, the average discharging rate is the same as the recharging rate since in each save-then-transmit period, all energy will be used for transmission. Therefore, the stationary distribution of $\{B_t\}$ exists. Moreover, it can be approximated as a Brownian motion.

3.3.2 Solutions for i.i.d. Case

In this subsection, we focus on the case when $\{H_t\}_{t\geq 1}$ and $\{E_t\}_{t\geq 1}$ are both i.i.d., respectively. As a special case of the one studied in the previous subsection, the optimal stopping rule of this case still exists. Taking one step further, the corresponding optimal stopping rule is simplified to bear a pure-threshold structure.

Proposition 3.3.3 When $\{H_t\}_{t\geq 1}$ and $\{E_t\}_{t\geq 1}$ are i.i.d. with finite means and variances,

respectively, the optimal stopping rule T^* for problem (3.6) has the following form:

$$T^* = \min\left\{t \geq 1 : R(\mathbf{F}_t) \geq \gamma\right\}. \tag{3.10}$$

where γ is a fixed real number.

The proof is given in Appendix B. Moreover, we note that the expected value of T^* corresponds to the average length of the save-then-transmit period, i.e., the mean delay. The next proposition (proved in Appendix B.4) shows that for a fixed threshold, the delay performance is improved with the proposed multi-channel access.

Proposition 3.3.4 Given a fixed $\gamma > 0$, $\mathbb{E}[T^*]$ is decreasing polynomially over p_s.

Following Proposition 3.3.3 and Lemma 3.3.1, we have

$$\begin{aligned} 0 &= \sup_{T \in \mathcal{T}_1} \mathbb{E}[R(\mathbf{F}_T) - \lambda^* T] \\ &= \mathbb{E}\left[R\left(\mathbf{F}_{T^*}\right) I\left(R(\mathbf{F}_{T^*}) \geq \gamma\right)\right] - \lambda^* \mathbb{E}[T^*], \end{aligned}$$

where $I(\cdot)$ is the indicator function. Then, we obtain

$$\lambda^* = \max_{\gamma \geq 0} \frac{\mathbb{E}\left[R\left(\mathbf{F}_{T^*}\right) I\left(R(\mathbf{F}_{T^*}) \geq \gamma\right)\right]}{\mathbb{E}\left[T^*\right]}. \tag{3.11}$$

Conjecture: λ^* is a quasi-concave function over γ.

Our conjecture will be validated via numerical results in Section 2.6. Such a conjecture enables us to apply simple search method, e.g., bisection search, to find the optimal threshold.

3.4 Throughput with Conventional Power Supply

In this section, we investigate the throughput of the MU with a conventional power supply (i.e., a conventional battery) in the discussed multi-channel access system, which will serve as performance benchmarks for our proposed schemes. Note that we only need to change the EH constraints into the average power constraint, and keep the same channel and access models as before.

Under the conventional power supply, the MU does not need to work in a save-then-transmit cycle, and is able to probe channels at each time slot. Accordingly, now the target is to find the average throughput over the entire operation time. With the instant transmission rate R_t given by (3.4), finding the optimal power allocation is equivalent to solving the following optimization problem:

$$\max_{P_t, P_t^c} \quad \lim_{K\to\infty} \frac{1}{K} \sum_{t=1}^{K} \left(\log\left(1 + H_t P_t\right) + \log\left(1 + \phi_t H_t^c P_t^c\right)\right) \tag{3.12}$$

$$\text{s.t.} \quad \lim_{K\to\infty} \frac{1}{K} \sum_{t=1}^{K} \left(P_t + \phi_t P_t^c + 1_{\{\min\{P_t, P_t^c\}>0\}} C + S\right) \leq B; \tag{3.13}$$

$$P_t, P_t^c \geq 0, \text{ for } t = 1, \ldots, K,$$

where B is the average power limit. The optimal power allocation is given in the next proposition.

Proposition 3.4.1 The optimal power allocation of problem (3.12) is given as

$$P_t^* = \left(\frac{1}{\xi^*} - \frac{1}{H_t}\right)^+, P_t^{c,*} = \begin{cases} \left(\frac{1}{\xi^*} - \frac{1}{H_t^c}\right)^+, & \text{if } \phi_t = 1, \\ 0, & \text{if } \phi_t = 0, \end{cases} \tag{3.14}$$

where ξ^* satisfies the average power constraint (3.13).

Proof: For any feasible solution $\{P_t, P_t^c\}$, there exists a ξ such that $\mathbb{P}\{\min\{P_t, P_t^c\} >$

$0\} = \mathbb{P}\{H_t > \xi\} + p_s\mathbb{P}\{H_t^c > \xi\}$. With this ξ, constraint (3.13) is rewritten as

$$\mathbb{E}\left[P_t + \phi_t P_t^c\right] \leq B - S - C\left(\mathbb{P}\{H_t > \xi\} + p_s\mathbb{P}\{H_t^c > \xi\}\right). \tag{3.15}$$

Then, problem (3.12) with the above constraint could be easily solved following the classic water-filling solution [25], where the optimal solution is given by

$$P_t' = \left(\frac{1}{\xi'} - \frac{1}{H_t}\right)^+, P_t^{c'} = \begin{cases} \left(\frac{1}{\xi'} - \frac{1}{H_t^c}\right)^+, & \text{if } \phi_t = 1, \\ 0, & \text{if } \phi_t = 0, \end{cases}$$

where ξ' satisfies (3.15). Then, it remains to show that $\xi' = \xi$ and the value is unique.

We first show $\xi' \geq \xi$ by contradiction. Suppose that $\xi' < \xi$. By applying power allocation $\{P_t', P_t^{c'}\}$, the average total power consumption is given by

$$\begin{aligned} &\mathbb{E}\left[P_t' + \phi_t P_t^{c'} + 1_{\{\min\{P_t', P_t^{c'}\}>0\}} C + S\right] \\ =&B + C\left(\mathbb{P}\{H_t > \xi'\} - \mathbb{P}\{H_t > \xi\} + p_s(\mathbb{P}\{H_t^c > \xi'\} - \mathbb{P}\{H_t^c > \xi\})\right) \\ >&B, \end{aligned}$$

which violates constraint (3.13). Thus, we obtain $\xi' \geq \xi$. If $\xi' > \xi$, it follows that

$$\begin{aligned} &\mathbb{E}\left[P_t' + \phi_t P_t^{c'} + 1_{\{\min\{P_t', P_t^{c'}\}>0\}} C + S\right] \\ =&B + C\left(\mathbb{P}\{H_t > \xi'\} - \mathbb{P}\{H_t > \xi\} + p_s(\mathbb{P}\{H_t^c > \xi'\} - \mathbb{P}\{H_t^c > \xi\})\right) \\ \leq&B, \end{aligned}$$

which means that some energy is wasted, and ξ' is not the optimal threshold. Thus, there must be $\xi' = \xi$ in order to utilize all available energy. Note that the optimal ξ^* is unique. It is observed that if ξ^* increases from zero to infinity, the left-hand side of equation (3.13)

monotonically decreases from positive infinity to zero, which implies that there exists a unique $\xi = \xi^*$ to make the above equation hold. Thus, the proposition is proved. ■

3.5 Conclusion

In this chapter, we considered a HetNet uplink with multi-channel access, where each EH-powered MU has deterministic access to a private channel linked to the cellular BS, and random access to a common channel linked to a local AP. As such, the MU could fulfil a transmission via its private channel or both private and common channels. By jointly taking advantage of channel-energy variation and common channel sharing, we proposed an opportunistic transmission scheme that allows the transmitter to properly probe the channel-energy state, such that the average transmission rate is maximized. In particular, we formulated the average throughput maximization problem as an optimal stopping problem of rate-of-return. By applying the optimal stopping theory, we proved that the optimal stopping rule exists and has a state-dependent and threshold-based structure in general. Moreover, when the private channel gains and EH rates are i.i.d., respectively, the optimal stopping rule turned out to be a simple pure-threshold policy. We also found the optimal power allocation scheme for the transmitter powered by a conventional power supply, to serve as the performance benchmark.

4. MULTIUSER ENERGY DIVERSITY IN ENERGY HARVESTING WIRELESS COMMUNICATIONS

4.1 Introduction

For conventional systems with constant power supplies, the multiuser diversity can be exploited when multiple users have independently fading channels. When more users present, it is more likely that the scheduler could find a user with a favorable channel condition. Therefore, the sum or average capacity increases as the number of users getting large. The multiuser diversity gain mainly comes from the effective channel gain [56], i.e., from h_i to $\max_{1\leq i\leq N} h_i$, where h_i denotes the channel power gain. In particular, multiuser diversity with random access or random number of users has been studied in [43, 46], and the scaling of the throughput over the number of users was shown to be on the order of $O(\log(N) + \log\log(N))$ [46].

Obviously, if all users have identical additive Gaussian channels, there is no multiuser diversity gain, given that all signal channels are the same and the transmission power is constant. However, when powered by energy harvesters, transmitters may have different battery levels because the energy harvesting (EH) rates are random. Then, the variation of battery levels among different users may result in a potential throughput gain over the benchmark, i.e., a point-to-point EH communication system.

In this chapter, we revisit the concept of multiuser diversity in EH communications, but from a new angle. We study multiuser diversity with respect to the energy availability. To facilitate the analysis, we eliminate the effect of fading channel by considering additive white Gaussian noise (AWGN) channel models only. We investigate the scaling of the available energy across all the users and the scaling of average throughput.

Specifically, assuming that the EH rates are i.i.d. across different users and over time,

we explore the multiuser diversity gain over AWGN channels under both the centralized and distributed access schemes:

- For the centralized case, we first discover the stationary distribution of the overall battery level, and further analyze the asymptotic behavior of the overall battery level when the number of users goes to infinity. We show that both the greedy scheduling, i.e., choosing the user with the highest available energy at each time, and the rate-suboptimal TDMA access schemes, are all able to explore the multiuser energy diversity, where the average throughput increases on a scale of $\log(\mu N)$, with μ denoting the mean of energy arrival rate and N denoting the number of users.

- For the distributed case, the distribution of energy levels is derived as a function of the channel contention probability, and we show that multiuser energy diversity can be efficiently exploited if the contention probability is on the scale of $O\left(\frac{1}{N}\right)$.

The rest of this chapter is organized as follows. The system model is given in Section 4.2. Then, the multiuser energy diversity is discussed under both centralized and distributed access schemes in Section 4.3. Finally, this chapter is concluded in Section 4.4.

4.2 System Model

In a common multiuser scenario, where multiple transmitter-receiver pairs share one channel for communications, the interference, usually described as packet collisions among users, dominates the unreliability of communication, which significantly impairs the system throughput performance. Thus, we are interested in studying how multiuser diversity affects the system throughput.

To eliminate the multiuser diversity imposed by the channel effect and focus on that form the EH effect, an AWGN channel is adopted for each communication link. Moreover, if two or more transmitters transmit at the same time slot, collisions occur and no data get

through[1], where length of a time slot is unified (such that the power per slot is of the same magnitude as the corresponding energy per time slot). Suppose that at time slot t, only the n-th transmitter transmits, the received signal $y_t^{(n)}$ is given by

$$y_t^{(n)} = \sqrt{P_t^{(n)}} x_t^{(n)} + z_t^{(n)}, \tag{4.1}$$

where $P_t^{(n)}$ is the transmission power, $x_t^{(n)}$ is the transmit signal of unit power, and $z_t^{(n)}$ is the circularly symmetric complex Gaussian (CSCG) noise with zero mean and unit variance. The transmission rate over one time slot could be expressed as $\log\left(1 + P_t^{(n)}\right)$ [56].

We assume that the EH rates among different transmitters are i.i.d., and each transmitter has a battery with infinite battery capacity[2]. Specifically, let $E_t^{(n)}$ denote the EH rate of the n-th transmitter at time slot t, which is a Bernoulli random variable such that an energy unit arrives with probability p. Furthermore, $\left\{E_t^{(n)}\right\}$ are assumed to be also i.i.d. across time. In addition, the transmitter is able to work in an energy-full-duplex fashion [57], i.e., it can supply and harvest energy at the same time. Let $B_t^{(n)}$ denote the energy level of the n-th user at the beginning of time slot t. The power for data transmission at each slot follows a greedy strategy, i.e., the transmitter uses all available energy for data transmission when it accesses the channel.

4.3 Multiuser Energy Diversity

In this section, we investigate the multiuser energy diversity under the centralized and distributed access schemes, respectively.

[1]This is a typical channel model for studying medium access protocols [46].

[2]It is worth pointing out that if the transmitter has no battery but with a constant channel, the analysis is similar to the case with a constant power supply but over i.i.d. fading channel.

4.3.1 Centralized Access

Assume that the central controller is able to know the energy state information (ESI) of all transmitters at the beginning of each time slot. Here, we consider a greedy scheduling: In each time slot, the controller picks the transmitter with the highest energy level. As such, the transmission power can be written as $M_t = \max_{1\leq n\leq N}\left\{B_t^{(n)}\right\}$, and the instantaneous rate is given by

$$R_t^{gr}(N) = \log\left(1 + M_t\right). \tag{4.2}$$

We use $\mu = p$ to denote the mean of EH rate, and $\sigma^2 = p(1-p)$ to denote the variance. Noth that our analysis in this subsection is not limited to the Bernoulli energy arrival model; it works for any arrival model with finite mean and variance.

We aim to analyze the stationary asymptotic behavior of $R_t^{gr}(N)$. The key is to understand how M_t behaves with a large N when $t \to \infty$. First, we quantify the battery levels when $t \to \infty$. The following lemma provides a clue to discover the distribution of the battery levels.

Lemma 4.3.1 Energy levels of all transmitters are stable, i.e., $\lim_{t\to\infty}\mathbb{P}\left\{B_t^{(n)} = \infty\right\} = 0$ *for any* $n \in \{1, 2, \ldots, N\}$.

The proof is given in Appendix C. Note that this lemma also holds for the case when EH rates are only i.i.d. across time, but not i.i.d. across different transmitters.

Following Lemma 4.3.1, we have the next proposition.

Proposition 4.3.1 When $\left\{E_t^{(n)}\right\}$ *are i.i.d. across different transmitters and over time, under the greedy scheduling policy* $\{M_t\}$*, there is*

$$\lim_{t\to\infty}\mathbb{P}\left\{B_t^{(n)} = M_t\right\} = \frac{1}{N}, \tag{4.3}$$

for any $n \in \{1, 2, \ldots, N\}$.

Proof: Since the energy levels of all transmitters are stable as $t \to \infty$ by Lemma 4.3.1, it follows that each transmitter could be chosen to transmit with non-zero probability. Also, given that EH rates are i.i.d. across different transmitters and over time, we obtain by symmetry that $\lim_{t\to\infty} \mathbb{P}\left\{B_t^{(n)} = M_t\right\} = \frac{1}{N}$ for any $1 \leq n \leq N$. ■

Remark 4.3.1 This also implies that the stationary probability that a transmitter achieves the highest energy level among all transmitters is $1/N$. *Then, the waiting time for a transmitter to fulfil a transmission satisfies a geometric distribution with parameter* $1/N$.

In the following, we only keep the transmitter index n when it is necessary for the presentation; otherwise we remove it since all transmitters are identical to our interests. Based on Proposition 4.3.1 and Remark 4.3.1, we obtain the distribution of energy levels at an arbitrary transmitter, which is given as

$$B_t \xrightarrow{d} B = \begin{cases} E_1, & \frac{1}{N}; \\ E_1 + E_2, & \frac{1}{N}\frac{N-1}{N}; \\ E_1 + E_2 + E_3, & \frac{1}{N}\left(\frac{N-1}{N}\right)^2; \\ \cdots, & \cdots, \end{cases} \tag{4.4}$$

as $t \to \infty$, where the notation $\xrightarrow{d}$ denotes the convergence in distribution. In other words, we have

$$B = \sum_{i=1}^{S} E_i, \tag{4.5}$$

where $S \sim Geo(\frac{1}{N})$. Then, we obtain

$$M_t \xrightarrow{d} M = \max_{1\leq n\leq N} \left\{B^{(n)}\right\} \text{ as } t \to \infty, \tag{4.6}$$

in which $B^{(n)}$ is from (4.5) for transmitter n. Next, we first analyze the asymptotic behavior of M when the number of transmitters gets large; and then consider the scaling of the

throughput.

4.3.1.1 Scaling of energy level

It is necessary to discover how the energy level B behaves as $N \to \infty$; then we move on to M. In the next lemma, we present the strong law of large numbers (SLLN) for the random sum B.

Lemma 4.3.2 Given $\mu = \mathbb{E}[E] < \infty$, the stationary energy level B satisfies

$$\frac{B - \mu S}{S} \overset{N\to\infty}{\longrightarrow} 0 \ \textit{a.s.}, \tag{4.7}$$

where $S \sim Geo(\frac{1}{N})$.

The proof is given in Appendix C. Lemma 4.3.2 also implies that $\mathbb{E}[B] = N\mu$. Next, we present the central limit theorem for the random sum B.

Proposition 4.3.2 Given $\{E_t\}$ are i.i.d. and $\mu = \mathbb{E}[E_t] < \infty$, B satisfies

$$\frac{B - \mu S}{\sigma\sqrt{S}} \overset{d}{\to} X, \tag{4.8}$$

as $N \to \infty$, where $X \sim \mathcal{N}(0, 1)$.

The proof is given in Appendix C.

Based on Proposition 4.3.2, we obtain that

$$\frac{M - \mu S}{\sigma\sqrt{S}} = \max_{1\le n\le N}\left\{\frac{B^{(n)} - \mu S}{\sigma\sqrt{S}}\right\} \overset{d}{\to} \max_{1\le n\le N}\{X_n\}, \text{ as } N \to \infty,$$

where $X_n \sim \mathcal{N}(0, 1)$. Moreover, we can further approximate the distribution of $\max_{1\le n\le N}\{X_n\}$ according to the next lemma [10, 19].

Lemma 4.3.3 If $X_n \sim \mathcal{N}(0,1)$ for $1 \leq n \leq N$, the distribution of $Z_N = \max\{X_1, X_2, \ldots, X_N\}$ satisfies

$$\mathbb{P}\left\{a_N(Z_N - b_N) < x\right\} \to \exp(-e^{-x}) \tag{4.9}$$

as $N \to \infty$, where a_N and b_N are normalizing variables, which are given as

$$\begin{aligned} a_N &= \sqrt{2\ln N} \\ b_N &= \sqrt{2\ln N} - \frac{\ln\ln N + \ln 4\pi}{2\sqrt{2\ln N}}. \end{aligned}$$

Based on Lemma 4.3.3, we obtain the following proposition.

Proposition 4.3.3 The optimal transmit power M satisfies

$$a_N\left(\frac{M-\mu S}{\sigma\sqrt{S}} - b_N\right) \xrightarrow{d} Y, \text{ as } N \to \infty, \tag{4.10}$$

where a_N and b_N are given in Lemma 4.3.3, and the CDF of Y is $\exp(-e^{-x})$ for $x \in (-\infty, +\infty)$.

Proof: It can be directly proved by using Proposition 4.3.2 and Lemma 4.3.3. ■

4.3.1.2 Scaling of expected throughput

With the results about the transmission power M, we are now ready to investigate how the average throughput behaves. By Jensen's inequality, an upper bound of the optimal throughput can be derived as

$$\begin{aligned} R^{gr}(N) &= \lim_{t\to\infty} R_t^{gr}(N) = \mathbb{E}\left[\log\left(1+M\right)\right] \\ &\leq \log\left(1+\mathbb{E}\left[M\right]\right) = \widehat{R}^{gr}(N). \end{aligned} \tag{4.11}$$

Note that the upper bound $\widehat{R}^{gr}(N)$ could be very tight when $\mathbb{E}[M]$ is large, and thus we only focus on the behavior of $\widehat{R}^{gr}(N)$. The next lemma [48] is used to bound the mean of M.

Lemma 4.3.4 If $X_n \sim \mathcal{N}(0,1)$ for $1 \leq n \leq N$, then the mean of $Z_N = \max\{X_1, X_2, \ldots, X_N\}$ satisfies

$$\mathbb{E}[Z_N] \leq \sqrt{2\ln N} + o(1) \tag{4.12}$$

for large N, where $o(1)$ denotes the function such that $\lim_{N\to\infty} o(1) < \epsilon$ for any $\epsilon > 0$.

By Lemma 4.3.4, when N is large, we have

$$\mathbb{E}\left[\frac{M-\mu S}{\sigma\sqrt{S}}\right] = \mathbb{E}\left[\max_{1\leq n\leq N}\{X_n\}\right] \leq \sqrt{2\ln N} + 1. \tag{4.13}$$

Therefore, we obtain an approximated upper bound for $\mathbb{E}[M]$, i.e., for large N,

$$\begin{aligned}\mathbb{E}[M] &\lessapprox \mu N + \sigma\mathbb{E}\left[\sqrt{S}\right]\left(\sqrt{2\ln N}+1\right)\\ &= \mu N + o(N).\end{aligned} \tag{4.14}$$

Note that this approximation is more accurate if the variable S is deterministic to be N. Furthermore, we could bound $\mathbb{E}[M]$ from below such that

$$\mu N \leq \mathbb{E}[M],$$

since $\mu N = \mathbb{E}[B] \leq \mathbb{E}[M]$. Finally, it follows that

$$\widehat{R}(N) = O\left(\log(\mu N)\right), \tag{4.15}$$

where $O\left(\log(\mu N)\right)$ denotes the function such that $\lim_{N\to\infty} \frac{O(\log(\mu N))}{\log(\mu N)} < \infty$.

Another centralized scheme considered here is the fixed TDMA, where each user transmits periodically. In this case, the transmission power is $B = \sum_{i=1}^{N} E_i$ for any user, and we have $\mathbb{E}[B] = N\mu$, which implies that the transmission rate grows on the scale of $\log(\mu N)$. Since the gap $\sigma\sqrt{N}\left(\sqrt{2\ln N} + 1\right)$ of the transmission power in (4.14) grows slowly, it is expected that the throughput achieved by TDMA is almost the same as the greedy scheduling when $N \to \infty$. One of the advantages of TDMA compared to the greedy algorithm is that TDMA has less complexity since the controller does not need to track the energy level of each user. The performance of TDMA will be also numerically validated in Section 4.3.3.

4.3.2 Distributed Access

Suppose that the n-th user contents for the channel use with probability q_n at the very beginning of each time slot; then the successful contention probability of the n-th user is

$$Q_n = q_n \prod_{j\neq n}(1 - q_j). \tag{4.16}$$

Here, we assume that channel contention consumes negligible time and energy as we focus on investigating the order-wise throughput performance. If the n-th transmitter successfully occupies the channel, it transmits during the current time slot by using all its available energy (i.e., greedy power utilization). Under this access and power control scheme, the

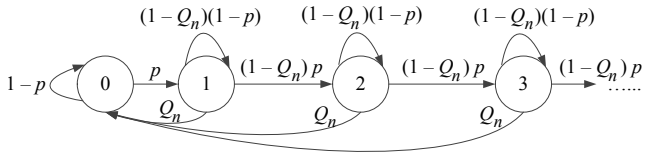

Figure 4.1: The transition of energy levels.

average throughput across the whole system is given by

$$\begin{aligned} R(N) &= \sum_{n=1}^{N} q_n \prod_{j\neq n}(1-q_j)\mathbb{E}\left[\log\left(1+B^{(n)}\right)\right] \\ &\leq \sum_{n=1}^{N} Q_n \log\left(1+\mathbb{E}\left[B^{(n)}\right]\right) \\ &= \widehat{R}_d(N) \end{aligned} \tag{4.17}$$

Again, it is worth noticing that when $\mathbb{E}\left[B^{(n)}\right]$ is large, $R(N) \approx \widehat{R}_d(N)$. Then, we aim to discover the asymptotic behavior of $\widehat{R}_d(N)$.

Following the Bernoulli energy arrival model, the state transition of energy levels is depicted in Fig. 4.1. Accordingly, the transition probability matrix of the energy level is given by

$$W = \begin{bmatrix} 1-p & p & 0 & \cdots \\ Q_n & (1-Q_n)(1-p) & (1-Q_n)p & \\ Q_n & 0 & (1-Q_n)(1-p) & (1-Q_n)p \\ \vdots & & & \ddots \end{bmatrix} \tag{4.18}$$

We can observe that this Markov chain is irreducible and aperiodic. Moreover, we obtain the stationary distribution of energy levels from the following proposition.

Proposition 4.3.4 There exists a unique stationary distribution $\pi = [\pi_0\ \pi_1\ \pi_2 \cdots]$*, where*

$$\pi_0 = \frac{Q_n}{p + Q_n}, \tag{4.19}$$

$$\pi_i = \left(\frac{(1-Q_n)p}{1-(1-Q_n)(1-p)}\right)^i \frac{\pi_0}{1-Q_n}, \tag{4.20}$$

for $i = 1, 2, \ldots$.

The proof is given in Appendix C.

Next, we analyze the scaling laws of the battery energy and the average throughput. Note that

$$\lim_{N\to\infty} Q_n = 0. \tag{4.21}$$

Then, we compute the average energy level as

$$\begin{aligned}
\mathbb{E}[B^{(n)}] =& \frac{p}{1-(1-Q_n)(1-p)} \frac{Q_n}{p+Q_n} + \sum_{i=2}^{\infty} i \left(\frac{(1-Q_n)p}{1-(1-Q_n)(1-p)}\right)^i \frac{\pi_0}{1-Q_n} \\
=& \frac{p}{Q_n + p}\left(\frac{p}{Q_n} + 1 - p\right) \\
\approx& pQ_n^{-1},
\end{aligned} \tag{4.22}$$

when Q_n is small. If all users apply the same channel contention strategy, it follows that

$$\begin{aligned}
\widehat{R}_d(N) &= \sum_{n=1}^{N} Q_n \log\left(1 + \mathbb{E}\left[B^{(n)}\right]\right) \\
&= NQ_n \log\left(1 + \mathbb{E}\left[B^{(n)}\right]\right) \\
&\approx NQ_n \log\left(pQ_n^{-1}\right)
\end{aligned} \tag{4.23}$$

when $N \to \infty$. Next, we consider some specific random access strategies and discuss how the multiuser energy diversity can be exploited.

4.3.2.1 ALOHA (uniform contention)

When transmitters contend with probability $q_n = 1/N^\alpha$, for $\alpha > 0$, we obtain $Q_n = \frac{1}{N^\alpha}\left(1 - \frac{1}{N^\alpha}\right)^{N-1}$. The next proposition provides the optimal α which maximizes (4.23).

Proposition 4.3.5 Define α^* as

$$\alpha^* = \arg\max_{\alpha>0} \widehat{R}_d(N), \tag{4.24}$$

for large N. Then, there is $\alpha^* = 1$, and the maximum average throughput is given as

$$\widehat{R}_d(N) \approx \frac{1}{e}\log\left(peN\right). \tag{4.25}$$

Proof: Note that we have

$$\begin{aligned}\lim_{N\to\infty}\left(1 - \frac{1}{N^\alpha}\right)^{N-1} &= \lim_{N\to\infty} e^{(N-1)\log\left(1-\frac{1}{N^\alpha}\right)} \\ &\approx \lim_{N\to\infty} e^{-\frac{N-1}{N^\alpha}} \\ &= \lim_{N\to\infty} e^{-N^{1-\alpha}},\end{aligned}$$

where the second approximation results from $\lim_{x\to 0}\frac{\log(1+x)}{x} = 1$. Thus, we obtain

$$\lim_{N\to\infty}\left(1 - \frac{1}{N^\alpha}\right)^{N-1} = \begin{cases} 0, & 0 < \alpha < 1; \\ e^{-1}, & \alpha = 1; \\ 1, & 1 < \alpha. \end{cases}$$

Next, we check $\widehat{R}_d(N)$ in (4.23) for all possible α.

When $0 < \alpha < 1$ and N is large, we obtain

$$\widehat{R}_d(N) \approx NQ_n \log\left(pQ_n^{-1}\right) = \frac{N^{1-\alpha}}{e^{N^{1-\alpha}}} \log\left(pe^{N^{1-\alpha}}\right) \to 0$$

as $N \to \infty$.

When $1 < \alpha$, similar to the case $0 < \alpha < 1$, it can be verified that $\widehat{R}_d(N) \to 0$ as $N \to \infty$.

When $\alpha = 1$, we obtain $Q_n \to \frac{1}{N}\frac{1}{e}$. It follows that $\mathbb{E}[B] \approx peN$, which leads to (4.25). In all, the proposition is proved. ■

4.3.2.2 Energy-aware contention

Here, we consider an energy-aware contention such that the transmitter only contends for the channel use when the battery $B \geq pe \log N$, which means that the transmitter acts only when its energy level is higher than a threshold. If the energy level meets the threshold, the transmitter will contend for the channel use with probability $\frac{1}{N}$. Therefore, the overall channel contention probability for user n is given by

$$\begin{aligned} q_n =& \frac{1}{N}\mathbb{P}\left\{B^{(n)} \geq pe \log N\right\} \\ =& \frac{1}{N}\frac{p}{p+Q_n}\left(\frac{(1-Q_n)p}{1-(1-Q_n)(1-p)}\right)^{pe\log N}. \end{aligned}$$

It is expected that the energy-aware contention strategy is strictly better than ALOHA in terms of average throughput. Note that when N is large, it follows that

$$q_n \approx \frac{1-\epsilon}{N},$$

where ϵ is dependent on N. Then, the total number of transmitters that would join channel

contentions is $N(1-\epsilon)$. The successful channel contention for user n is given by

$$Q_n = \frac{1-\epsilon}{N}\left(1-\frac{1-\epsilon}{N}\right)^{N(1-\epsilon)-1} \approx \frac{1-\epsilon}{N}e^{-(1-\epsilon)^2},$$

since $\lim_{N\to\infty}\left(1-\frac{1-\epsilon}{N}\right)^{N(1-\epsilon)-1} = e^{-(1-\epsilon)^2}$. Therefore, we obtain

$$\mathbb{E}[B] \approx \frac{e^{(1-\epsilon)^2}}{1-\epsilon}pN,$$

and

$$\widehat{R}_d(N) \approx (1-\epsilon)e^{-(1-\epsilon)^2}\log\left(\frac{e^{(1-\epsilon)^2}}{1-\epsilon}pN\right). \tag{4.26}$$

Unfortunately, it is extremely difficult to directly prove that when N is large, the average throughput in (4.26) should be strictly larger than that in (4.25). Instead, we numerically verify this result by testing the following two normalized functions based on (4.25) and (4.26):

$$f_1(x) = \log(N),\ f_2(x) = \frac{1}{x}\log(xN),$$

for $x \in (0,1]$, where N is a large number such that $N > \frac{1}{x}$ for all chosen x. In Fig. 4.2, we draw the values of functions f_1 and f_2 over $(0,1]$, where the minimum x is set to be 0.001, and N is set to be 1001. Obviously, f_2 stays above f_1 over the entire region as long as N is large enough.

From the above observation, we conclude that when N is large, the throughput in (4.26) could be strictly larger than that in (4.25). In addition, we also numerically compare the throughput performance of different contention strategies in the next subsection, where it will be shown again that the improved energy-aware contention scheme outperforms the

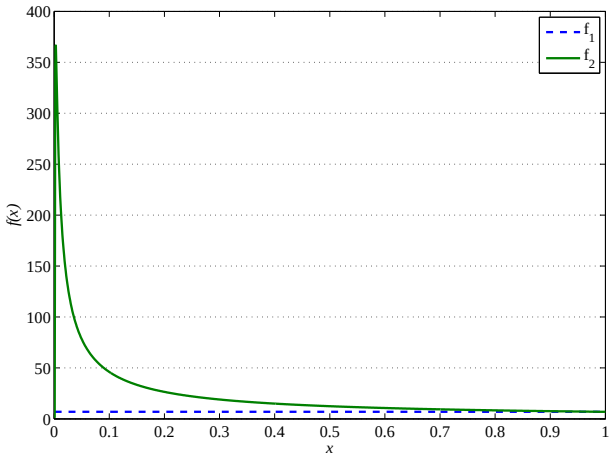

Figure 4.2: Comparison of functions f_1 and f_2.

ALOHA uniform scheme.

4.3.3 Discussions

In this subsection, we provide more insights on the average throughput based on the results in the previous two subsections, and discuss where the multiuser energy diversity gain comes from.

First, we numerically compare the average throughput under different centralized and distributed schemes in Fig. 4.3. Here, we set two benchmarks. The first benchmark is the throughput when each user has a fix power supply under the centralized access scheme. This is also equivalent to the point-to-point case since the throughput is always a constant over an AWGN channel given a fixed transmission power. The second benchmark is the throughput achieved by a point-to-point EH communication system over an additive Gaussian channel, where the transmitter adopts a greedy power utilization stratety[3]. The second benchmark is lower than the first one due to the concavity of the throughput function and

[3]Note that for Gaussian channel, the greedy power utilization strategy is not a capacity achieving power allocation strategy. The capacity achieving power allocation strategy is discussed in [47, 57], and the corresponding throughput is the same as the first benchmark.

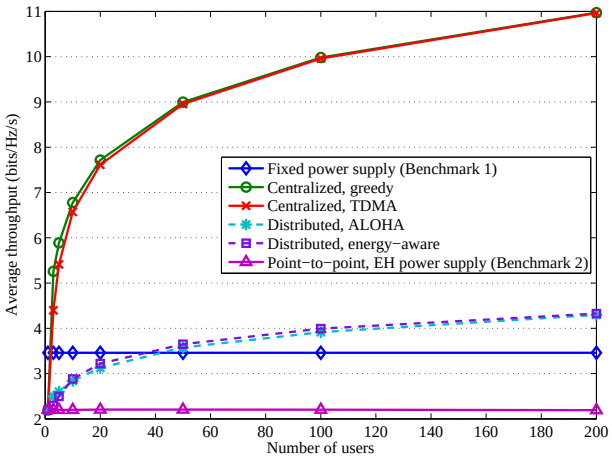

Figure 4.3: The average throughput in different access schemes.

the randomness of the transmission power.

We observe that all the scheduling schemes discussed in the previous two subsections can somehow exploit the multiuser energy diversity. For the centralized schemes, the greedy scheduling can achieve better performance than TDMA, while their performances get close when N is large, which agrees with our discussion in Section 4.3.1. For the distributed schemes, the energy-aware access achieves a slightly higher throughput than ALOHA, which also validates our analysis in the previous section. In addition, we also observe that the distributed scheme has a throughput loss against centralized schemes as $N \to \infty$, which results from the channel contentions in random access schemes. This observation is similar to the case with conventional multiuser diversity in fading channels, where the ALOHA has a throughput loss $\frac{1}{e}$ compared to the centralized protocol [46].

Moreover, in Fig. 4.4, we numerically compare the average throughput when the transmission power is normalized by the average waiting time, which is N. Such normalization eliminates the throughput contribution of the increase of total available energy accumulated over time. We observe that only the centralized greedy scheduling can achieve a

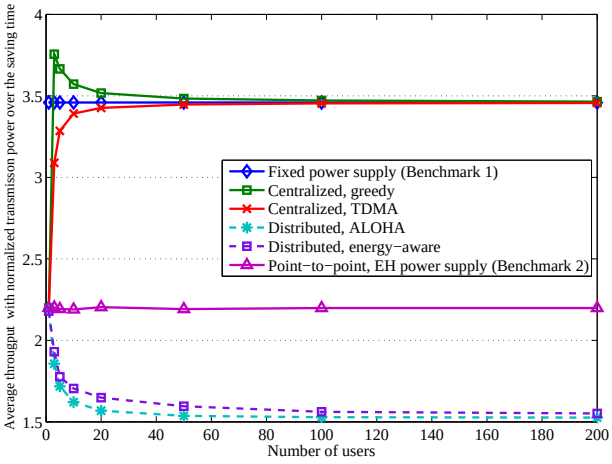

Figure 4.4: The average throughput with normalized transmission power in different access schemes.

throughput gain over both benchmarks, and TDMA only has a gain over the second benchmark while it can approach the first benchmark. This implies that compared to the second benchmark, the multiuser energy diversity gain comes from two aspects:

1. The increase in total available energy accumulated over time (power gain);

2. The improvement in effective transmission power (diversity gain):

   - for the greedy scheduling, improved from $E_t^{(1)}$ to $\max_{1\leq n\leq N} \frac{1}{N} B_t^{(n)}$;
   - for TDMA, improved from $E_t^{(1)}$ to $\frac{1}{N}\sum_{t=1}^{N} E_t^{(1)}$.

Note that the normalized average throughput of two centralized schemes is "upper-bounded" by that achieved by a fixed power supply as $N \to \infty$, which implies that multiuser diversity gain mainly comes from the power gain when N is large. We also observe that the distributed schemes have a "negative" diversity gain when we eliminate the effect of energy accumulation. It implies that the ALOHA-based access cannot effectively explore the randomness of energy levels since the users are not coordinated well.

Next, we make some remarks on the asymptotic distributions of the transmission power under either centralized or distributed access schemes. The main result is given in the next proposition.

Proposition 4.3.6 When EH rates are i.i.d. across transmitters and over time, the transmission power has a heavy-tailed distribution when $N \to \infty$ under either the centralized optimal access scheme or the distributed access scheme.

The definition of a heavy-tailed distribution is as follows (see Appendix 5 in [5]): The random variable B has a heavy-tailed distribution if

$$\lim_{x\to\infty} e^{\lambda x}\mathbb{P}\left\{B > x\right\} = \infty \tag{4.27}$$

for all $\lambda > 0$. Thus, the key idea of the proof is to verify that the asymptotic distribution of the transmission power satisfies (4.27), and the detailed proof is given as follows.

Proof: For the centralized case, it is straightforward to show that the distribution $\exp\left(-e^{-x}\right)$ is "heavy-tailed". For the distributed case, we have

$$\mathbb{P}\left\{B > x\right\} = \left(\frac{(1-Q_n)p}{1-(1-Q_n)(1-p)}\right)^x \cdot \frac{1-(1-Q_n)(1-p)}{Q_n}\frac{\pi_0}{(1-Q_n)} \to 1$$

as $N \to \infty$, for $x > 2$, due to (4.21). Therefore, we have

$$\lim_{x\to\infty}\lim_{N\to\infty} e^{\lambda x}\mathbb{P}\left\{B > x\right\} = \lim_{x\to\infty} e^{\lambda x} = \infty$$

for any $\lambda > 0$, which proves the proposition. ■

Remark 4.3.2 Proposition 4.3.6 considers the probability of "rare event" that some transmitter has a very high instantaneous transmission power, which leads to a burst throughput.

4.4 Conclusions

In this chapter, the multiuser energy diversity gain was investigated. For centralized access schemes, it was shown that the average throughput increases on a scale of $\log(\mu N)$, and the multiuser diversity gain comes from two aspects: the increase of total available energy accumulated over time; and the improvement in effective transmission power. Under the distributed access schemes, the average throughput could increase as well when the access strategy is carefully designed.

5. CONCLUSION AND FUTURE DIRECTION*

In this dissertation, we studied the opportunistic scheduling for EH-based wireless networks in two different scenarios and investigate the multiuser energy diversity.

The first scenario is an *ad hoc* network with multiple transmitter-receiver pairs, in which all transmitters are capable of harvesting renewable energy from the environment and compete for one shared channel by random access. A distributed opportunistic scheduling (DOS) framework with two-stage probing and save-then-transmit energy utilization was proposed by quantifying the roles of both the energy and channel state information.

The second is an uplink transmission scenario under a heterogeneous network hierarchy, where each EH-based mobile user (MU) has deterministic access to the large network, but only dynamic access to a small network with certain probability shared by multiple MUs. Applying a simple yet efficient "save-then-transmit" scheme, the throughput maximization problem is cast as a "rate-of-return" optimal stopping problem. The optimal solution is investigated for the general Markovian channel states and energy arrivals, followed by the i.i.d. case.

Finally, the scaling law of the throughput of the EH-based network is studied under both centralized and distributed access schemes. It is found that the multiuser diversity gain comes from two aspects: the increase of total harvested energy accumulated over time; and the improvement in effective transmission power.

Besides the above studies on EH-based wireless communications, this new and high-potential subject still has many research problems that are worth of investigating. We

*Part of this chapter is reprinted, with permission, from [Hang Li, Jie Xu, Rui Zhang and Shuguang Cui, "A general utility optimization framework for energy harvesting based wireless communications." *Communications Magazine, IEEE*, 53(4):79–85, 2015]

briefly present some promising directions or future work as the closing of this dissertation.

1) Case with EH Receiver. Most existing studies on EH based communications have considered EH at the transmitter side only, by assuming that the receivers are powered by a stable energy supply. When the receiver is powered by EH, a similar EH constraint like in the EH transmitter case needs to be applied, but with a key difference that the energy used at the receiver is for decoding the signal instead of sending it at the transmitter. As a preliminary work along this new direction, [41] showed that the detection and decoding operations dominate the energy cost for EH receivers, and the energy cost is nondecreasing over both the sampling rate and the decoding complexity. Thus, the communication rate should be designed by taking into account the energy availability at both the EH transmitter and EH receiver.

2) Cross-Layer Design. In practical systems, the data arrives at the transmitter with random timing and amounts in general. In such cases, the transmitter needs to deal with the uncertainties in both energy and data arrivals, and it is thus beneficial to jointly schedule the energy usage and data packet transmission based on the channel conditions [28]. As another example, consider a wireless network with multiple EH transmitters sharing the same limited channel resources for communications, for which there is a necessity for the design of energy-aware medium access control (MAC) to optimize the system throughput. In general, a cross-layer design approach should be further investigated to achieve more efficient operation of EH based communication systems.

3) Hybrid Energy Sources and Imperfect Energy Storage Devices. Due to the random and intermittent characteristics of practical EH sources, using renewable energy alone may not be sufficient to provide reliable operation of wireless systems with large power demands, e.g., in base stations. To maintain their reliable operations, it is wise to use hybrid energy sources by efficiently integrating the renewable energy with the conventional energy (such as fuel generators). On the other hand, energy storage devices (ESDs) with

imperfect charging-discharging efficiency and a finite capacity may be employed in the system. In general, how to optimally design the energy management policies with hybrid energy sources and/or imperfect ESDs to achieve the maximum utility in EH based communications still remains largely open, while some initial results have been obtained [14].

4) RF EH with Dedicated WET. In addition to the conventional EH sources such as wind and solar power as well as ambient radio frequency (RF) transmissions, deploying dedicated power transmission nodes in the network for delivering controllable energy over the air to distributed communication devices (e.g., sensors) has drawn growing interests recently. The devices can either harvest RF energy from the signal transmitted by the power transmission nodes, or decode the information in it, or even use part of the energy harvested to decode the information and the remaining energy to transmit or relay other information [64]. The RF signal enabled WET is a very promising technique for powering low-power wireless communication devices such as those in sensor networks and personal/body area networks, even with its practically limited energy transfer efficiency, which actually could be alleviated by some new techniques such as highly directional massive MIMO [64]. Clearly, such WET powered communication brings a new avenue for the future research of EH based systems.

REFERENCES

[1] Norman Abramson. The throughput of packet broadcasting channels. *Communications, IEEE Transactions on*, 25(1):117–128, 1977.

[2] Jeffrey G Andrews. Seven ways that hetnets are a cellular paradigm shift. *Communications Magazine, IEEE*, 51(3):136–144, 2013.

[3] Jeffrey G Andrews, Holger Claussen, Mischa Dohler, Sundeep Rangan, and Mark C Reed. Femtocells: past, present, and future. *Selected Areas in Communications, IEEE Journal on*, 30(3):497–508, 2012.

[4] Matthew Andrews, Krishnan Kumaran, Kavita Ramanan, Alexander Stolyar, Phil Whiting, and Rajiv Vijayakumar. Providing quality of service over a shared wireless link. *Communications Magazine, IEEE*, 39(2):150–154, 2001.

[5] Søren Asmussen. *Applied probability and queues*, volume 51. Springer Science & Business Media, 2003.

[6] Nicole Bäuerle and Ulrich Rieder. *Markov decision processes with applications to finance*. Springer Science & Business Media, 2011.

[7] Marc Beaudin, Hamidreza Zareipour, Anthony Schellenberglabe, and William Rosehart. Energy storage for mitigating the variability of renewable electricity sources: An updated review. *Energy for Sustainable Development*, 14(4):302–314, 2010.

[8] Mehdi Bennis, Meryem Simsek, Andreas Czylwik, Walid Saad, Stefan Valentin, and Merouane Debbah. When cellular meets wifi in wireless small cell networks. *Communications Magazine, IEEE*, 51(6):44–50, 2013.

[9] Patrick Billingsley. *Probability and measure*. John Wiley & Sons, 2008.

[10] Anton Bovier. Extreme values of random processes. *Lecture Notes Technische Universität Berlin*, 2005.

[11] Stephen Boyd and Lieven Vandenberghe. *Convex optimization*. Cambridge University Press, 2004.

[12] Vikram Chandrasekhar and Jeffrey G Andrews. Uplink capacity and interference avoidance for two-tier femtocell networks. *Wireless Communications, IEEE Transactions on*, 8(7):3498–3509, 2009.

[13] Dipak Chatterjee. *Real analysis*. PHI Learning Pvt. Ltd., 2012.

[14] Yeow-Khiang Chia, Sumei Sun, and Rui Zhang. Energy cooperation in cellular networks with renewable powered base stations. In *Wireless Communications and Networking Conference (WCNC)*, pages 2542–2547. IEEE, 2013.

[15] I Chih-Lin, Corbett Rowell, Shuangfeng Han, Zhikun Xu, Gang Li, and Zhengang Pan. Toward green and soft: a 5g perspective. *Communications Magazine, IEEE*, 52(2):66–73, 2014.

[16] Susan Combs. The energy report. 2008. `http://www.window.state.tx.us/specialrpt/energy`, accessed March 2014.

[17] Bert JM De Vries, Detlef P Van Vuuren, and Monique M Hoogwijk. Renewable energy sources: Their global potential for the first-half of the 21st century at a global level: an integrated approach. *Energy Policy*, 35(4):2590–2610, 2007.

[18] Harpreet S Dhillon, Ying Li, Pavan Nuggehalli, Zhouyue Pi, and Jeffrey G Andrews. Fundamentals of heterogeneous cellular networks with energy harvesting. *Wireless Communications, IEEE Transactions on*, 13(5):2782–2797, 2014.

[19] Paul Embrechts, Thomas Mikosch, and Claudia Klüppelberg. Modelling extremal events: for insurance and finance. 1997.

[20] Thomas S. Ferguson. Optimal stopping and applications. 2006. Lecture notes, http://www.math.ucla.edu/~tom/Stopping/Contents.html, accessed October 2013.

[21] Thomas S Ferguson and James B MacQueen. Some time-invariant stopping rule problems. *Optimization*, 23(2):155–169, 1992.

[22] Robert G Gallager. *Discrete stochastic processes*. Kluwer Academic Publishers, 1996.

[23] David Gamarnik and John Tsitsiklis. 6.436j fundamentals of probability, Fall 2008. Massachusetts Institute of Technology: MIT OpenCourseWare, http://ocw.mit.edu, accessed December 2015.

[24] Amitabha Ghosh, Nitin Mangalvedhe, Rapeepat Ratasuk, Bishwarup Mondal, Mark Cudak, Eugene Visotsky, Timothy A Thomas, Jeffrey G Andrews, Ping Xia, Han Shin Jo, et al. Heterogeneous cellular networks: from theory to practice. *Communications Magazine, IEEE*, 50(6):54–64, 2012.

[25] Andrea J Goldsmith and Pravin P Varaiya. Capacity of fading channels with channel side information. *Information Theory, IEEE Transactions on*, 43(6):1986–1992, 1997.

[26] Xiaowen Gong, TPS Chandrashekhar, Junshan Zhang, and H Vincent Poor. Opportunistic cooperative networking: to relay or not to relay? *Selected Areas in Communications, IEEE Journal on*, 30(2):307–314, 2012.

[27] Jayavardhana Gubbi, Rajkumar Buyya, Slaven Marusic, and Marimuthu Palaniswami. Internet of things (iot): A vision, architectural elements, and future directions. *Future Generation Computer Systems*, 29(7):1645–1660, 2013.

[28] D. Gunduz, K. Stamatiou, N. Michelusi, and M. Zorzi. Designing intelligent energy harvesting communication systems. *Communications Magazine, IEEE*, 52(1):210–216, January 2014.

[29] Mesud Hadzialic, Branko Dosenovic, Merim Dzaferagic, and Jasmin Musovic. Cloud-ran: innovative radio access network architecture. In *ELMAR, 55th International Symposium*, pages 115–120. IEEE, 2013.

[30] Chin Keong Ho and Rui Zhang. Optimal energy allocation for wireless communications with energy harvesting constraints. *Signal Processing, IEEE Transactions on*, 60(9):4808–4818, 2012.

[31] Chuan Huang, Rui Zhang, and Shuguang Cui. Throughput maximization for the gaussian relay channel with energy harvesting constraints. *Selected Areas in Communications, IEEE Journal on*, 31(8):1469–1479, 2013.

[32] Kaibin Huang. Spatial throughput of mobile ad hoc networks powered by energy harvesting. *Information Theory, IEEE Transactions on*, 59(11):7597–7612, 2013.

[33] Fabio Iannello, Osvaldo Simeone, and Umberto Spagnolini. Medium access control protocols for wireless sensor networks with energy harvesting. *Communications, IEEE Transactions on*, 60(5):1381–1389, 2012.

[34] Vikram Kanodia, Ashutosh Sabharwal, and E Knightly. Moar: a multi-channel opportunistic auto-rate media access protocol for ad hoc networks. In *Broadband Networks, First International Conference on*, pages 600–610. IEEE, 2004.

[35] Mohamed Kashef and Anthony Ephremides. Optimal packet scheduling for energy harvesting sources on time varying wireless channels. *Communications and Networks, Journal of*, 14(2):121–129, 2012.

[36] Hongseok Kim and Gustavo De Veciana. Leveraging dynamic spare capacity in wireless systems to conserve mobile terminals' energy. *Networking, IEEE/ACM Transactions on*, 18(3):802–815, 2010.

[37] Hang Li, Chuan Huang, Ping Zhang, Shuguang Cui, and Junshan Zhang. Distributed opportunistic scheduling for energy harvesting based wireless networks: a two-stage probing approach. *Networking, IEEE/ACM Transactions on*, 24(3):1618–1631, June 2016.

[38] Xin Liu, Edwin KP Chong, and Ness B Shroff. A framework for opportunistic scheduling in wireless networks. *Computer Networks*, 41(4):451–474, 2003.

[39] David Lopez-Perez, Ismail Guvenc, Guillaume De La Roche, Marios Kountouris, Tony QS Quek, and Jie Zhang. Enhanced intercell interference coordination challenges in heterogeneous networks. *Wireless Communications, IEEE*, 18(3):22–30, 2011.

[40] Shixin Luo, Rui Zhang, and Teng Joon Lim. Optimal save-then-transmit protocol for energy harvesting wireless transmitters. *Wireless Communications, IEEE Transactions on*, 12(3):1196–1207, 2013.

[41] Hajar Mahdavi-Doost and Roy D Yates. Fading channels in energy-harvesting receivers. In *Information Sciences and Systems (CISS), 48th Annual Conference on*, pages 1–6. IEEE, 2014.

[42] Bhargav Medepally, Neelesh B Mehta, and Chandra R Murthy. Implications of energy profile and storage on energy harvesting sensor link performance. In *Global Telecommunications Conference*, pages 1–6. IEEE, 2009.

[43] Adarsh B Narasimhamurthy, Cihan Tepedelenlioğlu, and Yuan Zhang. Multi-user diversity with random number of users. *Wireless Communications, IEEE Transactions*

on, 11(1):60–64, 2012.

[44] Omur Ozel, Kaya Tutuncuoglu, Jing Yang, Sennur Ulukus, and Aylin Yener. Transmission with energy harvesting nodes in fading wireless channels: Optimal policies. *Selected Areas in Communications, IEEE Journal on*, 29(8):1732–1743, 2011.

[45] Goran Peskir and Albert Shiryaev. *Optimal stopping and free-boundary problems*. Springer, 2006.

[46] Xiangping Qin and Randall A Berry. Distributed approaches for exploiting multiuser diversity in wireless networks. *Information Theory, IEEE Transactions on*, 52(2):392–413, 2006.

[47] Ramachandran Rajesh, Vinod Sharma, and Pramod Viswanath. Capacity of gaussian channels with energy harvesting and processing cost. *Information Theory, IEEE Transactions on*, 60(5):2563–2575, 2014.

[48] Justin Romberg. Maximum of a sequence of gaussian random variables. 2012. `http://cnx.org/contents/8bd316d8-6442-4f5a-a597-aef1d6202f87@1`, accessed March 2015.

[49] Sumudu Samarakoon, Mehdi Bennis, Walid Saad, and Matti Latva-Aho. Enabling relaying over heterogeneous backhauls in the uplink of femtocell networks. In *Modeling and Optimization in Mobile, Ad Hoc and Wireless Networks (WiOpt), 10th International Symposium on*, pages 75–80. IEEE, 2012.

[50] Alireza Seyedi and Biplab Sikdar. Energy efficient transmission strategies for body sensor networks with energy harvesting. *Communications, IEEE Transactions on*, 58(7):2116–2126, 2010.

[51] Vinod Sharma, Utpal Mukherji, Vinay Joseph, and Shrey Gupta. Optimal energy management policies for energy harvesting sensor nodes. *Wireless Communications,*

IEEE Transactions on, 9(4):1326–1336, 2010.

[52] Tao Shu and Marwan Krunz. Throughput-efficient sequential channel sensing and probing in cognitive radio networks under sensing errors. In *Mobile Computing and Networking, 15th Annual International Conference on*, pages 37–48. ACM, 2009.

[53] Wolfgang Stadje. An optimal stopping problem with two levels of incomplete information. *Mathematical Methods of Operations Research*, 45(1):119–131, 1997.

[54] Sujesha Sudevalayam and Purushottam Kulkarni. Energy harvesting sensor nodes: survey and implications. *Communications Surveys & Tutorials, IEEE*, 13(3):443–461, 2011.

[55] PS Thejaswi, Junshan Zhang, Man-On Pun, H Vincent Poor, and Dong Zheng. Distributed opportunistic scheduling with two-level probing. *Networking, IEEE/ACM Transactions on*, 18(5):1464–1477, 2010.

[56] David Tse and Pramod Viswanath. *Fundamentals of wireless communication*. Cambridge University Press, 2005.

[57] Sennur Ulukus, Aylin Yener, Elza Erkip, Osvaldo Simeone, Michele Zorzi, Pulkit Grover, and Kaibin Huang. Energy harvesting wireless communications: a review of recent advances. *Selected Areas in Communications, IEEE Journal on*, 33(3):360–381, 2015.

[58] Pramod Viswanath, David N. C. Tse, and Rajiv Laroia. Opportunistic beamforming using dumb antennas. *Information Theory, IEEE Transactions on*, 48(6):1277–1294, 2002.

[59] Hui Wang. Introduction to stochastic control theory, chapter 3. 2006. `http://www.dam.brown.edu/people/huiwang/classes/am226/Archive/stop.pdf`, accessed April 2015.

[60] Xiaofei Wang, Athanasios V Vasilakos, Min Chen, Yunhao Liu, and Ted Taekyoung Kwon. A survey of green mobile networks: opportunities and challenges. *Mobile Networks and Applications*, 17(1):4–20, 2012.

[61] David Williams. *Probability with martingales*. Cambridge University Press, 1991.

[62] Ping Xia, Vikram Chandrasekhar, and Jeffrey G Andrews. Open vs. closed access femtocells in the uplink. *Wireless Communications, IEEE Transactions on*, 9(12):3798–3809, 2010.

[63] Qinqing Zhang and Saleem A Kassam. Finite-state markov model for rayleigh fading channels. *Communications, IEEE Transactions on*, 47(11):1688–1692, 1999.

[64] Rui Zhang and Chin Keong Ho. Mimo broadcasting for simultaneous wireless information and power transfer. *Wireless Communications, IEEE Transactions on*, 12(5):1989–2001, 2013.

[65] Dong Zheng. *Physical-layer aware control and optimization in stochastic wireless networks*. PhD thesis, Arizona State University. 2007.

[66] Dong Zheng, Weiyan Ge, and Junshan Zhang. Distributed opportunistic scheduling for ad hoc networks with random access: an optimal stopping approach. *Information Theory, IEEE Transactions on*, 55(1):205–222, 2009.

APPENDIX A

SOME PROOFS FOR CHAPTER 2

A.1 Proof of Proposition 2.3.1

For the first part of Proposition 2.3.1, it follows by Theorem 1 in Chapter 3 of [20] that $N^*(\lambda)$ exists and $S^*(\lambda)$ is attained by this $N^*(\lambda)$ if the following two conditions are satisfied:

(C1) $\limsup_{N\to\infty} r_N(\lambda) \leq r_{-\infty}(\lambda)$ a.s.;

(C2) $\mathbb{E}\left[\sup_{N\geq 1} r_N(\lambda)\right] < \infty$,

where $r_N(\lambda)$ is given by (2.4). As we pointed out in Section 3.2.1, the energy level $B_{N,0}$ is stationary for $N \geq 1$. Although $\{R_N(M_N^*)\}_{N\geq 1}$ are independent, it may not be identically distributed with respect to h_N and $B_{N,0}$. However, it is not too difficult to show that (C1) and (C2) hold. The idea is that we first consider that every transmitter has the same statistics; then we apply the channel contention probability as the summation coefficients over all transmitters.

For (C1), if we assume that all transmitters have the same statistics as transmitter i, then $\{R_N^i(M_N^*)\}_{N\geq 1}$ become i.i.d.. Since $\mathbb{E}\left[R_N^i(M_N^*)\right] < \infty$ according to Section 3.2.2, and the accumulated cost $\lambda T_N = \lambda l\left(K_N + \sum_{n=1}^{N-1}(K_n + M_n^*)\right) \to \infty$ as $N \to \infty$ a.s., we obtain that $\mathbb{P}\left\{\limsup_{N\to\infty} r_N^i(\lambda) = -\infty\right\} = 1$. Recall from Section 3.2.1 that the channel is occupied by transmitter i with probability Q_i and $\sum_{i=1}^{I} \frac{Q_i}{Q} = 1$, we obtain that

$$1 = \sum_{i=1}^{I} \frac{Q_i}{Q} \mathbb{P}\left\{\limsup_{N\to\infty} r_N^i(\lambda) = -\infty\right\} = \mathbb{P}\left\{\limsup_{N\to\infty} r_N(\lambda) = -\infty\right\},$$

which proves that (C1) holds.

For (C2), it can be shown that

$$\begin{aligned}\mathbb{E}\left[\sup_{N\geq 1} r_N^i(\lambda)\right] &= \mathbb{E}\left[\sup_{N\geq 1}\left(\left(R_N^i(M_N^*)-\lambda\right)L-\lambda T_N\right)\right] \\ &\leq \mathbb{E}\left[\sup_{N\geq 1}\left(R_N^i(M_N^*)-\lambda(lN+L)\right)\right], \end{aligned} \tag{A.1}$$

due to the fact that $K_n \geq 1$ and $M_n^* \geq 0$ for $1 \leq n \leq N$. Since $\mathbb{E}\left[\left(R_N^i(M_N^*)\right)^2\right] < \infty$, it follows that the right-hand side of (B.1) is finite by Theorem 1 in Chapter 4 of [20]. Similar to the technique in the proof of (C1), we have

$$\mathbb{E}\left[\sup_{N\geq 1} r_N(\lambda)\right] = \sum_{i=1}^{I}\frac{Q_i}{Q}\mathbb{E}\left[\sup_{N\geq 1} r_N^i(\lambda)\right] < \infty,$$

which shows that (C2) also holds.

For the second part, we know that with the cost $\lambda l K_N$ at the N-th CP for any $N \geq 1$, the successful transmitter could choose one of three actions: transmits immediately with reward $(R_N(0)-\lambda)L$; or gives up the channel immediately, and obtains the optimal expected net reward $S^*(\lambda)$ based on the property of time invariance described in Section 2.3.1; or starts EP and obtains the expected net reward $\mathbb{E}\left[U_1(\mathcal{F}_{N,1}) \mid \mathcal{F}_{N,0}\right]$. Thus, by the optimal stopping theory [20, 21], $S^*(\lambda)$ satisfies the *optimality equation* under (C2) as

$$S^*(\lambda) = -\lambda l K_N + \max\left\{S^*(\lambda), (R_N(0)-\lambda)L, E\left[U_1(\mathcal{F}_{N,1}) \mid \mathcal{F}_{N,0}\right]\right\},$$

which is equivalent to (2.10).

A.2 Proof of Proposition 2.3.2

For 1), we show the concavity of function $y(x)$ by checking its second-order derivative over $[0, 1)$, which is given by

$$y''(x) = -\frac{(a+b)^2}{(1-x)\left[a+1+(b-1)x\right]^2} \leq 0.$$

Therefore, $y(x)$ is concave over $[0, 1)$ [11]. To prove the second part of 1), we check the first-order derivative of $y(x)$, which is given by

$$y'(x) = -\log\left(1+\frac{a+bx}{1-x}\right) + \frac{a+b}{1-x+a+bx}. \tag{A.2}$$

It is easy to see that as $x \to 1^-$, the first term of the right-hand side of (A.2) goes to negative infinity, while the second term is bounded. Hence, $y'(x)$ is strictly negative as $x \to 1^-$. Therefore, part 1) is proved.

Next, we prove 2). By checking the second-order derivative of $g(x)$, we obtain

$$g''(x) = -\frac{a^2}{(1-x)(a+1-x)^2} \leq 0,$$

which implies that $g(x)$ is concave. For the second part of 2), we consider the first-order derivative of $g(x)$, which is given by

$$g'(x) = -\log\left(1+\frac{a}{1-x}\right) + \frac{a}{1-x+a}. \tag{A.3}$$

Since $g''(x) \leq 0$, it follows that

$$\max_{0\leq x<1} g'(x) = g'(0) = -\log(1+a) + \frac{a}{1+a}.$$

Moreover, due to the fact that $\frac{\mathrm{d}}{\mathrm{d}a}\left(-\log\left(1+a\right)+\frac{a}{1+a}\right) = -\frac{a}{(1+a)^2} \leq 0$ for arbitrary $a \geq 0$, we obtain

$$\max_{0\leq x<1} g'(x) = g'(0) \leq \left(-\log\left(1+a\right)+\frac{a}{1+a}\right)\Big|_{a=0} = 0,$$

which proves the second part of 2).

A.3 Proof of Proposition 2.3.3

According to Part 1) of Proposition 2.3.2, we obtain that $G(\rho)$ is concave over $\rho \in [0,1)$, which means that $G'(\rho) = \frac{\mathrm{d}G(\rho)}{\mathrm{d}\rho}$ is decreasing over $[0,1)$ and attains its maximum at $\rho = 0$. Then, finding the maximum of $G(\rho)$ boils down to two cases:

1. $G'(\rho)|_{\rho=0} < 0$: It follows that $G(\rho)$ is decreasing over $[0,1)$, and $\rho^* = 0$ is the optimum.

2. $G'(\rho)|_{\rho=0} \geq 0$: The point ρ_0, satisfying $G'(\rho)|_{\rho=\rho_0} = 0$, lies on the right-hand side of $\rho = 0$. By Part 1) of Proposition 2.3.2, $G'(\rho) < 0$ as $\rho \to 1^-$, which implies that $\rho_0 \in [0,1)$. Since the optimal point $\rho^* \leq \frac{B_{max}\delta - B_0}{LE}$ due to (2.13), it follows that $\rho^* = \min\left\{\rho_0, \frac{B_{max}\delta - B_0}{LE}\right\}$.

Note that $G'(\rho)|_{\rho=0} \geq 0$ is equivalent to $\frac{C+D}{1+C} \geq \log(1+C)$, where $C = \frac{|h|^2 B_0}{L\sigma^2} \geq 0$, $D = \frac{|h|^2 E}{\sigma^2} \geq 0$, and $G'(\rho)|_{\rho=\rho_0} = 0$ is equivalent to

$$\log\left(1+\frac{C+D\rho_0}{1-\rho_0}\right) = \frac{C+D}{1-\rho_0+C+D\rho_0}. \tag{A.4}$$

Next, we show that when $\frac{C+D}{1+C} \geq \log(1+C)$, (A.4) has a unique solution. For $\rho \in [0,1)$, the left-hand side of (A.4) is increasing over ρ from $\log\left(1+C\right)$ to $+\infty$. For its right-hand side, we have the following two cases:

1. $D \geq 1$: The right-hand side of (A.4) decreases from $\frac{C+D}{1+C}$ to 1. Since $\frac{C+D}{1+C} \geq \log(1+C)$, there exists a unique solution ρ_0 for (A.4);

2. $0 \leq D < 1$: The right-hand side of (A.4) increases from $\frac{C+D}{1+C}$ to 1. If the first-order derivative of the left-hand side of (A.4) is always greater than that of the right-hand side, there must be only one solution for (A.4) when $\frac{C+D}{1+C} \geq \log(1+C)$. Thus, we check their first-order derivatives: For the left-hand side of (A.4), we obtain

$$\frac{\mathrm{d}}{\mathrm{d}\rho} \log\left(1 + \frac{C + D\rho}{1-\rho}\right) = \frac{C+D}{(1-\rho)\left(1+C+(D-1)\rho\right)}; \tag{A.5}$$

for the right-hand side, we have

$$\frac{\mathrm{d}}{\mathrm{d}\rho}\left(\frac{C+D}{1-\rho+C+D\rho}\right) = \frac{(C+D)(1-D)}{\left(1+C+(D-1)\rho\right)^2}. \tag{A.6}$$

Thus, by calculating the difference between (A.5) and (A.6), we arrive at

$$\begin{aligned} &\frac{C+D}{(1-\rho)\left(1+C+(D-1)\rho\right)} - \frac{(C+D)(1-D)}{\left(1+C+(D-1)\rho\right)^2} \\ =&\frac{(C+D)^2}{(1-\rho)\left(1+C+(D-1)\rho\right)^2} \geq 0. \end{aligned} \tag{A.7}$$

Therefore, there exists a unique solution ρ_0 satisfying (A.4).

In conclusion, the proposition is proved.

Remark: Since it is proved that ρ_0 is unique in (A.4), ρ_0 can be found just by adopting a simple one-dimension searching method, e.g., bisection search.

A.4 Proof of Proposition 2.4.1

To prove this proposition, we construct an axillary "super" Markov chain in which each state is a "super" vector of aggregated energy levels across the whole network, whose

transition probability matrix does not change over time t. Afterwards, we prove that such a "super" Markov chain has a unique steady-state distribution. Then, we show that for any time t in the original Markov chain, one iteration for updating Π_t^i for $1 \leq i \leq I$ in Algorithm 2.1 is equivalent to the evolution of the state distribution in the "super" Markov chain, thereby proving the convergence of Algorithm 2.1.

To construct such a "super" Markov chain, we need to jointly consider the states of energy levels across all transmitters. Let $\mathbf{\Sigma}$ denote the set of all possible battery states over the whole system, i.e.,

$$\mathbf{\Sigma} = \{\mathbf{u} = (u_1 \ \cdots \ u_I) : u_1 \in \mathbf{\Delta}_1, \cdots, u_I \in \mathbf{\Delta}_I\}. \tag{A.8}$$

Furthermore, we use $\mathbf{B}_t$ to denote the battery state of the system at time t, and thus we have $\mathbf{B}_t \in \mathbf{\Sigma}$. Note that the number of elements in $\mathbf{\Sigma}$ is $\left(\left\lceil \frac{B_{max}\delta}{E^1 l} \right\rceil + 1\right) \times \cdots \times \left(\left\lceil \frac{B_{max}\delta}{E^I l} \right\rceil + 1\right)$.

Suppose that $\mathbf{B}_t = \mathbf{u}$. There are $I + 1$ possible events at time t: A transmission is performed by transmitter i, where $1 \leq i \leq I$, or no transmission happens.

If the i-th transmitter transmits, there is $\mathbf{B}_{t+1} = \mathbf{v}_i$, where $\mathbf{v}_i \in \mathbf{\Sigma}$ and

$$\mathbf{v}_i = \begin{pmatrix} \min\{u_1 + E^1 L, B_{max}\delta\} \\ \cdots \\ 0 \\ \cdots \\ \min\{u_I + E^I L, B_{max}\delta\} \end{pmatrix}^T,$$

in which the i-th element is zero. According to (2.24), the corresponding transition probability is given by

$$p_{\mathbf{u},\mathbf{v}_i} = Q_i p_{tr}^i(u_i), \ 1 \leq i \leq I. \tag{A.9}$$

If no transmission happens, all transmitters just harvest energy for one time slot. Then, we obtain $\mathbf{B}_{t+1} = \mathbf{w}$, where $\mathbf{w} \in \mathbf{\Sigma}$ and

$$\mathbf{w} = \begin{pmatrix} \min\{u_1 + E^1 l, B_{max}\delta\} \\ \cdots \\ \min\{u_i + E^i l, B_{max}\delta\} \\ \cdots \\ \min\{u_I + E^I l, B_{max}\delta\} \end{pmatrix}^T .$$

The corresponding transition probability is just the complement of the transmission probability over all other possible I cases, which is given by

$$p_{\mathbf{u},\mathbf{w}} = 1 - \sum_{i=1}^{I} Q_i p_{tr}^i(u_i). \tag{A.10}$$

Therefore, $\{\mathbf{B}_t\}_{t\geq 0}$ is a unichain [22], i.e., a finite-state Markov process that contains a single recurrent class. By calculating the transition probability for each $\mathbf{u} \in \mathbf{\Sigma}$, we obtain the transition probability matrix $\mathbf{P}$ for $\{\mathbf{B}_t\}_{t\geq 0}$. Clearly, $\mathbf{P}$ is a stochastic matrix and is invariant over time. Therefore, there exists a unique probability vector $\mathbf{\Pi}$ such that $\mathbf{\Pi} = \mathbf{\Pi}\mathbf{P}$ holds [22]. In fact, $\mathbf{\Pi}$ is the steady-state distribution of $\{\mathbf{B}_t\}_{t\geq 0}$.

So far, we have constructed a "super" Markov chain $\{\mathbf{B}_t\}_{t\geq 0}$ for the whole system, for which the steady-state distribution exists and is unique. Therefore, by the iteration

$\mathbf{\Pi}_{t+1} = \mathbf{\Pi}_t\mathbf{P}$, we have $\lim_{t\to\infty} \mathbf{\Pi}_t = \mathbf{\Pi}$. Thus, it suffices to show that

$$\mathbf{\Pi}_{t+1} = \mathbf{\Pi}_t\mathbf{P} \Leftrightarrow \begin{cases} \Pi^1_{t+1} = \Pi^1_t\mathbf{P}^1_t, \\ \cdots \\ \Pi^i_{t+1} = \Pi^i_t\mathbf{P}^i_t, \qquad t \geq 0, \\ \cdots \\ \Pi^I_{t+1} = \Pi^I_t\mathbf{P}^I_t. \end{cases} \tag{A.11}$$

If (A.11) is true, the state distribution of each transmitter converges to the unique steady-state distribution.

Next, we are going to show that both the directions "$\Rightarrow$" and "$\Leftarrow$" of (A.11) hold. For notational simplicity, we omit the time index t. In fact, the direction "$\Leftarrow$" is the same as constructing the "super" Markov chain as discussed earlier. If the system is at state $\mathbf{u} = \left(b_1E^1l \cdots b_IE^Il\right)$, where $b_i \in \left\{0, 1, 2, \cdots, \left\lfloor \frac{B_{max}\delta}{E^il} \right\rfloor, B_{max}\right\}$, $1 \leq i \leq I$, the probability $\mathbf{\Pi}(\mathbf{u})$ is the joint probability over all transmitters, i.e., $\mathbf{\Pi}(\mathbf{u}) = \prod_{i=1}^{I} \pi^i_{b_i}$. The way of constructing transition probability matrix $\mathbf{P}$ is given by (A.9) and (A.10), which can be obtained directly from (2.24) for $\{\mathbf{P}^i\}$. Thus, both $\mathbf{\Pi}$ and $\mathbf{P}$ can be obtained from the right-hand side of (A.11).

For the direction "$\Rightarrow$" of (A.11), we need to show how we obtain $\{\Pi^i\}$ and $\{\mathbf{P}^i\}$ from the left-hand side of (A.11). We consider $\{\Pi^i\}$ first. Given the state distribution $\mathbf{\Pi}$ of the system, there exists an one-to-one mapping from each element of $\mathbf{\Sigma}$ to that of $\mathbf{\Pi}$. Let $\mathbf{\Pi}(\mathbf{u})$ denote the probability of the system staying at state $\mathbf{u} \in \mathbf{\Sigma}$. Obviously, there is $\sum_{\mathbf{u}\in\mathbf{\Sigma}} \mathbf{\Pi}(\mathbf{u}) = 1$. Then, we consider the subset of $\mathbf{\Sigma}$ such that transmitter i stays at state $u \in \mathbf{\Delta}_i$, i.e.,

$$\mathbf{\Sigma}_{u_i=u} = \left\{\mathbf{u} = (u_1 \cdots u_i \cdots u_I) : u_1 \in \mathbf{\Delta}_1, \cdots, u_i = u, \cdots, u_I \in \mathbf{\Delta}_I\right\}. \tag{A.12}$$

Clearly, (A.12) satisfies $\bigcup_{u\in\mathbf{\Delta}_i}\mathbf{\Sigma}_{u_i=u}=\mathbf{\Sigma}$. Then, the probability that transmitter i stays at state $u=bE^il$, where $b\in\left\{0,1,2,\cdots,\left\lfloor\frac{B_{max}\delta}{E^il}\right\rfloor,B_{max}\right\}$, is equal to the probability that the system is staying at $\mathbf{\Sigma}_{u_i=u}$, i.e.,

$$\pi_b^i=\mathbb{P}\left\{\mathbf{\Sigma}_{u_i=u}\right\}=\sum_{\mathbf{u}\in\mathbf{\Sigma}_{u_i=u}}\mathbf{\Pi}(\mathbf{u}). \tag{A.13}$$

In this way, we can obtain the state distribution Π^i for transmitter i such that $\Pi^i=[\pi_0^i\cdots\pi_b^i\cdots\pi_{B_{max}}^i]$.

Next, we consider $\{\mathbf{P}^i\}$. When transmitter i stays at the energy state $u\in\mathbf{\Delta}_i$, it can transfer to state 0, v_1, or v_2 , where $v_1=\min\{u+E^iL,B_{max}\delta\}$, and $v_2=\min\{u+E^il,B_{max}\delta\}$. Accordingly, from $\mathbf{\Sigma}_{u_i=u}$, there are three possible cases:

1. $\mathbf{\Sigma}_{u_i=u}\rightarrow\mathbf{\Sigma}_{u_i=0}$: For each state $\mathbf{u}\in\mathbf{\Sigma}_{u_i=u}$, there is only one possible route to $\mathbf{\Sigma}_{u_i=0}$ with probability $Q_ip_{tr}^i(u)$ such that transmitter i transmits and goes into state 0. In fact, such transition probability does not change for any $\mathbf{u}\in\mathbf{\Sigma}_{u_i=u}$. Thus, by taking all possible states into account, the transition probability can be computed by

$$p_{u,0}^i=\mathbb{P}\left\{\mathbf{\Sigma}_{u_i=u}\rightarrow\mathbf{\Sigma}_{u_i=0}\mid\mathbf{\Sigma}_{u_i=u}\right\}=\frac{Q_ip_{tr}^i(u)\mathbb{P}\left\{\mathbf{\Sigma}_{u_i=u}\right\}}{\mathbb{P}\left\{\mathbf{\Sigma}_{u_i=u}\right\}}=Q_ip_{tr}^i(u), \tag{A.14}$$

   which is equal to (2.24).

2. $\mathbf{\Sigma}_{u_i=u}\rightarrow\mathbf{\Sigma}_{u_i=v_1}$: For each state $\mathbf{u}\in\mathbf{\Sigma}_{u_i=u}$, there are $I-1$ possible routes to $\mathbf{\Sigma}_{u_i=v_1}$. We pick the route caused by transmitter $j\neq i$, i.e., the j-th transmitter transmits. Suppose that at state $\mathbf{u}$, the transmitter j is in the energy state $bE^jl\in\mathbf{\Delta}_j$. The probability of staying at $\mathbf{\Sigma}_{u_i=u,u_j=bE^jl}$ is given as $\pi_b^j\mathbb{P}\left\{\mathbf{\Sigma}_{u_i=u}\right\}$ by (A.13). Thus, the transition $\mathbf{\Sigma}_{u_i=u,u_j=bE^jl}\rightarrow\mathbf{\Sigma}_{u_i=v_1,u_j=0}$ describes the transition of transmitter i from state u to state v_1 caused by transmitter j with energy level $u_j=bE^jl$.

Similarly as in (A.14), the transition probability for this case is given by

$$\begin{aligned}
&\mathbb{P}\left\{\boldsymbol{\Sigma}_{u_i=u,u_j=bE^jl} \to \boldsymbol{\Sigma}_{u_i=v_1,u_j=0} \mid \boldsymbol{\Sigma}_{u_i=u,u_j=bE^jl}\right\} \\
=&\frac{Q_j p_{tr}^j(bE^jl)\mathbb{P}\left\{\boldsymbol{\Sigma}_{u_i=u,u_j=bE^jl}\right\}}{\mathbb{P}\left\{\boldsymbol{\Sigma}_{u_i=u,u_j=bE^jl}\right\}} \\
=&Q_j p_{tr}^j(bE^jl).
\end{aligned}$$

When we extend to other transmitters besides i, and consider all possible states for each transmitter, we obtain the probability of the one step transition $\boldsymbol{\Sigma}_{u_i=u} \to \boldsymbol{\Sigma}_{u_i=v_1}$ as

$$\begin{aligned}
&\mathbb{P}\left\{\boldsymbol{\Sigma}_{u_i=u} \to \boldsymbol{\Sigma}_{u_i=v_1} \mid \boldsymbol{\Sigma}_{u_i=u}\right\} \\
=&\frac{\mathbb{P}\left\{\boldsymbol{\Sigma}_{u_i=u} \to \boldsymbol{\Sigma}_{u_i=v_1},\ \boldsymbol{\Sigma}_{u_i=u}\right\}}{\mathbb{P}\left\{\boldsymbol{\Sigma}_{u_i=u}\right\}} \\
=&\frac{1}{\mathbb{P}\left\{\boldsymbol{\Sigma}_{u_i=u}\right\}} \sum_{j\neq i}\sum_{b=0}^{B_{max}} \Big(\mathbb{P}\left\{\boldsymbol{\Sigma}_{u_i=u,u_j=bE^jl}\right\} \\
&\qquad \cdot \mathbb{P}\left\{\boldsymbol{\Sigma}_{u_i=u} \to \boldsymbol{\Sigma}_{u_i=v_1} \mid \boldsymbol{\Sigma}_{u_i=u,u_j=bE^jl}\right\}\Big) \\
=&\frac{1}{\mathbb{P}\left\{\boldsymbol{\Sigma}_{u_i=u}\right\}} \sum_{j\neq i}\sum_{b=0}^{B_{max}} \Big(\mathbb{P}\left\{\boldsymbol{\Sigma}_{u_i=u,u_j=bE^jl}\right\} \\
&\cdot \mathbb{P}\left\{\boldsymbol{\Sigma}_{u_i=u,u_j=bE^jl} \to \boldsymbol{\Sigma}_{u_i=v_1,u_j=0} \mid \boldsymbol{\Sigma}_{u_i=u,u_j=bE^jl}\right\}\Big) \\
=&\frac{1}{\mathbb{P}\left\{\boldsymbol{\Sigma}_{u_i=u}\right\}} \sum_{j\neq i}\sum_{b=0}^{B_{max}} \pi_b^j \mathbb{P}\left\{\boldsymbol{\Sigma}_{u_i=u}\right\} Q_j p_{tr}^j(bE^jl) \\
=&\sum_{j\neq i}\sum_{b=0}^{B_{max}} \pi_b^j Q_j p_{tr}^j(bE^jl). \qquad \text{(A.15)}
\end{aligned}$$

Thus, (A.15) is equivalent to (2.26).

3. $\boldsymbol{\Sigma}_{u_i=u} \to \boldsymbol{\Sigma}_{u_i=v_2}$: The transition probability for this case can be obtained by taking the complement of (A.14) and (A.15), which is equivalent to (2.27).

Therefore, we obtain all possible transitions for transmitter i at time t, for which the corresponding transition probabilities can be computed as well. Thus, $\{\Pi^i\}$ and $\{\mathbf{P}^i\}$ are obtained from $\mathbf{\Pi}$ and $\mathbf{P}$, which proves the direction "$\Rightarrow$" of (A.11).

Overall, the convergence of Algorithm 2.1 is proved.

APPENDIX B

SOME PROOFS FOR CHAPTER 3

B.1 Proof of Proposition 3.3.1

According to the optimal stopping theory [20,21], the existence of the optimal stopping rule could be proved by checking the following two conditions: For a given $\lambda > 0$,

C1: $\mathbb{E}\left[\sup_{T\geq 1} G_T(\lambda)\right] < \infty$;

C2: $\limsup_{T\to\infty} G_T(\lambda) \leq G_\infty = -\infty$ a.s..

We first check C1 and C2 for $B_{max} < +\infty$ and $B_{max} = +\infty$, respectively.

- $B_{max} < +\infty$: For C1, we have $\sup_{T\geq 1} G_T(\lambda) \leq \sup_{T\geq 1} R(\mathbf{F}_T)$. Since the channel gains are finite a.s., and the battery capacity is finite, the expectation of the transmission rate is finite as well, which proves that C1 holds. For C2, we only need to show that for any large negative real number $\nu < 0$, there exists a $K \geq 0$ a.s. such that for all $T \geq K$, $G_T(\lambda) = R(\mathbf{F}_T) - \lambda T < \nu$. In fact, for any T, $\mathbb{E}\left[R(\mathbf{F}_T)\right] < \infty$, which implies that $\mathbb{P}\left\{R(\mathbf{F}_T) = \infty\right\} = 0$. However, the term λT will increase to infinity as $T \to \infty$. Thus, when $T \geq K$, $R(\mathbf{F}_T) - \lambda T$ can be as small as we want a.s., i.e., $R(\mathbf{F}_T) - \lambda T < \nu$ a.s., which proves that C2 holds.

- $B_{max} = +\infty$: For this case, we check C2 first. Recall the expression of $R(\mathbf{F}_T)$ in (3.4) and B_T is given as

$$B_T = \sum_{i=1}^{T-1} E_i - S\sum_{i=1}^{T-1} 1_{\{B_i > S+C\}},$$

then, we have

$$\begin{aligned}
&R(\mathbf{F}_T) - \lambda T \\
\leq &\log\left(\frac{1+H_T(B_T-S-C)^+}{2^{\lambda T/2}}\right) + \log\left(\frac{1+H_T^c\phi_T(B_T-S-C)^+}{2^{\lambda T/2}}\right) \\
\leq &\log\left(\frac{1+H_T\left(E_{max}T-S-C\right)^+}{2^{\lambda T/2}}\right) \\
&+\log\left(\frac{1+H_T^c\phi_T\left(E_{max}T-S-C\right)^+}{2^{\lambda T/2}}\right), a.s.. \qquad \text{(B.1)}
\end{aligned}$$

By noticing the maximum EH rate $E_{max} < +\infty$ and using L'H$\hat{o}$pital's rule [13], the first term in (B.1) satisfies

$$\lim_{T\to\infty}\frac{1+H_T\left(E_{max}T-S-C\right)^+}{2^{\lambda T/2}} \leq \lim_{T\to\infty}\frac{H_T E_{max}}{\frac{\lambda\ln 2}{2}2^{\lambda T/2}} = 0.$$

We could apply a similar check for the second term of (B.1). Thus, C2 holds. For C1, we could use the above results of C2 and obtain that $\forall\epsilon > 0$, there exists an $N > 0$ such that $\mathbb{E}\left[\sup_{T\geq 1} G_T(\lambda)\right] < \mathbb{E}\left[\sup_{1\leq T\leq N}(R(\mathbf{F}_T)-\lambda T)\right] + \epsilon$. Since the channel gains are finite a.s., and for all $1 \leq T \leq N$, $\mathbb{E}[B_T] = \mathbb{E}\left[\sum_{i=1}^{T-1} E_i - S\sum_{i=1}^{T-1} 1_{\{B_i>S+C\}}\right] < \infty$, we obtain $\mathbb{E}\left[\sup_{1\leq T\leq N}(R(\mathbf{F}_T)-\lambda T)\right] < \infty$, which implies that C1 holds.

Therefore, both C1 and C2 hold for either $B_{max} < +\infty$ or $B_{max} = +\infty$, which implies that the optimal stopping rule exists.

Next, we derive the optimal stopping rule. Consider the remaining maximum expected reward $V_t(\mathbf{F}_t)$ given by (3.7), which is further rewritten as

$$\begin{aligned} V_t(\mathbf{F}_t) &= \sup_{T \in \mathcal{T}_t} \mathbb{E}\left[R(\mathbf{F}_T) - \lambda(T-(t-1)) \mid \mathbf{F}_t\right] - \lambda(t-1) \\ &= \sup_{T \in \mathcal{T}_1} \mathbb{E}\left[R(\mathbf{F}_T) - \lambda T) \mid \mathbf{F}_t\right] - \lambda(t-1) \\ &= V_1(\mathbf{F}_t) - \lambda(t-1). \end{aligned} \tag{B.2}$$

Meanwhile, $V_t(\mathbf{F}_t)$ satisfies the dynamic programming equation [6, 59]:

$$V_t(\mathbf{F}_t) = \max\left\{R(\mathbf{F}_t) - \lambda t, \mathbb{E}\left[V_{t+1}(\mathbf{F}_{t+1}) \mid \mathbf{F}_t\right]\right\}. \tag{B.3}$$

Therefore, the optimal stopping rule has the following form

$$\begin{aligned} T^* &= \min\left\{t \geq 1 : R(\mathbf{F}_t) - \lambda t = V_t(\mathbf{F}_t)\right\} \\ &= \min\left\{t \geq 1 : R(\mathbf{F}_t) - \lambda t = V_1(\mathbf{F}_t) - \lambda(t-1)\right\} \\ &= \min\left\{t \geq 1 : R(\mathbf{F}_t) - \lambda = V_1(\mathbf{F}_t)\right\}, \end{aligned}$$

where the second equation holds due to (B.2). By letting $\lambda = \lambda^*$, we obtain the form of T^* as shown in (3.8).

Finally, we compute λ^*. By Lemma 3.3.1, λ^* makes the following equation hold:

$$\begin{aligned} 0 = &\sup_{T \in \mathcal{T}_1} \mathbb{E}[G_T(\lambda)] \\ =&\mathbb{E}\left[\max\left\{R(\mathbf{F}_1) - \lambda^*, \mathbb{E}\left[V_2(\mathbf{F}_2) \mid \mathbf{F}_1\right]\right\}\right] \\ =&\mathbb{E}\left[\max\left\{R(\mathbf{F}_1) - \lambda^*, -\lambda^* + \mathbb{E}\left[V_1(\mathbf{F}_2) \mid \mathbf{F}_1\right]\right\}\right]. \end{aligned}$$

Thus, we could obtain λ^* by some simple rearrangements.

B.2 Proof of Proposition 3.3.2

Recalling Proposition 3.3.1 that the optimal stopping rule T^* has the form given in (3.8) and thus is finite a.s.. Then, given some $\epsilon > 0$, there exists an $M \geq 2$ such that for all $t \geq M$, we have $\mathbb{P}(T^* = t) < \epsilon$. Therefore, when we consider the expected value of $V_1(\mathbf{F}_1)$, we could just focus on a finite horizon, i.e., $1 \leq t \leq M$. Then, by the dynamic programming algorithm [6, 20, 59], we have

$$\begin{aligned} V_1(\mathbf{F}_t) &= \max\left\{R(\mathbf{F}_t), \mathbb{E}\left[V_1(\mathbf{F}_{t+1}) \mid \mathbf{F}_t\right]\right\} - \lambda^*, \text{ for } t = 1, 2, \ldots, M-1 \\ V_1(\mathbf{F}_M) &= R(\mathbf{F}_M) - \lambda^*. \end{aligned}$$

Now, we show that λ^* is strictly increasing over p_s by contradiction. First, we fix λ^*, and let p_s increase to $p_s + \Delta$, where Δ is a small positive real number. Then, we move backward. Note that at step $t = M$, $V_1(\mathbf{F}_M)$ only depends on $\mathbf{F}_M$ and does not change with p_s. At $t = M - 1$, we observe that

$$\begin{aligned} &\mathbb{E}\left[V_1(\mathbf{F}_M) \mid \mathbf{F}_{M-1}\right] \\ =&(p_s + \Delta)\mathbb{E}\left[R(H_M, H_M^c) - R(H_M, 0) \mid \mathbf{F}_{M-1}\right] + \mathbb{E}\left[R(H_M, 0) \mid \mathbf{F}_{M-1}\right] - \lambda^*. \end{aligned}$$

Note that the private channel could not be strictly better than the common channel [3], i.e., it is unrealistic that $\min_{H_M \in \mathcal{H}} H_M > \max_{H_M^c \in \mathcal{H}_c} H_M^c$. It follows that

$$\mathbb{E}\left[R(H_M, H_M^c) - R(H_M, 0) \mid \mathbf{F}_{M-1}\right] > 0. \tag{B.4}$$

Thus, we have that $\mathbb{E}\left[R(\mathbf{F}_M) - \lambda^* \mid \mathbf{F}_{M-1}\right]$ strictly increases as p_s increases to $p_s + \Delta$.

Suppose that at $t = k$ for $2 \leq k \leq M - 1$, $\mathbb{E}\left[V_1(\mathbf{F}_{k+1}) \mid \mathbf{F}_k\right]$ strictly increases as p_s

increases to $p_s + \Delta$. Since the expected value of $R(\mathbf{F}_k)$ also strictly increases following a similar argument as we discussed at step $t = M - 1$, we have that the expected value of $\max\{R(\mathbf{F}_k), \mathbb{E}[V_1(\mathbf{F}_{k+1}) \mid \mathbf{F}_k]\}$ strictly increases. Then, at $t = k - 1$, we have

$$\mathbb{E}[V_1(\mathbf{F}_k) \mid \mathbf{F}_{k-1}] = \mathbb{E}[\max\{R(\mathbf{F}_k), \mathbb{E}[V_1(\mathbf{F}_{k+1}) \mid \mathbf{F}_k]\} \mid \mathbf{F}_{k-1}] - \lambda^*, \tag{B.5}$$

which strictly increases and thus implies that such an increment holds for all $t = 1, 2, \ldots, M-1$.

At the step $t = 1$, we have

$$\mathbb{E}[V_1(\mathbf{F}_1)] = \mathbb{E}[\max\{R(\mathbf{F}_1), \mathbb{E}[V_1(\mathbf{F}_2) \mid \mathbf{F}_1]\}] - \lambda^*, \tag{B.6}$$

where $\mathbb{E}[\max\{R(\mathbf{F}_1), \mathbb{E}[V_1(\mathbf{F}_2) \mid \mathbf{F}_1]\}]$ should also strictly increase as p_s increase to $p_s + \Delta$. However, we recall from Proposition 3.3.1 that $\mathbb{E}[V_1(\mathbf{F}_1)] = 0$, which is attained by T^* and λ^*. It implies that in order to make $\mathbb{E}[V_1(\mathbf{F}_1)] = 0$, the value λ^* should not be fixed and must strictly increase accordingly, which contradicts the assumption in the first step that λ^* is fixed. Thus, λ^* strictly increases as p_s increases. Finally, this proposition is proved by letting $\epsilon \to 0$ (i.e., M is large enough).

B.3 Proof of Proposition 3.3.3

Since the optimal stopping rule is given by (3.8) based on Proposition 3.3.1, we could further rearrange the rule as

$$\begin{aligned} T^* &= \inf\{t \geq 1 : V_1(\mathbf{F}_t) - R(\mathbf{F}_t) + \lambda^* = 0\} \\ &= \inf\{t \geq 1 : \Lambda(\mathbf{F}_t) = 0\}. \end{aligned}$$

The function $\Lambda(\cdot)$ is defined by $\Lambda(\mathbf{F}_t) = V_1(\mathbf{F}_t) - R(\mathbf{F}_t) + \lambda^*$, where $\mathbf{F}_t = \{\phi_t, B_t, E_{t-1}, H_t, H_t^c\} \in \mathcal{F}$. The following properties of $\Lambda(\mathbf{F}_t)$ play a key role in the proof of this proposition:

1. $\Lambda(\mathbf{F}_t) \geq 0$ for all $\mathbf{F}_t$;
2. $\mathbb{E}[\Lambda(\mathbf{F}_t) \mid B_t] < +\infty$ for all $B_t \geq 0$. Moreover, $\mathbb{E}[\Lambda(\mathbf{F}_t) \mid B_t] = 0$ when B_t is large enough;
3. $\mathbb{E}[\Lambda(\mathbf{F}_{t+1}) \mid \mathbf{F}_t] < +\infty$ for all $B_t \geq 0$. Moreover, $\mathbb{E}[\Lambda(\mathbf{F}_{t+1}) \mid \mathbf{F}_t] = 0$ when B_t is large enough;
4. $\Lambda(\mathbf{F}_t) = 0$ when $R(\mathbf{F}_t)$ is large enough.

If all the above properties are true, it follows that $\forall \epsilon > 0$, there exists $\gamma \geq 0$ such that $\Lambda(\mathbf{F}_t) \leq \epsilon$ whenever $R(\mathbf{F}_t) > \gamma$, which implies that the stopping rule T^* has the form given by (3.10) (similar to the technique used in [21]). In the following, we prove the four properties.

For Property 1), it is straightforward to see that

$$\begin{aligned}\Lambda(\mathbf{F}_t) &= V_1(\mathbf{F}_t) - R(\mathbf{F}_t) + \lambda^* \\ &= \max\left\{R(\mathbf{F}_t) - \lambda^*_{\mathbf{F}_1}, -\lambda^* + \mathbb{E}\left[V_1(\mathbf{F}_{t+1}) \mid \mathbf{F}_t\right]\right\} - R(\mathbf{F}_t) + \lambda^* \\ &= \max\left\{0, \mathbb{E}\left[V_1(\mathbf{F}_{t+1}) \mid \mathbf{F}_t\right] - R(\mathbf{F}_t)\right\} \geq 0. \end{aligned} \tag{B.7}$$

For Property 2), suppose that the transmitter does not stop channel-energy probing until time t; then starting at t, we should have $T \in \mathcal{T}_t = \{T \geq t : \mathbb{E}[T] < \infty\}$. Thus, $\mathbb{E}[\Lambda(\mathbf{F}_t) \mid B_t]$ could be written as

$$\mathbb{E}[\Lambda(\mathbf{F}_t) \mid B_t] = \sum_{n \geq t} \mathbb{P}(T = n)\mathbb{E}[\Lambda(\mathbf{F}_t) \mid B_t, T = n] < \infty,$$

due to $\mathbb{P}(T = +\infty) = 0$. Then, with a fixed $T = n$ such that $t \leq n < \infty$, along with Property 1), $\mathbb{E}[\Lambda(\mathbf{F}_t) \mid B_t, n]$ is expanded as

$$\begin{aligned}
0 \leq & \mathbb{E}[\Lambda(\mathbf{F}_t) \mid B_t, n] \\
= & \mathbb{E}\left[R(\mathbf{F}_n) - R(\mathbf{F}_t) - \lambda^* n \mid B_t\right] + \lambda^* \\
\leq & (1 - p_s)\mathbb{E}\left[\log\left(\frac{1 + HB_n}{1 + HB_t}\right)\right] \qquad \text{(B.8)} \\
& + p_s\left(\mathbb{E}\left[\log\left(\frac{1 + HP_n}{1 + HP_t}\right) + \log\left(\frac{1 + H^c P_n^c}{1 + H^c P_t^c}\right)\right]\right), \qquad \text{(B.9)}
\end{aligned}$$

where the second inequality holds due to $-\lambda^* n + \lambda^* \leq 0$ for $n \geq t$. Note that we do not put the time index n on H and H^c since $\{H_t\}_{t \geq 1}$ and $\{H_t^c\}_{t \geq 1}$ are i.i.d., respectively. Next, we want to show that both (B.8) and (B.9) are finite and could be as small as we want with a large B_t, which would complete the proof for 2).

- For (B.8): by plugging $B_n = B_t + \sum_{i=t}^{n-1} E_i - S\sum_{i=t}^{n-1} 1_{\{B_i > S+C\}}$, we obtain

  $$(B.8) = (1 - p_s)\mathbb{E}\left[\log\left(1 + \frac{H\left(\sum_{i=t}^{n-1} E_i - S\sum_{i=t}^{n} 1_{\{B_i > S+C\}} - C\right)^+}{1 + HB_t}\right)\right] < +\infty$$

  since H has finite mean and $\{E_j\}_{t \leq j \leq n-1}$ are i.i.d. with finite mean as well. Moreover, if $B_t \to \infty$, $(B.8) \to 0$.

- For (B.9): Since $P_n + P_n^c = (B_n - C - S)^+$, and both H and H^c have finite means, respectively, it follows that (B.9) is finite. When the transmitter occupies the common channel at time $T \geq t$, there are three possible events by Lemma 3.2.1: If $\left|\frac{1}{H^c} - \frac{1}{H}\right| \geq (B_n - C - S)^+$, allocating all power to one of the two channels; otherwise, allocating the power to both channels at a certain ratio. Note that the probability of any above event happening does not depend on n if B_t is large enough.

To see this point, we let

$$
\begin{aligned}
Q &= \mathbb{P}\left(\left|\frac{1}{H^c}-\frac{1}{H}\right| < (B_t - C - S)^+\right), \\
q_1 &= \mathbb{P}\left(\left|\frac{1}{H^c}-\frac{1}{H}\right| \geq (B_t - C - S)^+, H > H^c\right), \\
q_2 &= \mathbb{P}\left(\left|\frac{1}{H^c}-\frac{1}{H}\right| \geq (B_t - C - S)^+, H < H^c\right).
\end{aligned}
$$

When B_t is large, there is

$$
\mathbb{P}\left(\left|\frac{1}{H^c}-\frac{1}{H}\right| < \left(B_t + \sum_{i=t}^{n-1} E_i - S\sum_{i=t}^{n} 1_{\{B_i > S+C\}} - C\right)+\right) \approx Q,
$$

and similarly, we have

$$
\begin{aligned}
\mathbb{P}\left(\left|\frac{1}{H^c}-\frac{1}{H}\right| \geq (B_n - S - C)^+, H > H^c\right) &\approx q_1, \\
\mathbb{P}\left(\left|\frac{1}{H^c}-\frac{1}{H}\right| \geq (B_n - S - C)^+, H < H^c\right) &\approx q_2.
\end{aligned}
$$

Then, by applying Q, q_1 and q_2, we can expand (B.9) as

$$
\begin{aligned}
&(B.9) \approx \\
&p_s\left(q_1\mathbb{E}\left[\log\left(\frac{1+H(B_n - S - C)^+}{1+hB_t}\right)\right] + q_2\mathbb{E}\left[\log\left(\frac{1+H^c(B_n - S - C)^+}{1+h^cB_t}\right)\right]\right) \\
&\quad + p_sQ\mathbb{E}\left[\log\frac{\left(1+H(B_n - S - C)^+ + \frac{H}{H^c}\right)\left(1+H^c(B_n - S - C)^+ + \frac{H^c}{H}\right)}{\left(1+HB_t + \frac{H}{H^c}\right)\left(1+H^cB_t + \frac{H^c}{H}\right)}\right].
\end{aligned}
$$

Similarly as the reasoning in (B.8), we obtain that $(B.9) \to 0$ as $B_t \to \infty$.

Therefore, we conclude that $\mathbb{E}[\Lambda(\mathbf{F}_t) \mid B_t]$ is finite and could be arbitrarily small when B_t is large enough.

For 3), we expend $\mathbb{E}[\Lambda(\mathbf{F}_{t+1}) \mid \mathbf{F}_t]$ as

$$\begin{aligned}&\mathbb{E}[\Lambda(\mathbf{F}_{t+1}) \mid \mathbf{F}_t] = \mathbb{E}[\Lambda(\mathbf{F}_{t+1}) \mid B_t] \\ =&\sum_{e\in\mathcal{E}} P(E_t = e)\mathbb{E}[\Lambda(\mathbf{F}_{t+1}) \mid B_t],\end{aligned}$$

since only $\{B_t\}$ are correlated over time. By Property 2), we know $\mathbb{E}[\Lambda(\mathbf{F}_{t+1}) \mid B_t]$ is finite and thus $\mathbb{E}[\Lambda(\mathbf{F}_{t+1}) \mid \mathbf{F}_t]$ is finite since $\mathcal{E}$ is a finite space. Moreover, by Property 2), we have $\mathbb{E}[\Lambda(\mathbf{F}_{t+1}) \mid B_t] \to 0$ as $B_t \to \infty$. Therefore, it follows that $\mathbb{E}[\Lambda(\mathbf{F}_{t+1}) \mid \mathbf{F}_t]$ could be as small as we want when B_t is large enough.

By now, we are ready to show Property 4). We could rewrite (B.7) as

$$\begin{aligned}\Lambda(\mathbf{F}_t) &= \max\left\{0, \mathbb{E}\left[V_1(\mathbf{F}_{t+1}) \mid \mathbf{F}_t\right] - R(\mathbf{F}_t)\right\} \\ &= \max\left\{0, \mathbb{E}\left[\Lambda(\mathbf{F}_{t+1}) + R(\mathbf{F}_{t+1}) - \lambda^* \mid \mathbf{F}_t\right] - R(\mathbf{F}_t)\right\}.\end{aligned}$$

Next, we show Property 4) by contradiction. Suppose that $\Lambda(\mathbf{F}_t) > 0$ for all $R(\mathbf{F}_t) \geq 0$, then we have

$$\mathbb{E}\left[\Lambda(\mathbf{F}_{t+1}) + R(\mathbf{F}_{t+1}) \mid \mathbf{F}_t\right] > R(\mathbf{F}_t) + \lambda^*. \tag{B.10}$$

For the left-hand side (LHS) of (B.10), $\mathbb{E}\left[R(\mathbf{F}_{t+1}) \mid \mathbf{F}_t\right]$ is finite for any fixed B_t, and $\mathbb{E}\left[\Lambda(\mathbf{F}_{t+1}) \mid \mathbf{F}_t\right]$ is either a finite number or a arbitrarily small positive number if B_t is large enough. Then, we choose $K < +\infty$ and $B_t = B_{max}$ such that the LHS of (B.10) is upper-bounded by K. With such K and B_t, we have

$$K > \mathbb{E}\left[\Lambda(\mathbf{F}_{t+1}) + R(\mathbf{F}_{t+1}) \mid \mathbf{F}_t\right] > R(\mathbf{F}_t) + \lambda^*. \tag{B.11}$$

However, for the right-hand side (RHS) of (B.10) with the same B_t, $R(\mathbf{F}_t)$ could be arbitrarily large if H_t and H_t^c are large enough. Then, there always exists an $M > 0$ such that when $H_t, H_t^c > M$, $R(\mathbf{F}_t) > K$, which leads to the contradiction with the inequality (B.11). Therefore, we obtain that $\Lambda(\mathbf{F}_t) = 0$ when $R(\mathbf{F}_t)$ is large enough.

Overall, we have shown that all four properties hold, and we conclude that the optimal stopping rule has a pure-threshold structure given by (3.10).

B.4 Proof of Proposition 3.3.4

Given some $\gamma > 0$, we let $q_t(p_s) = \mathbb{P}\left(R(H_t, \phi_t H_t^c) \geq \gamma\right)$. Based on the form of the stopping rule T^* given by (3.10), we obtain

$$\mathbb{E}\left[T^*\right] = q_1(p_s) + \sum_{t=2}^{\infty} t q_t(p_s) \prod_{n=1}^{t-1} (1 - q_n(p_s)).$$

Since $\mathbb{E}\left[T^*\right] < \infty$, it follows that $\forall \epsilon, \epsilon_0 > 0$, there exists $N > 0$ such that $\mathbb{P}\left(T^* = t\right) = q_t(p_s) \prod_{n=1}^{t-1}(1-q_n(p_s)) < \epsilon$ for all $t \geq N$, and $\sum_{t=N}^{\infty} t q_t(p_s) \prod_{n=1}^{t-1}(1-q_n(p_s)) < \epsilon_0$. Note that the generality still holds to let $q_N(p_s) = \epsilon$ since $\mathbb{P}(T^* = N) = \epsilon \prod_{n=1}^{N-1}(1 - q_n(p_s)) < \epsilon$. Then, we have

$$\begin{aligned}
\mathbb{E}\left[T^*\right] &= q_1(p_s) + \sum_{t=2}^{N} t q_t(p_s) \prod_{n=1}^{t-1} (1 - q_n(p_s)) + \epsilon_0 \\
&= \epsilon_0 + q_1(p_s) + (1 - q_1(p_s)) \cdot \left(2q_2(p_s) + (1 - q_2(p_s)) \cdot \right. \\
&\quad \left. \cdots \left((N-1) q_{N-1}(p_s) + (1 - q_{N-1}(p_s)) N \epsilon \right) \cdots \right).
\end{aligned}$$

We introduce $U_t = t q_t(p_s) + (1 - q_t(p_s)) U_{t+1} = t + (1 - q_t(p_s))\left(U_{t+1} - t\right)$, where we notice $U_{t+1} - t > 0$. With this notation, we have $\mathbb{E}\left[T^*\right] = \epsilon_0 + U_1$.

Next, we show the monotonicity of $\mathbb{E}\left[T^*\right]$ by using the mathematical induction in a "backward" fashion: From a very large number N back to $t = 1$. First, we check U_N. It is

true since $U_N = N\epsilon$, which is independent with p_s. Then, suppose that U_{k+1} is decreasing over p_s for $k = 2, \ldots, N-1$; we check $U_k = k + (1 - q_k(p_s))(U_{k+1} - k)$. For $q_k(p_s)$, we have

$$\begin{aligned} q_k(p_s) =& \mathbb{P}\left(R(H_k, 0) \geq \gamma\right) + \\ & p_s \left(\mathbb{P}\left(R(H_k, H_k^c) \geq \gamma\right) - \mathbb{P}\left(R(H_k, 0) \geq \gamma\right)\right), \end{aligned}$$

where $\mathbb{P}\left(R(H_k, H_k^c) \geq \gamma\right) \geq \mathbb{P}\left(R(H_k, 0) \geq \gamma\right)$ due to $R(H_k, H_k^c) \geq R(H_k, 0)$. It follows that $q_k(p_s)$ is an increasing linear function of p_s, and then $1 - q_k(p_s)$ is deceasing. Since both $(1 - q_k(p_s))$ and $(U_{k+1} - k)$ are nonnegative and decreasing, U_k is decreasing as well. Moreover, U_k is a polynomial function of p_s due to the linearity of $q_k(p_s)$ and the iteration function, i.e., $U_k = k + (1 - q_k(p_s))(U_{k+1} - k)$. Thus, we obtain that $\mathbb{E}[T^*] = U_1 + \epsilon_0$ is a polynomial function and decreasing over p_s. By letting $\epsilon_0 \to 0$, we are done with the proof for this proposition.

APPENDIX C

SOME PROOFS FOR CHAPTER 4

C.1 Proof of Lemma 4.3.1

We prove this proposition by contradiction. Suppose that transmitter 1 does not satisfy the condition, i.e., $\lim_{t\to\infty} \mathbb{P}\left\{B_t^{(1)} = \infty\right\} > 0$. Note that such an event will happen only when transmitter 1 keeps saving for an infinite number of time slots starting from, say, the k_1-th time slot, given the condition that the EH rate has finite nonnegative mean μ and variance σ^2. That is, as $t \to \infty$, we have

$$\left\{B_t^{(1)} = \infty\right\} \Leftrightarrow \left\{\sum_{i=k_1}^{t-1} E_i^{(1)} = \infty\right\}.$$

Moreover, if the event $\left\{\sum_{i=k_1}^{t} E_i^{(1)} = \infty\right\}$ happens as $t \to \infty$, according to the access scheme M_t, it is equivalent to the event that the energy level of transmitter 1 is never the highest among those of all transmitters after time k, i.e.,

$$\left\{\sum_{i=k_1}^{t-1} E_i^{(1)} = \infty\right\} \Leftrightarrow \left\{\sum_{i=k_1}^{t-1} E_i^{(1)} \leq \max_{n\neq 1}\left\{B_t^{(n)}\right\} = \infty\right\}$$

as $t \to \infty$. Then, if the event $\left\{\max_{n\neq 1}\left\{B_t^{(n)}\right\} = \infty\right\}$ happens, there must exist at least one transmitter, say the 2-nd transmitter, such that it starts saving from time k_2 for an

infinite number of time slots, i.e.,

$$\left\{\sum_{i=k_1}^{t-1} E_i^{(1)} \leq \max_{n\neq 1}\left\{B_t^{(n)}\right\} = \infty\right\}$$
$$\Rightarrow \left\{\sum_{i=k_1}^{t} E_i^{(1)} \leq \sum_{i=k_2}^{t-1} E_i^{(2)} = \infty\right\} \text{ as } t \to \infty.$$

Similar to the case of transmitter 1, if the 2nd transmitter also saves for an infinite number of time slots, there must be

$$\left\{\sum_{i=k_2}^{t-1} E_i^{(2)} \leq \max_{n\neq 1,2}\left\{B_t^{(n)}\right\} = \infty\right\} \text{ as } t \to \infty.$$

Analogously, it directly implies that all N transmitters must keep saving energy for infinite numbers of times slots. However, this cannot happen since by using the optimal access $\{M_t\}_{t\geq 1}$, a transmitter is chosen to fulfil a transmission in each time slot. Hence, all N transmitters cannot keep saving energy forever, which contradicts the assumption that the event $\left\{B_t^{(1)} = \infty\right\}$ exists as $t \to \infty$. Therefore, the lemma is proved.

C.2 Proof of Lemma 4.3.2

We need to show that for $\forall \epsilon > 0$,

$$\mathbb{P}\left\{\lim_{N\to\infty}\left|\frac{B-\mu S)}{S}\right| > \epsilon\right\} = 0. \tag{C.1}$$

Let $X_i = E_i - \mu$. Note that SLLN holds for $X_1, X_2, \ldots, X_k$, i.e., $\sum_{i=1}^{k} X_i/k \to 0$ as $k \to \infty$ with probability 1, which implies

$$\sum_{k=1}^{\infty} \mathbb{P}\left\{\left|\sum_{i=1}^{k} X_i\right| > k\epsilon\right\} < \infty. \tag{C.2}$$

Define

$$A_k = \left\{ \left| \sum_{i=1}^{S} X_i \right| > S\epsilon, S = k \right\};\ F_N = \bigcup_{k \geq N} A_k.$$

Then, we have

$$\mathbb{P}\left\{ \lim_{N\to\infty} \left| \frac{B - \mu S}{S} \right| > \epsilon \right\} = \mathbb{P}\left\{ \bigcap_{N=1}^{\infty} F_N \right\} = \mathbb{P}\left\{ A_k \text{ i.o.} \right\},$$

where i.o. stands for "infinitely often". Next, we need to show $\mathbb{P}\left\{ A_k \text{ i.o.} \right\} = 0$.

$$\begin{aligned} &\sum_{k=1}^{\infty} \mathbb{P}\left\{ A_k \right\} = \sum_{k=1}^{\infty} \mathbb{P}\left\{ \left| \sum_{i=1}^{k} X_i \right| > k\epsilon \mid S = k \right\} \mathbb{P}\left\{ S = k \right\} \\ \leq &\sum_{k=1}^{\infty} \mathbb{P}\left\{ \left| \sum_{i=1}^{k} X_i \right| > k\epsilon \right\} < \infty. \end{aligned}$$

Therefore, $\mathbb{P}\left\{ A_k \text{ i.o.} \right\} = 0$, which implies that the convergence (4.7) holds by the Bore-Cantelli lemma [61].

C.3 Proof of Proposition 4.3.2

Let

$$\frac{B - \mu S}{\sigma\sqrt{S}} = \sum_{i=1}^{S} \frac{E_i - \mu}{\sigma\sqrt{S}} = \sum_{i=1}^{S} \frac{Y_i}{\sqrt{S}} \tag{C.3}$$

Then, we calculate its characteristic function as

$$\begin{aligned}
&\mathbb{E}\left[\exp\left(t\sum_{i=1}^{S-1}\frac{Y_i}{\sqrt{S}}\right)\right] = \mathbb{E}\left[\prod_{i=1}^{S}\exp\left(\frac{Y_i}{\sqrt{S}}\right)\right] \\
=&\sum_{s=1}^{\infty}\mathbb{E}\left[\prod_{i=1}^{s}\exp\left(\frac{Y_i}{\sqrt{s}}\right)\middle| S=s\right]\mathbb{P}\left\{S=s\right\} \\
=&\sum_{s=1}^{\infty}\left(\mathbb{E}\left[\exp\left(\frac{Y_i}{\sqrt{s}}\right)\right]\right)^s\mathbb{P}\left\{S=s\right\} \\
=&\sum_{s=1}^{\infty}\left(1-\frac{t^2}{2s}+o\left(\frac{t^2}{s}\right)\right)^s\mathbb{P}\left\{S=s\right\}. \qquad \text{(C.4)}
\end{aligned}$$

Note that for a large s, we have the approximation: $\left(1-\frac{t^2}{2s}+o\left(\frac{t^2}{s}\right)\right)^s \approx e^{-\frac{t^2}{2}}$ when $s \geq K$. Thus, we obtain

$$\begin{aligned}
(C.4) =&\sum_{s=1}^{K-1}\left(1-\frac{t^2}{2s}+o\left(\frac{t^2}{s}\right)\right)^s\mathbb{P}\left\{S=s\right\} \\
&+\sum_{s\geq K}e^{-\frac{t^2}{2}}\mathbb{P}\left\{S=s\right\}. \qquad \text{(C.5)}
\end{aligned}$$

Further, by letting $N \to \infty$, we have

$$\begin{aligned}
\lim_{N\to\infty}(C.5) =& \lim_{N\to\infty}\sum_{s=1}^{K-1}\left(1-\frac{t^2}{2s}+o\left(\frac{t^2}{s}\right)\right)^s\mathbb{P}\left\{S=s\right\} \\
&+e^{-\frac{t^2}{2}}\lim_{N\to\infty}\sum_{s\geq K}\mathbb{P}\left\{S=s\right\} \\
=&e^{-\frac{t^2}{2}}\lim_{N\to\infty}\mathbb{P}\left\{S\geq K\right\} = e^{-\frac{t^2}{2}}.
\end{aligned}$$

Thus, we obtain that the characteristic function of $\frac{B-\mu S}{\sigma\sqrt{S}}$ converges to $e^{-\frac{t^2}{2}}$ as $N \to \infty$. Finally, by the L$\acute{e}$vy's continuity theorem (Chapter 18 in [61]), we obtain the conclusion.

C.4 Proof of Proposition 4.3.4

The model given by Fig. 4.1 is an Markov chain with an infinite countable state space, and it has a unique stationary distribution if and only if it has at least one positive recurrent state according to Theorem 26.3 in [23]. However, it is difficult to directly show that a state is positive recurrent. Thus, we first derive the form of the stationary distribution $\pi = [\pi_1 \ \pi_2 \ \cdots]$, and then show that it is unique.

Assume $\sum_{i=0}^{\infty} \pi_i = 1$. Then, by solving $\pi = \pi W$, where W is the transition probability matrix given by (4.18), we have

$$\begin{aligned}
\pi_0 = \frac{Q_n}{p + Q_n}, \ \pi_1 &= \frac{p}{1 - (1 - Q_n)(1 - p)} \pi_0 \\
\pi_2 &= \frac{(1 - Q_n)p}{1 - (1 - Q_n)(1 - p)} \pi_1 \\
\pi_3 &= \frac{(1 - Q_n)p}{1 - (1 - Q_n)(1 - p)} \pi_2 \\
&\cdots
\end{aligned}$$

Thus, we obtain that π is given by (4.19) and (4.20). Next, we check $\sum_{i=0}^{\infty} \pi_i = 1$, which

can be verified as follows:

$$\begin{aligned}
\sum_{i=0}^{\infty} \pi_i =& \pi_0 + \frac{p}{1-(1-Q_n)(1-p)}\pi_0 + \\
& \sum_{i=2}^{\infty} \left(\frac{(1-Q_n)p}{1-(1-Q_n)(1-p)} \right)^i \frac{\pi_0}{(1-Q_n)} \\
=& \pi_0 + \frac{p}{1-(1-Q_n)(1-p)}\pi_0 + \\
& \frac{(1-Q_n)p^2}{1-(1-Q_n)(1-p)} \frac{\pi_0}{Q_n} \\
=& \frac{1}{p+Q_n} \left(Q_n + \frac{Q_n p}{Q_n + (1-Q_n)p} \right. \\
& \left. + \frac{(1-Q_n)p^2}{Q_n + (1-Q_n)p} \right) \\
=& \frac{1}{p+Q_n} \frac{(Q_n+p)^2 - Q_n p(Q_n+p)}{Q_n + (1-Q_n)p} = 1.
\end{aligned}$$

Thus, π is a stationary distribution. We observe that state zero is positive recurrent since $\frac{1}{\pi_0} < \infty$, and thus the stationary distribution π is unique by Theorem 26.3 in [23].